DESIGN AND ANALYSIS OF
TYPE-2 FUZZY LOGIC SYSTEMS

WU, DONGRUI

Acknowledgements

Contents

Summary

Type-1 fuzzy logic systems (FLSs), constructed from type-1 fuzzy sets introduced by Zadeh in 1965, have been successfully applied to many fields. However, research has shown that the ability of type-1 fuzzy sets to model and minimize the effect of uncertainties is limited. A reason may be that a type-1 fuzzy set is certain in the sense that for each input, there is a crisp membership grade.

The concept of type-2 fuzzy sets was proposed by Zadeh in 1975 to overcome this limitation. The uncertainties in the shape and position of a a type-2 set is modeled by a blur membership function (MF) called the footprint of uncertainty (FOU). A type-2 FLS is an entity that characterizes its input or output domains with one or more type-2 fuzzy sets. Compared to type-1 FLSs, type-2 FLSs have extra mathematical dimensions and they are useful in circumstances where it is difficult to determine an exact MF for a fuzzy set. They can, therefore, better handle uncertainties and have the potential to outperform their type-1 counterparts. However, many properties of type-2 FLSs remain unclear so far.

This thesis aims at providing insights into the fundamental properties of type-2 FLSs and improving their performance. First, it shows that type-2 FLSs can achieve a better compromise between accuracy/performance and interpretability than their type-1 counterparts. Then a simplified type-2 FLS structure is proposed to reduce the heavy computational cost of traditional type-2 FLSs. This makes type-2 FLSs more suitable for real-time applications. Next, the original concept of Equivalent Type-1 Sets (ET1Ss) of a type-2 FLS is introduced and used to analyze the properties of the type-2 FLSs. The ET1Ss are also used to show that a type-2

PI-like FLS may be equivalent to a type-1 PI FLS with adaptive PI gains in certain input ranges. This provides insights into why type-2 FLSs may generate smoother input-output maps than their type-1 counterparts. Finally conclusions are drawn and future research directions are outlined.

List of Tables

List of Figures

Chapter 1

Introduction

Our knowledge of many problems may be classified to two categories: 1) **Objective knowledge** and 2) **Subjective knowledge** [**?**]. The former are sensory measurements and mathematical models that are derived according to physical laws. i.e. the transfer function of a system. The latter comes from human experts who describe their knowledge about the system in natural languages [2]. It represents linguistic information that may be impossible to quantify using traditional mathematics. e.g. the operation rule for a chemical process :

IF the water level is low, THEN open the valve a little.

Both types of knowledge are useful for solving practical problems. **Fuzzy logic**, originally proposed by Lotif Zadeh in 1965 [3], is a way to coordinate the two classes of knowledge. It emulates a human's ability to reason and solve problems using imprecise information. Its underlying modes of reasoning are approximate. This leads to the concept of **fuzzy logic system** (**FLS**). FLSs are knowledge-based systems consisting of linguistic "IF-THEN" rules that can be constructed using the knowledge of experts in the given field of interest.

1.1   Type-1 Fuzzy Logic

Type-1 fuzzy set is a generalization of the crisp set, whose **membership grades** can only be 0 or 1. A fuzzy set A is defined on a *universe of discourse* X and is

characterized by a membership grade $\mu_A(x)$ that takes on values in the interval $[0, 1]$. When X is continuous, A is commonly written as :

$$A = \int_X \mu_A(x)/x \qquad (1.1)$$

Here $\int$ does not denote integration; it denotes the collection of all points $x \in X$ with associated membership grade $\mu_A(x)$.

A type-1 FLS is constructed completely by type-1 fuzzy sets. It contains four components—rule base, fuzzifier, inference engine and defuzzifier, as shown in Figure 1.1.
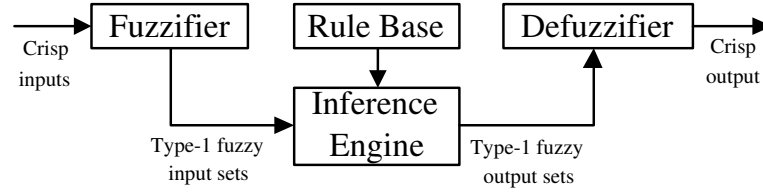
Figure 1.1: A type-1 FLS

The rule base is a collection of IF-THEN statements in the following form :

R^l: IF x_1 is X_1^l and $\cdots$ and x_p is X_p^l,   THEN y is Y^l

where X_i^l $(i = 1, \ldots, p)$ and Y^l are type-1 fuzzy sets in U_i and V, respectively, and $\mathbf{x} = (x_1, \ldots, x_p) \in U_1 \times U_2 \times \cdots \times U_p \equiv \mathbf{U}$ and $y \in V$ are linguistic variables. More specifically, $\mathbf{x}$ is the input to the FLS and y is the output. The IF-part of a rule is its ***antecedent***, and the THEN-part is its ***consequent***. Fuzzy sets are associated with terms that appear in the antecedents or consequents of rules, and with the inputs to and output of the FLS. They are called ***membership functions*** (**MFs**), which provide a measure of the degree of similarity of an element to the fuzzy set. For type-1 fuzzy sets, the MFs are totally certain.

The fuzzifier performs a mapping from the crisp input $\mathbf{x} = (x_1, \ldots, x_p)$ into

fuzzy sets in **U**. In the fuzzy inference engine, fuzzy logic principles are used to combine the fuzzy IF-THEN rules in the fuzzy rule base into a mapping from the fuzzy sets in **U** to fuzzy sets in V. The defuzzifier performs a mapping from fuzzy sets in V to a crisp output $y \in V$.

1.2 Type-1 Fuzzy Modeling and Control: A Review

Type-1 FLSs have been successfully applied in many areas, including data mining [4–10], time-series prediction [11–16], communication and networks [17–21], etc. Fuzzy modeling and control is the most common application area of fuzzy logic [2, 22–30]. The milestone of the application of ***fuzzy logic controllers*** (**FLCs**) is universally considered to be the experiments on steam control described by Mamdani and Assilian [31–33]. The fuzzy model introduced by Mamdani is also known as the ***Mamdani model***. It is the most widely model used by FLCs. All the results reported in this thesis assume this model.

The early applications of fuzzy control were based on the idea to mimic the control actions of human operators [34]. In this case, a priori knowledge is used and the final FLC performs as well as an human operator. Fuzzy control is suitable when the system is only partly known, difficult to describe by a white-box model, and few measurements are available, or the system is highly nonlinear. However, extensive experience in operating the process should be available to the FLC designers.

Many fuzzy control architectures are related to simple control algorithms, such

as the widely used PID controllers. Nonlinearities and exceptions, which are difficult to realize with conventional controllers, can be handled relatively easily by FLCs. In conventional control, many additional measures have to be included for the proper functioning of the controller: anti-reset windup, proportional kick, retarded integral action, etc. These tricks can be built in naturally in a fuzzy PID-like controller. Moreover, other types of local nonlinearities can easily be built in since a FLC can be viewed as a nonlinear mapping [35].

Models play an important role in many advanced controllers. There are several possibilities to model a system by applying fuzzy techniques such as models based on Mamdani fuzzy rules [34], models based on Takagi-Sugeno rules [36], fuzzy relational models [37] and a combination of them [38]. Some approaches to determine a fuzzy model are [39] :

- A fuzzy model can be obtained by using a priori knowledge about the system provided as rules by system designers and operators. However, knowledge acquisition may be cumbersome, costly, and time-consuming.

- A fuzzy model can be obtained by using available measurements and using identification methods, e.g., clustering methods to find the parameters and fuzzy terms of the rules describing the system. This method gives good results and can easily be interpreted in a linguistic way, thus providing a means for evaluating and validating the final model with knowledge from operators and experts [26].

The resulting fuzzy models can be used to develop FLCs [40]. An interesting application is the use of these models in **model-based predictive controllers** (**MBPCs**) [41–44]. Such controllers calculate the future output of a system for

different control sequences, and find the optimal control action while taking into account a desired behavior and constraints on system variables. The model of the process must be able to predict the future process output. Preferably, it should be based on an intuition so that it can be understood by an operator. In situations where conventional modeling approaches based on physical modeling or linear system identification cannot derive reliable models for complex or partly known systems, fuzzy modeling may give promising results.

Adaptive fuzzy control is a possibility to cope with time-varying and non-linear behavior of a system [45]. However, complicated measures are needed to keep the adaptive controllers functioning properly. In FLCs, exceptions can be easily implemented and their interpretation is more straight-forward to the user and designer. Generally, exception handling and safety guarding is implemented in a FLC in a transparent way with easy linguistic interpretations, while in conventional (adaptive) control it is more difficult. When the actual parameters of the controller are adapted according to the behavior of the overall system, an adaptive supervisory control algorithm may be used. The adaption should be related to some performance measure of the system. Some possibilities to apply fuzzy techniques are [39] :

- The performance criterion provides information as MFs, such as that the overshoot is too big, or within the specs. The supervision is done by rules relating these fuzzy performance measures (antecedents) to the settings of the controller to be adapted (consequents).

- A fuzzy model is used as a representation of the time-varying system. This model is adapted and used in a fuzzy control strategy.

- Depending on the situation, a choice is made between different control strategies (strategy switching). A fuzzy decision maker realizes this selection based on the requirements and actual state of the system and takes care of transient behavior.

As an autonomous system utilizes the supervisory methods described above, special attention should be paid to exception handling and safety guarding, which can be described quite easily by rules. The whole supervisory system can then be realized in a *fuzzy expert system*.

1.3 Type-2 Fuzzy Logic

Despite having a name which carries the connotation of uncertainty, research has shown that there may be limitations in the ability of type-1 FLSs to model and minimize the effect of uncertainties [?, 62]. One restriction being that a type-1 fuzzy set is certain in the sense that the membership grade for each input is a crisp value. Recently, type-2 fuzzy sets [46], characterized by MFs that are themselves fuzzy, have been attracting interest [?].

A FLS described using at least one type-2 fuzzy set is called a type-2 FLS. Type-2 FLSs have been used successfully in many applications, for example, time-series forecasting [?, 47], communication and networks [48–50], decision making [51–53], data and survey preprocessing [?, ?, 54], noise cancellation [55], word modeling [56, 57], phoneme recognition [58], plant monitoring and diagnostics [59, 60], etc.

Fuzzy control is the most widely used application of fuzzy set theory. A literature search reveals that type-2 FLSs are beginning to be employed in the field of control. A type-2 proportional controller was proposed in [61]. Interval type-2

FLCs were applied to mobile robot control [62], quality control of sound speakers [63], connection admission control in ATM networks [20]. A dynamical optimal training algorithms for type-2 fuzzy neural networks (T2FNN) was proposed in [64]. T2FNNs have been used in non-linear plant control [65,66] and truck back up control [64]. A comparison of the performances of type-1 and type-2 FLCs on a first-order time delay system was conducted in [67].

1.4 Aims and Scope of This Work

Type-2 fuzzy logic is still a relatively new concept. Many of its properties remain unclear. Though type-2 FLSs may have better abilities to handle uncertainties than their type-1 counterparts, the heavy computational cost of type-reduction may limit their usefulness in certain real-time applications. This work seeks to better understand the properties of type-2 FLSs, and tries to reduce their computational requirements. The specific aims are the follows :

1. To investigate whether a type-2 FLC can achieve better control performance than its type-1 counterpart with similar or more design parameters. That is, whether a type-2 FLC has better trade-off between accuracy and interpretability.

2. To reduce the computational cost by finding a simplified structure for real-time type-2 FLCs. The simplified type-2 FLC should be able to bring about computational savings without sacrificing the ability to handle modeling uncertainties.

3. To demonstrate that a type-2 FLS can be viewed as being equivalent to a collection of *equivalent type-1 fuzzy logic systems* and explain why

type-2 FLSs may be able to model more complex input-output maps than their type-1 counterparts.

4. To explain why type-2 FLCs generally are better at eliminating oscillations by introducing the concept of **equivalent proportional and integral gains**.

1.5   Organization of the Thesis

Chapter 2 deals with the groundwork that forms the basis of the research presented in this thesis. It introduces several important concepts on type-2 fuzzy sets and FLSs. The operations in each part of a type-2 FLS are described. An illustrative example is given at the end of the Chapter.

Chapter 3 focuses on advancing the understanding of type-2 fuzzy systems by studying the characteristics of type-2 FLCs. First, a method for using Genetic Algorithms (GAs) to evolve a type-2 FLC is presented. The type-2 FLC is then compared with another three GA evolved type-1 FLCs that have different number of design parameters. The study aims at investigating the ability of type-2 FLCs to handle uncertainties as well as the relationship between performance and rule base size. Via experiments, the ability of a type-2 FLC to cope with the complexity of the plant, and to handle uncertainties was compared with three type-1 FLC with different number of design parameters. By examining whether a type-2 FLC can achieve better control performance with fewer fuzzy sets/rules, the trade-off between accuracy and interpretability can be established.

One major disadvantage of type-2 FLCs is that they may not be suitable for real-time applications because they require large computational power, especially when there are many MFs and the rule base is large. In Chapter 4, a simplified

type-2 FLC that is more suitable for real-time control is proposed. The key idea is to only replace some critical type-1 fuzzy sets by type-2 sets. A type-2 FLCs with simplified structure is designed for a coupled-tank liquid level control process. Its performances is compared with two type-1 FLCs and a traditional type-2 FLC. Simulations and experiments are conducted to show whether the simplified type-2 FLC is able to bring about computational savings without sacrificing the ability to handle modeling uncertainties.

The objective of Chapter 5 is to gain a better understanding of type-2 FLSs by analyzing the manner in which the extra mathematical dimensions associated with FOU enable a type-2 FLS to differentiate itself from a type-1 FLS. Utilizing the fact that the input-output relationships of both type-2 and type-1 FLSs are fixed once their parameters are selected, a group of **equivalent type-1 sets** (**ET1Ss**) that re-produces the input-output relationship of the type-2 FLS can be identified. A type-2 FLS may, therefore, be viewed as being equivalent to a collection of **equivalent type-1 FLSs** (**ET1FLSs**), and the role of the type-reducer is to select an *equivalent membership grade* from which the firing level of a rule can be calculated. Via the concepts of ET1Ss and ET1FLSs, properties of a type-2 FLS can be studied. The proposed technique for converting a type-2 FLS into a group of ET1FLSs is also useful as it provides a framework for extending the entire wealth of type-1 fuzzy control/identification/design/analysis techniques to type-2 systems.

Chapter 6 studies the characteristics of an interval type-2 PI fuzzy controller. The **equivalent PI gains** for a double-input single-output PI-like type-2 FLC are found. The change patterns of the PI gains with respect to the change of

inputs are also studied. This may help understand why type-2 FLCs are generally better at eliminating oscillations, and provide insights into how to evolve faster type-reducers theoretically.

Finally, Chapter 7 draws conclusions from the results presented in this Thesis, and suggests possible directions for future work.

Chapter 2

Background and Preliminaries

The concept of type-2 fuzzy set was introduced by Zadeh in 1975 as an extension of the type-1 set [46]. It is characterized by fuzzy membership grades. An *interval type-2 fuzzy set* $\tilde{A}$ in X is defined as [?] :

$$\widetilde{A} = \int_{x \in X} \int_{u \in J_x \subseteq [0,1]} 1/(x,u) = \int_{x \in X} \left[\int_{u \in J_x \subseteq [0,1]} 1/u \right] / x \qquad (2.1)$$

where x is the *primary variable* with domain X; u is the *secondary variable*, which has domain J_x at each $x \in X$; J_x is called the *primary membership* of x. For interval type-2 sets, the *secondary grades* of $\widetilde{A}$ all equal 1. Uncertainty about $\widetilde{A}$ is conveyed by the union of all of the primary memberships called the *footprint of uncertainty* (FOU) of $\widetilde{A}$; i.e.

$$FOU(\widetilde{A}) = \bigcup_{x \in X} J_x \qquad (2.2)$$

Examples of type-2 fuzzy sets are shown in Figure 2.1. The FOU is shown as the shaded region. It represents the uncertainties in the shape and position of the type-1 fuzzy set. The FOU is bounded by an *upper MF* and a *lower MF*, both of which are type-1 MFs. Consequently, the membership grade of each element in a type-2 fuzzy set is a fuzzy set $[l, r]$, where l and r are membership grades on the lower and upper MFs. Type-2 sets are extremely useful in circumstances where it is difficult to determine the exact MF for a fuzzy set; hence, they are useful for incorporating uncertainties.
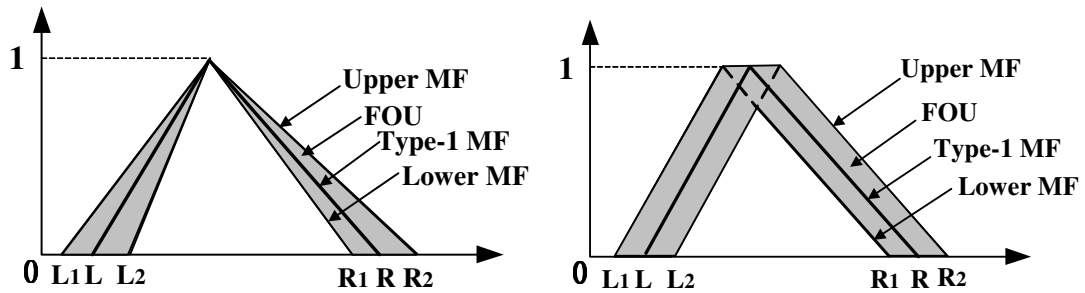
(a) A type-2 fuzzy set evolved by blurring the width of a triangular type-1 fuzzy set

(b) A type-2 fuzzy set evolved by blurring the apex of a triangular type-1 fuzzy set

Figure 2.1: Type-2 fuzzy sets

FLSs constructed using type-2 fuzzy sets are called *type-2 FLSs* to distinguish them from the traditional type-1 FLSs. For all the results reported in this thesis, interval singleton type-2 FLSs [?] are employed. "*Interval*" means that the input/output domains are characterized by interval type-2 sets [47]. The term "*singleton*" denotes that the fuzzifier converts the input signals of the FLS into fuzzy singletons.

Figure 2.2 shows the schematic diagram of a type-2 FLS. It is similar to its type-1 counterpart, the major difference being that at least one of the fuzzy sets in the rule base is type-2. Hence, the output of the inference engine are type-2 sets and a type-reducer is needed to convert them into a type-1 set before defuzzification can be carried out. In the following subsections the operations in a interval singleton type-2 FLS are described in detail.
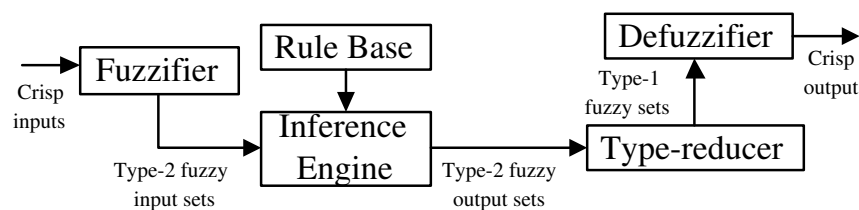
Figure 2.2: A type-2 FLS

2.1 Fuzzification

Consider the rule base of a type-2 FLS consisting of N rules assuming the following form :

$$\widetilde{R}^l: \quad \text{IF } x_1 \text{ is } \widetilde{X}_1^l \text{ and } \cdots \text{ and } x_p \text{ is } \widetilde{X}_p^l, \quad \text{THEN } y \text{ is } \widetilde{Y}^l$$

where $\widetilde{X}_i^l$ $(i = 1, \ldots, p)$ and $\widetilde{Y}^l$ are type-2 fuzzy sets, and $\mathbf{x} = (x_1, \ldots, x_p)$ and y are linguistic variables.

The fuzzifier maps a crisp point $\mathbf{x} = (x_1', x_2', \ldots, x_p')$ into a type-2 fuzzy set $\widetilde{A}_{\mathbf{x}}$. In this thesis we focus on the *type-2 singleton fuzzifier* [?]. This means $\mu_{\widetilde{X}_i}(x_i) = 1/1$ when $x_i = x_i'$ and $\mu_{\widetilde{X}_i}(x_i) = 1/0$ when $x_i \neq x_i'$, for all $i = 1, 2, \ldots, p$.

2.2 Inference

The inference engine matches the fuzzy singletons with the fuzzy rules in the rule base. To compute unions and intersections of type-2 sets, compositions of type-2 relations are needed. Just as the sup-star composition is the backbone computation for a type-1 FLS, the extended sup-star composition is the backbone for a type-2 FLS [?].

The first step in the extended sup-star operation is to obtain the firing set $\sqcap_{j=1}^{p} \mu_{\widetilde{X}_j^i}(x_j) \equiv F^i(\mathbf{x})$ by performing the input and antecedent operations. As only interval type-2 sets are used and the *meet* operation is implemented by the product t-norm, the firing set is the following type-1 interval set :

$$F^i(\mathbf{x}) = [\underline{f}^i(\mathbf{x}), \overline{f}^i(\mathbf{x})] \equiv [\underline{f}^i, \overline{f}^i] \tag{2.3}$$

where $\underline{f}^i(\mathbf{x}) = \underline{\mu}_{\widetilde{X}_1^i}(x_1) \star \underline{\mu}_{\widetilde{X}_2^i}(x_2)$ and $\overline{f}^i(\mathbf{x}) = \overline{\mu}_{\widetilde{X}_1^i}(x_1) \star \overline{\mu}_{\widetilde{X}_2^i}(x_2)$. The term $\underline{\mu}_{\widetilde{X}_j^i}(x_j)$ and $\overline{\mu}_{\widetilde{X}_j^i}(x_j)$ are the lower and upper membership grades of $\mu_{\widetilde{X}_j^i}(x_j)$. Next, the

firing set, $F^i(\mathbf{x})$, is combined with the consequent fuzzy set of the ith rule, $\mu_{\widetilde{Y}^i}$, using the product t-norm to derive the fired output consequent sets. The combined output fuzzy set may then be obtained using the maximum t-conorm.

2.3 Type-reduction and Defuzzification

Since the output of the inference engine are type-2 fuzzy sets, they must be type-reduced before the defuzzifier can be used to generate a crisp output. This is the main structural difference between type-1 and type-2 FLSs. The most commonly used type-reduction method is the center-of-sets type-reducer, which may be expressed as [?] :

$$Y_{cos}(\mathbf{x}) = \int_{y^1 \in Y^i} \cdots \int_{y^N \in Y^i} \int_{f^1 \in F^i(\mathbf{x})} \cdots \int_{f^N \in F^i(\mathbf{x})} \left[1 \left/ \frac{\sum\limits_{i=1}^{N} f^i y^i}{\sum\limits_{i=1}^{N} f^i} \right. \right] = [y_l, \ y_r] \quad (2.4)$$

where $F^i(\mathbf{X}) = [\underline{f}^i, \overline{f}^i]$ is the interval firing level of the ith rule, $Y^i = [y_l^i, \ y_r^i]$ is an interval type-1 set corresponding to the centroid of the interval type-2 consequent set $\widetilde{Y}^i$ [?] :

$$C_{\widetilde{Y}^i} = \int_{\theta_1 \in J_{x_1}} \cdots \int_{\theta_N \in J_{x_N}} 1 \left/ \frac{\sum_{i=1}^{N} x_i \theta_i}{\sum_{i=1}^{N} \theta_i} \right. = [y_l^i, \ y_r^i] \quad (2.5)$$

Equation (2.4) may be computed using the Karnik-Mendel iterative method [?] as follows :

> *Set $y^i = y_l^i$ for $i = 1, \ldots, N$;*
> *Arrange y^i in ascending order;*
> *Set $f^i = \frac{\underline{f}^i + \overline{f}^i}{2}$ for $i = 1, \ldots, N$;*
> *$y' = \frac{\sum_{i=1}^{N} y^i f^i}{\sum_{i=1}^{N} f^i}$;*
> *do*
> > *$y'' = y'$;*
> > *Find $k \in [1, N-1]$ such that $y^k \leq y' \leq y^{k+1}$;*

$$\text{Set } f^i = \overline{f}^i \text{ for } i \leq k$$
$$\text{Set } f^i = \underline{f}^i \text{ for } i \geq k+1;$$
$$y' = \frac{\sum_{i=1}^N y^i f^i}{\sum_{i=1}^N f^i};$$
$$\text{while } y' \neq y''$$
$$y_l = y';$$

$$\text{Set } y^i = y_r^i \text{ for } i = 1, \ldots, N;$$
$$\text{Arrange } y^i \text{ in ascending order;}$$
$$\text{Set } f^i = \frac{\underline{f}^i + \overline{f}^i}{2} \text{ for } i = 1, \ldots, N;$$
$$y' = \frac{\sum_{i=1}^N y^i f^i}{\sum_{i=1}^N f^i};$$
$$\text{do}$$
$$\qquad y' = y'';$$
$$\qquad \text{Find } k \in [1, N-1] \text{ such that } y^k \leq y' \leq y^{k+1};$$
$$\qquad \text{Set } f^i = \underline{f}^i \text{ for } i \leq k$$
$$\qquad \text{Set } f^i = \overline{f}^i \text{ for } i \geq k+1;$$
$$\qquad y' = \frac{\sum_{i=1}^N y^i f^i}{\sum_{i=1}^N f^i};$$
$$\text{while } y' \neq y''$$
$$y_r = y';$$

The main idea of the above procedure is to find a switch point for both y_l and y_r. Let's take y_l for example. y_l is the minimum of $Y_{cos}(\mathbf{x})$. Since y_l^i increases from the left to the right along the horizontal axis of Figure 2.3(a), generally we should choose the upper membership grade for the y_l^i on the left and the lower membership grade for the y_l^i on the right. The Karnik-Mendel procedure finds the switch point y_l^k. For $i \leq k$, the upper membership grades are used to calculate y_l; for $i > k$, the lower membership grades are used. This will ensure y_l be the minimum. For y_r, the idea is similar; except that for $i \leq k$, the lower membership grades are used to calculate y_r; for $i > k$, the upper membership grades are used, as shown in Figure 2.3(b).

It has been proven that this iterative procedure converges super-exponentially [68]. Once y_l and y_r are obtained, they can be used to calculate the crisp output.

(a) Computing y_l: switch from the UMF to the LMF

(b) Computing y_r: switch from the LMF to the UMF
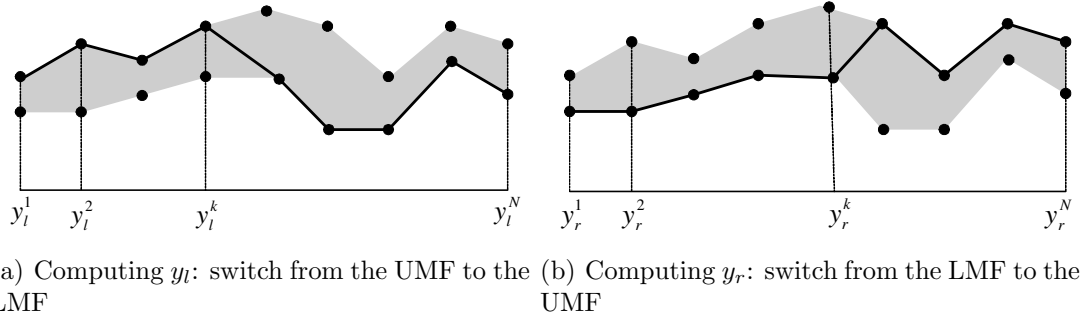
Figure 2.3: Illustration of the switch points in computing y_l and y_r. The switch points are found by the Karnik-Mendel algorithms [1].

Since the type-reduced set is an interval type-1 set, the defuzzified output is :

$$y = \frac{y_l + y_r}{2} \tag{2.6}$$

2.4 Example of a Type-2 FLS

In this section, the mathematical operations in a type-2 FLS are illustrated using an example. Consider a baseline type-1 FLS that has two inputs (x_1 and x_2) and one output (y). It is assumed that each input domain consists of two type-1 MFs, shown as the dark thick lines in Figure 2.4.

(a) Input MFs of x_1

(b) Input MFs of x_2
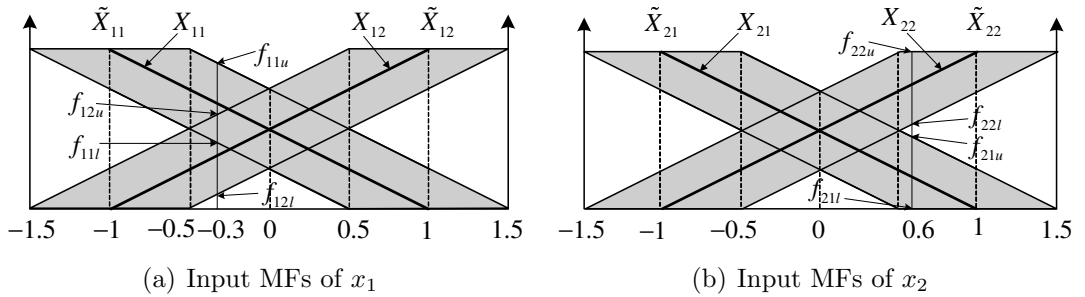
Figure 2.4: MFs of the two FLSs

A type-2 FLS is obtained by equipping the four fuzzy sets used to partition the input domains of the baseline type-1 FLS with FOUs, shown as the shaded areas in Figure 2.4. The rule base also has four rules assuming the following form :

$$\widetilde{R}^{ij}: \quad \text{IF } x_1 \text{ is } \widetilde{X}_{1i} \text{ and } x_2 \text{ is } \widetilde{X}_{2j}, \text{ THEN } y \text{ is } \widetilde{Y}_{ij}. \quad i,j = 1,2$$

The complete rule base and the corresponding consequents are shown in Table 2.1.

Table 2.1: Rule base and consequents of the type-2 FLS

x_1 \ x_2	$\widetilde{X}_{21}$	$\widetilde{X}_{22}$
$\widetilde{X}_{11}$	$\widetilde{Y}_{11} = -1$	$\widetilde{Y}_{12} = -0.5$
$\widetilde{X}_{12}$	$\widetilde{Y}_{21} = 0.5$	$\widetilde{Y}_{22} = 1$

Consider an input vector $\mathbf{x} = (x_1, x_2) = (-0.3, 0.6)$. The firing strengths of the four type-2 input MFs are :

$$\widetilde{f}_{11} = [0.4,\ 0.9] \quad \widetilde{f}_{12} = [0.1,\ 0.6]$$

$$\widetilde{f}_{21} = [0,\ 0.45] \quad \widetilde{f}_{22} = [0.55,\ 1]$$

Thus, the firing levels of the four rules are :

Rule No.:	Firing Strength	$\rightarrow$	Consequent
$\widetilde{R}^{11}$:	$[0.4 \times 0, 0.9 \times 0.45] = [0, 0.405]$	$\rightarrow$	-1
$\widetilde{R}^{12}$:	$[0.4 \times 0.55, 0.9 \times 1] = [0.22, 0.9]$	$\rightarrow$	-0.5
$\widetilde{R}^{21}$:	$[0.1 \times 0, 0.6 \times 0.45] = [0, 0.27]$	$\rightarrow$	0.5
$\widetilde{R}^{22}$:	$[0.1 \times 0.55, 0.6 \times 1] = [0.055, 0.6]$	$\rightarrow$	1

For the type-2 FLS, the bounds of the type-reduced interval type-1 set obtained using the Karnik-Mendel type-reducer are :

$$y_l = \frac{0.405 \times (-1) + 0.22 \times (-0.5) + 0 \times 0.5 + 0.055 \times 1}{0.405 + 0.22 + 0 + 0.055} = -0.6765$$

$$y_r = \frac{0 \times (-1) + 0.22 \times (-0.5) + 0 \times 0.5 + 0.6 \times 1}{0 + 0.22 + 0 + 0.6} = 0.5976$$

Note here the switch of membership grades for y_l occurs at $\widetilde{R}^{11}$. That is, for consequent -1, the upper membership grade is employed to calculate y_l; for consequents -0.5, 0.5 and 1, the lower membership grades are used. For y_r, the switch occurs after the second rule. That is, for consequent -1 and -0.5, the

upper membership grades are employed to calculate y_r; for consequents 0.5 and 1,

the lower membership grades are used.

Finally, the crisp output of the type-2 FLS, y_2, is :

$$y_2 = \frac{y_l + y_r}{2} = \frac{-0.6765 + 0.5976}{2} = 0.03945$$

Chapter 3

Genetic Tuning and Performance Evaluation of Interval Type-2 FLCs

This Chapter seeks to contribute towards the design and understanding of type-2 fuzzy control. A genetic learning strategy for designing a type-2 fuzzy logic controller (FLC) to control non-linear plants is proposed. Genetic algorithm (GA), a global optimal search algorithm, has been widely used to design FLSs [64,69–71]. Due to the computational requirements, FLCs designed using GAs are generally evolved off-line using a model of the controlled process. As it is impossible for a model to capture all the characteristics of the actual plant, the performance of the type-1 FLC designed using GA and a theoretical model will inevitably deteriorate when it is applied to the real-world problem. The concept of type-2 fuzzy sets was introduced to enhance the uncertainty handling capability of FLS so an issue that is addressed herein is whether a type-2 FLC would cope better with modeling uncertainties, and thereby achieve better control performance than a type-1 FLC in practice. The study is performed by comparing the ability of type-1 and type-2 FLCs to control an uncertain liquid level plant.

One aspect that was considered in the comparative study is the number of design parameters or degrees of freedom that the FLCs have. It is well-known that the performance of a type-1 FLC may be improved by partitioning the input

domains with a larger number of fuzzy sets. Unfortunately, there is a trade-off between accuracy/performance and interpretability. A larger number of MFs results in a bigger rule base that would be harder for a human to interpret because of the curse of dimensionality. Since the FOU provides a type-2 fuzzy set with an additional mathematical dimension, the conjecture is that a type-2 FLC with a smaller rule base may be capable of providing performance comparable to a type-1 FLC that has more rules. Hence, another objective is to ascertain whether a type-2 FLC is able to provide better performance/accuracy without sacrificing rule base interpretability.

The rest of this Chapter is organized as follows : Section 3.1 briefly introduces GAs and approaches for designing type-2 FLCs. Next, details of the FLCs that were evolved by GA are covered in Section 3.2. Section 3.3 presents the comparative abilities of the FLCs to handle modelling uncertainties. Discussions are given in Section 4.3 before conclusions are drawn in Section 3.5.

3.1   Genetic Tuning of a Type-2 FLC

GA is a general-purpose search algorithm that uses principles inspired by natural population genetics to evolve solutions to problems. It was first proposed by Holland in 1975 [72]. GAs are theoretically and empirically proven to provide a robust search in complex spaces, thereby offering a valid approach to problems requiring efficient and effective searches [73–76].

Figure 3.1 shows the flow chart of a basic GA. First, a chromosome population is randomly generated. Each chromosome encodes a candidate solution of the optimization problem. The fitness of all individuals with respect to the optimization

```
┌─────────────────────┐
│ Initialize population│
│       Gen = 1        │
└─────────────────────┘
           │
           ▼
┌─────────────────────┐
│  Evaluate population │◄──┐
└─────────────────────┘   │
           │              │
           ▼              │
┌─────────────────────┐   │
│      Selection       │   │
└─────────────────────┘   │
           │              │
           ▼              │
┌─────────────────────┐   │
│      Crossover       │   │
└─────────────────────┘   │
           │              │
           ▼              │
┌─────────────────────┐   │
│      Mutation        │   │
└─────────────────────┘   │
           │              │
           ▼              │
┌─────────────────────┐   │
│    Gen = Gen + 1     │   │
└─────────────────────┘   │
           │         No   │
           ▼              │
    ◇ Gen > MaxGen ◇──────┘
           │ Yes
           ▼
┌─────────────────────┐
│   Output results     │
└─────────────────────┘
```
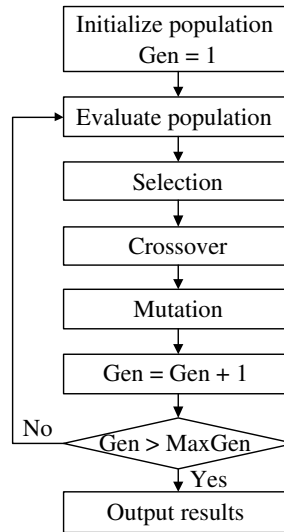
Figure 3.1: The flow chart of a basic GA

task is then evaluated by a scalar objective function (fitness function). According to Darwin's principle, highly fit individuals are more likely to be selected to reproduce offsprings. Genetic operators such as crossover and mutation are applied to the parents in order to produce a new generation of candidate solutions. As a result of this evolutionary cycle of selection, crossover and mutation, more and more suitable solutions to the optimization problem emerge within the population.

Increasingly, GA is used to facilitate FLCs design [77–80]. However, most of the works discuss type-1 FLC design. This Chapter focuses on genetic learning of type-2 FLCs. There are two very different approaches for selecting the parameters of a type-2 FLS [?]. One is the partially dependent approach, where a best possible type-1 FLS is designed first, and then used to initialize the parameters of a type-2 FLS. The other method is a totally independent approach, where all of the parameters of the type-2 FLC are tuned from scratch without the aid of an existing type-1 design.

One advantage offered by the partially dependent approach is smart initialization of the parameters of the type-2 FLS. Since the baseline type-1 fuzzy sets impose constraints on the type-2 sets, fewer parameters need to be tuned and the search space for each variable is smaller. Therefore, the computational cost needed to implement the GA is less so design flexibility is traded off for a lower computational burden. Type-2 FLCs designed via the partially dependent approach may be able to outperform the corresponding type-1 FLCs [70], although both the FLCs have the same number of MFs (resolution). However, the type-2 FLC has a larger number of degrees of freedom because type-2 fuzzy sets are more complex. The additional mathematical dimensions provided by the type-2 fuzzy sets enable a type-2 FLS to produce more complex input-output map without the need to increase the resolution. However, an open question is whether a type-1 FLS with a higher resolution, and therefore more degrees of freedom, would be able to match the modeling capability of a type-2 FLS. To address this issue, a comparative study involving type-2 and type-1 FLCs with similar number of degrees of freedom is performed. The totally independent approach is adopted so that the type-2 FLC evolved using GA has maximum design flexibility. Details about the FLCs are delineated in the following section.

3.2   Structure of the FLCs

Four double-inputs single-output FLCs with different degrees of freedom (design parameters) are studied. The input signals of all the FLCs are the feedback error, e, and the change of the error, $\dot{e}$, and the output signal is the change in the control signal, $\dot{u}$.

3.2.1 The Type-2 FLC, FLC_2

Each input domain of FLC_2 is partitioned by three interval type-2 fuzzy sets (Gaussian MFs with constant mean and uncertain variance) that are labeled as **N**, **Z** and **P** (refer to Figure 3.3(a)). In order to study the benefits of antecedent type-2 fuzzy sets, its effect is isolated by using five crisp numbers $\dot{u}_i$ $(i = 1, 2, \ldots, 5)$ as the consequents. Table 3.1 shows the fuzzy rule base used by the type-2 FLC. As the GA will only tune the MFs, the rules are fixed so a commonly used structure is employed.

A Gaussian MF with certain mean and uncertain variance can be completely defined by 3 parameters, m and $[\delta_1, \delta_2]$. The center-of-sets type-reducer and the height defuzzifier are means that the MFs of $\dot{u}$ are completely described by five distinct numbers (points). As FLC_2 has 6 input type-2 MFs and 5 different crisp outputs, FLC_2 has a total of $3 \times 6 + 5 = 23$ parameters.

Table 3.1: Rule base of FLC_2 and FLC_{1a}

e \ $\dot{e}$	$N_{\dot{e}}$	$Z_{\dot{e}}$	$P_{\dot{e}}$
N_e	$\dot{u}_1$	$\dot{u}_2$	$\dot{u}_3$
Z_e	$\dot{u}_2$	$\dot{u}_3$	$\dot{u}_4$
P_e	$\dot{u}_3$	$\dot{u}_4$	$\dot{u}_5$

3.2.2 The Type-1 FLC, FLC_{1a}

The structure and rule base of the type-1 FLC, FLC_{1a}, are the same as those of FLC_2. The only difference between FLC_{1a} and FLC_2 is that the input MFs of FLC_{1a} are type-1 (refer to Figure 3.3(b)). Product-sum inference and height defuzzification were employed. Since two parameters are sufficient to determine a Gaussian type-1 MF, the GA has to optimize a total of $2 \times 6 + 5 = 17$ parameters.

FLC_2 and FLC_{1a} have the same number of MFs and rules. Hence, comparing their performances may provide insights into the contributions made by the FOU.

3.2.3 The Type-1 FLC, FLC_{1b}

Each input of FLC_{1b} has 5 type-1 MFs in its universe of discourse, as shown in Figure 3.3(c). The rule base is given in Table 3.2. It is commonly used by Mamdani FLCs. FLC_{1b} has $2 \times 10 + 9 = 29$ parameters to be tuned. Compared to FLC_2, FLC_{1b} has 6 extra design parameters. They enable us to determine whether a type-2 FLC is able to outperform a type-1 FLC with similar number of degrees of freedom.

Table 3.2: Rule base of the type-1 FLC, FLC_{1b}

e \ $\dot{e}$	$NB_{\dot{e}}$	$NM_{\dot{e}}$	$Z_{\dot{e}}$	$PM_{\dot{e}}$	$PB_{\dot{e}}$
NB_e	$\dot{u}_1$	$\dot{u}_2$	$\dot{u}_3$	$\dot{u}_4$	$\dot{u}_5$
NM_e	$\dot{u}_2$	$\dot{u}_3$	$\dot{u}_4$	$\dot{u}_5$	$\dot{u}_6$
Z_e	$\dot{u}_3$	$\dot{u}_4$	$\dot{u}_5$	$\dot{u}_6$	$\dot{u}_7$
PM_e	$\dot{u}_4$	$\dot{u}_5$	$\dot{u}_6$	$\dot{u}_7$	$\dot{u}_8$
PB_e	$\dot{u}_5$	$\dot{u}_6$	$\dot{u}_7$	$\dot{u}_8$	$\dot{u}_9$

3.2.4 The Neuro-Fuzzy Controller, NFC

The fourth controller analyzed in this Chapter is a neuro-fuzzy controller similar to the one proposed in [81]. Its two inputs are characterized by 5 type-1 MFs, as shown in Figure 3.3(d). Though the input MFs are similar to those of FLC_{1b}, its rule base is quite different. The consequences of the 25 rules are different from each other (refer to Table 3.7(b)). Thus, there are $2 \times 10 + 25 = 45$ parameters to be tuned by GA.

3.3 Experimental Comparison

This section presents an experimental comparison of the characteristics of the four FLCs. The test platform is a non-linear second order liquid level process. Since the FLCs are tuned offline, the simulation model used for identifying the controller parameters is described in the following subsection.

3.3.1 The Coupled-tank System

The coupled-tank apparatus [82] shown in Figure 3.2 is used to assess the FLCs. It consists of two small tower-type tanks mounted above a reservoir that stores the water. Water is pumped into the top of each tank by two independent pumps, and the levels of water are measured by two capacitive-type probe sensors. Each tank is fitted with an outlet, at the side near the base. Raising the baffle between the two tanks allows water to flow between them. The amount of water that returns to the reservoir is approximately proportional to the square root of the height of water in the tank, which is the main source of nonlinearity in the system [82].
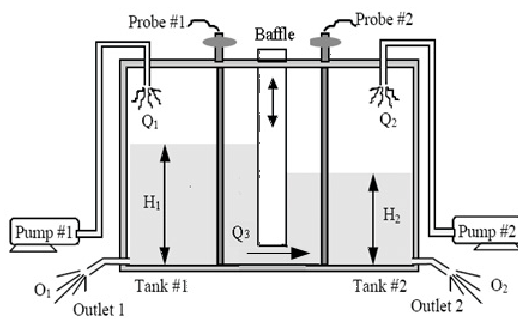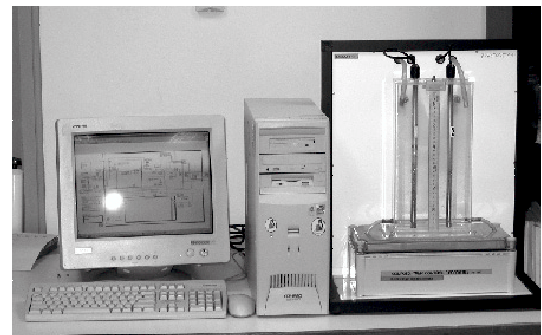
(a) Schematic diagram　　　　　　　　(b) Experimental Setup

Figure 3.2: The coupled-tank liquid-level control system

The dynamics of the coupled-tank apparatus can be described by the following

set of nonlinear differential equations :

$$A_1 \frac{dH_1}{dt} = Q_1 - \alpha_1 \sqrt{H_1} - \alpha_3 \sqrt{H_1 - H_2} \qquad (3.1a)$$

$$A_2 \frac{dH_2}{dt} = Q_2 - \alpha_2 \sqrt{H_2} + \alpha_3 \sqrt{H_1 - H_2} \qquad (3.1b)$$

where A_1, A_2 are the cross-sectional area of Tank #1, #2; H_1, H_2 are the liquid level in Tank #1, #2; Q_1, Q_2 are the volumetric flow rate (cm^3/sec) of Pump #1, #2; α_1, α_2, α_3 are the proportionality constant corresponding to the $\sqrt{H_1}$, $\sqrt{H_2}$ and $\sqrt{H_1 - H_2}$ terms. Note that here we assume $H_1 \geq H_2$, which is always satisfied in the experiments.

The coupled-tank apparatus can be configured as a second-order single-input single-output system by turning off Pump #2 and using Pump #1 to control the water level in Tank #2. Since Pump #2 is turned off, Q_2 equals zero and Equation (3.1b) reduces to :

$$A_2 \frac{dH_2}{dt} = -\alpha_2 \sqrt{H_2} + \alpha_3 \sqrt{H_1 - H_2} \qquad (3.2)$$

Equations (3.1a) and (3.2) are used to construct a simulation model of the coupled tank for the GA to evaluate the fitness of the candidate solutions. The parameters used are as follows :-

$$A_1 = A_2 = 36.52 \text{ cm}^2$$

$$\alpha_1 = \alpha_2 = 5.6186$$

$$\alpha_3 = 10$$

The area of the tank was measured manually while the discharge coefficients (α_1, α_2 and α_3) were found by measuring the time taken for a pre-determined change in the water levels to occur. Although the DC power source can supply between 0 and 5 Volts to the pumps, the maximum control signal is capped at

4.906 V which corresponds to an input flow rate of about 75 cm^3/sec. To compensate for the pump dead zone, the minimum control signal is chosen to be 1.646 V. A sampling period of 1 second is employed.

3.3.2   GA Parameters

The model of the coupled tank apparatus described in the previous subsection is constructed using physical laws and does not accurately reflect the characteristics of the practical plant. For example, it has been documented that the volumetric flow rate of the pumps in the coupled-tank apparatus used to produce the results is nonlinear, the system has non-zero transport delay and the sensor output is noisy [81]. Due to the presence of such modelling uncertainties, the performance of the FLCs designed using the simulation model will inevitably deteriorate when it is applied to the real-world problem. This work aims at studying whether the FOU of the type-2 FLC will enable it to cope better with the modelling uncertainties. To find the best possible FOU, there is a need to expose the FLCs to uncertain model parameters during the design phase because the input-output mapping of the type-2 FLC is fixed once the controller parameters are selected. Hence, four plants (I – IV) with the parameters shown in Table 3.3 are used to evaluate each chromosome. The sum of the integral of the time-weighted absolute errors (ITAEs) obtained from the 4 plants, defined as Equation (3.3), is used by the GA to evaluate the fitness of each candidate solution. It is taken to be the

$$F = \sum_{i=1}^{4} \alpha_i \left[\sum_{j=1}^{N_i} j * e_i(j) \right] \tag{3.3}$$

where $e_i(j)$ is the error between the setpoint and the actual level height at the jth sampling of the ith plant, α_i is the weight corresponding to the ITAE of the

Table 3.3: Plants used to assess fitness of candidate solutions

	I	II	III	IV
$A_1 = A_2$ (cm^2)	36.52	36.52	36.52	36.52
$\alpha_1 = \alpha_2$	5.6186	5.6186	5.6186	5.6186
α_3	10	10	10	8
Setpoint (cm)	$0 \to 15$	$0 \to 22.5 \to 7.5$	$0 \to 15$	$0 \to 15$
Transport delay (seconds)	0	0	2	0

i^{th} plant, and $N_i = 200$ is the number of sampling instants. There is a need to introduce α_i because the ITAE of the second plant is usually several times bigger than that of other plants. To ensure that the ITAE of the four plants can be reduced with equal emphasis, α_2 is defined as $\frac{1}{3}$ while the other weights are unity.

The GA parameters used to evolve the MFs of all the four FLCs in this Chapter are similar. A population size of 100 chromosomes coded in real number is used. Members of the first generation are randomly initialized and the GA terminates after 600 generations. The termination point was selected after an inspection of the fitness function verses generation plot revealing that the fitness function will settle within 600 generations. To ensure that the fitness function decreases monotonically, the best population in each generation enters the next generation directly. In addition, a generation gap of 0.8 is used during the reproduction operation so that 80% of the members in the new generation are determined by the selection scheme employed, while the remaining 20% are selected randomly from the intervals of adjustment. This strategy helps to prevent premature convergence of the population. The crossover rate is 0.8 and the mutation rate is 0.1. In order to enable finer adjustment to occur as the generation number (i) becomes bigger, the non-linear mutation [76] method defined in Equation (3.4) is used in the FLC

design.

$$x(i+1) = x(i) + \delta(i) \tag{3.4}$$

where

$$\delta(i) = \begin{cases} a \cdot \left[1 - \lambda^{\left(1 - \frac{i}{imax+1}\right)}\right], & \text{if } rand(1) > 0.5 \\ -a \cdot \left[1 - \lambda^{\left(1 - \frac{i}{imax+1}\right)}\right], & \text{otherwise} \end{cases}$$

$x(i)$ is the value of gene x in i^{th} generation, i_{max} is the maximum number of generations, λ and $rand(1)$ are random numbers in $[0, 1]$, and a is a constant associated with each input and output. In this Chapter a for each input is chosen to be 1/6 of the length of its universe of discourse, and a for the output is 1/10 of the length of its universe of discourse. Flexible position-coding strategy is applied in each input or output domain to improve the diversity of the members in each generation. Consequently, the genes in each sub-chromosome may not remain in the proper order after crossover and mutation, i.e. the center of the type-2 set corresponding to N_e may be larger than that of Z_e. Every sub-chromosome is, therefore, sorted before fitness evaluation is performed.

Since each input type-2 MF is determined by 3 parameters (m, δ_1, δ_2) and there are 6 input type-2 MFs and 5 different crisp outputs, each chromosome has $3 \times 6 + 5 = 23$ genes.

Figure 3.3 shows the MFs of the four FLCs evolved by the GA. The parameters of the four FLCs are listed in Table 3.4–3.7. Figure 3.4 shows the fitness value verses generation number curves of the four GAs. It indicates that the fitness values have converged. Another observation is that the additional mathematical dimension provided by the FOU enables the FLC_2 to achieve a lower ITAE than the other three type-1 FLCs, though FLC_2 has less parameters than two of the

type-1 FLCs. To further assess the performance of the FLCs, simulation and experimental study was conducted and the results are presented in the following subsection.

(a) MFs of FLC_2 (b) MFs of FLC_{1a}

(c) MFs of FLC_{1b} (d) MFs of NFC
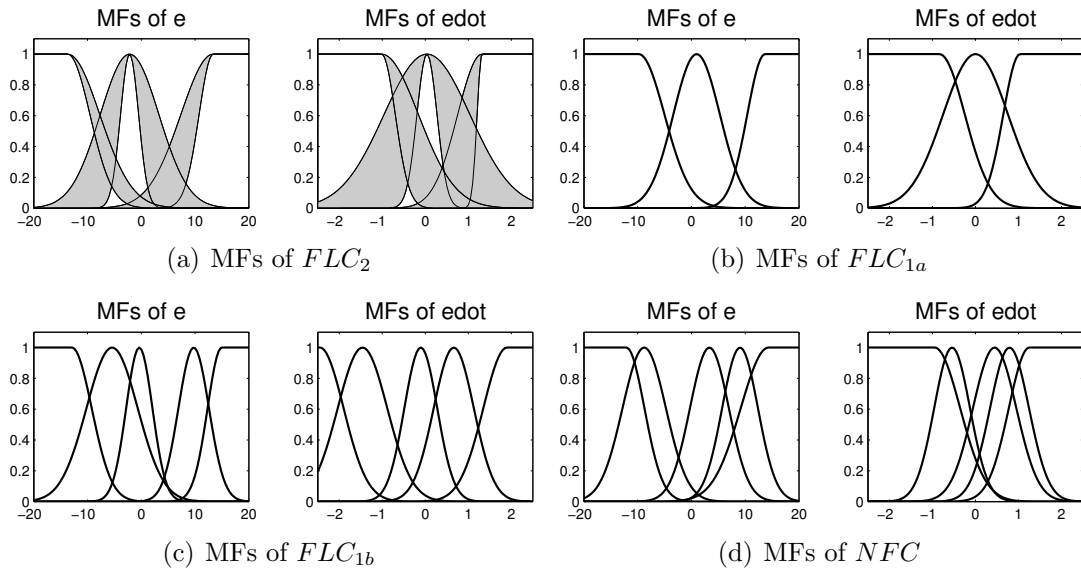
Figure 3.3: MFs of the four FLCs

Table 3.4: MFs of the type-2 FLC, FLC_2
(a) MFs of the inputs

	Input	N	Z	P
e	m	-13.6778	-2.1764	13.3864
	$[\delta_1, \delta_2]$	$[4.1385, 5.9727]$	$[1.6850, 5.4645]$	$[2.6457, 6.0475]$
$\dot{e}$	m	-1.0132	0.0393	1.3172
	$[\delta_1, \delta_2]$	$[0.3172, 0.8553]$	$[0.2342, 1.0000]$	$[0.1130, 0.5656]$

(b) MFs of the output

$\dot{u}_1$	$\dot{u}_2$	$\dot{u}_3$	$\dot{u}_4$	$\dot{u}_5$
-0.8091	-0.3429	0.0796	0.4656	0.7457

3.3.3 Performance Study

Figure 3.5 shows the step responses and the corresponding control signals obtained when the four FLCs were used to control the nominal plant. Performances of FLC_2,
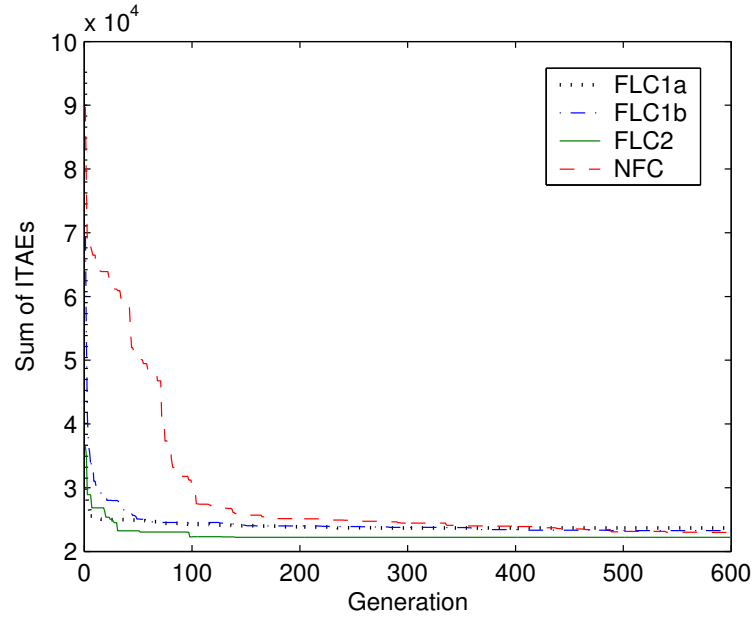
Figure 3.4: Relationship between generation and sum of ITAE

Table 3.5: MFs of the type-1 FLC, FLC_{1a}
(a) MFs of the inputs

	N_e	Z_e	P_e	$N_{\dot{e}}$	$Z_{\dot{e}}$	$P_{\dot{e}}$
m	-9.7890	0.9611	13.6741	-0.8344	0.0022	1.0366
δ	4.7869	4.3414	3.3040	0.5887	0.7562	0.3902

(b) MFs of the output

$\dot{u}_1$	$\dot{u}_2$	$\dot{u}_3$	$\dot{u}_4$	$\dot{u}_5$
-0.3449	-0.1406	0.0668	0.6201	0.8899

Table 3.6: MFs of of the type-1 FLC, FLC_{1b}

(a) MFs of the inputs

Input		NB	NM	Z	PM	PB
e	m	-12.9009	-5.4265	-0.3698	9.7432	14.9622
	δ	3.6845	4.7648	2.4434	2.8409	2.6371
$\dot{e}$	m	-2.4483	-1.4590	-0.1044	0.6618	1.8987
	δ	0.5499	0.5756	0.3823	0.4662	0.5499

(b) Rule Base and Consequents

e \ $\dot{e}$	$NB_{\dot{e}}$	$NM_{\dot{e}}$	$Z_{\dot{e}}$	$PM_{\dot{e}}$	$PB_{\dot{e}}$
NB_e	-0.7999	-0.6734	-0.2558	-0.1375	-0.0096
NM_e	-0.6734	-0.2558	-0.1375	-0.0096	0.2468
Z_e	-0.2558	-0.1375	-0.0096	0.2468	0.5219
PM_e	-0.1375	-0.0096	0.2468	0.5219	0.7295
PB_e	-0.0096	0.2468	0.5219	0.7295	0.8595

Table 3.7: MFs of the neuro-fuzzy controller, NFC

(a) MFs of the inputs

Input		NB	NM	Z	PM	PB
e	m	-12.0948	-8.7795	3.3386	9.0337	14.3214
	δ	3.3558	4.0363	3.6185	3.3313	5.1559
$\dot{e}$	m	-0.9471	-0.5429	0.4458	0.7916	1.2536
	δ	0.5923	0.4165	0.5046	0.4531	0.4781

(b) Rule Base and Consequents

e \ $\dot{e}$	$NB_{\dot{e}}$	$NM_{\dot{e}}$	$Z_{\dot{e}}$	$PM_{\dot{e}}$	$PB_{\dot{e}}$
NB_e	-0.3052	-0.3671	-0.3679	-0.1765	-0.3744
NM_e	-0.0074	0.2593	-0.1646	0.1657	-0.2463
Z_e	-0.0998	-0.0742	-0.0590	0.2755	0.2225
PM_e	-0.2286	0.1267	0.3988	0.1868	0.2677
PB_e	0.6778	0.1248	0.4227	0.1317	0.0201

FLC_{1a} and FLC_{1b} are comparable to NFC, a neurofuzzy controller reported in the literature [81]. The results also indicate that the FLCs evolved by GA are able to provide satisfactory control in spite of the pump non-linearity and the unmodelled transport delay (about 1~2 seconds based on our experiments).

(a) Simulation results   (b) Experiment results
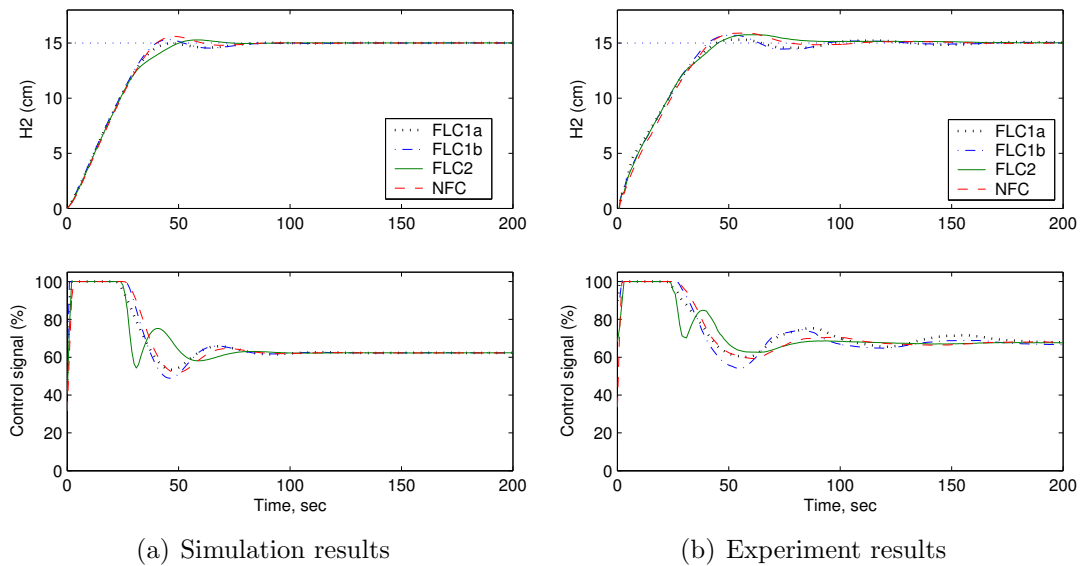
Figure 3.5: Step responses for the nominal plant

To test the ability of the FLCs to handle unmodelled dynamics, unmodelled transport delay was introduced into the feedback loop. First, a transport delay equal to 1 second (one sampling period) was artificially added to the nominal system. The step responses and the control signal are shown in Figure 3.6. When a 2 sampling periods transport delay was added to the system, the corresponding step responses and the control signal are shown in Figure 3.7. Although the simulation results indicated that the four FLCs should have similar performances, large oscillations were obtained when FLC_{1a} and FLC_{1b} were used to control the actual plant. For FLC_2 and NFC, the simulation results coincide with the experimental results more closely.

(a) Simulation results

(b) Experimental results
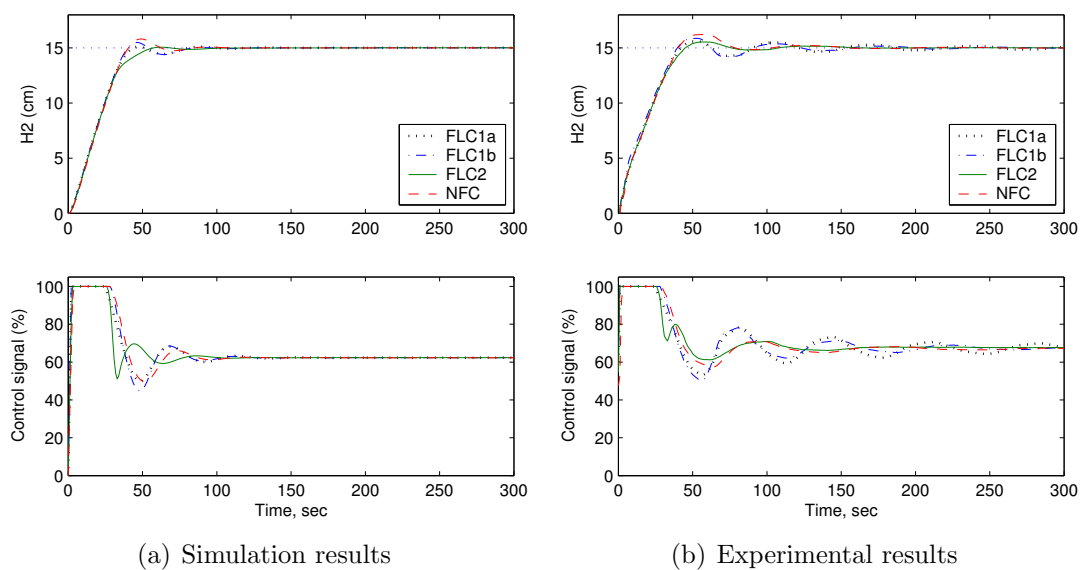
Figure 3.6: Step responses with a 1 sec transport delay

(a) Simulation results

(b) Experimental results
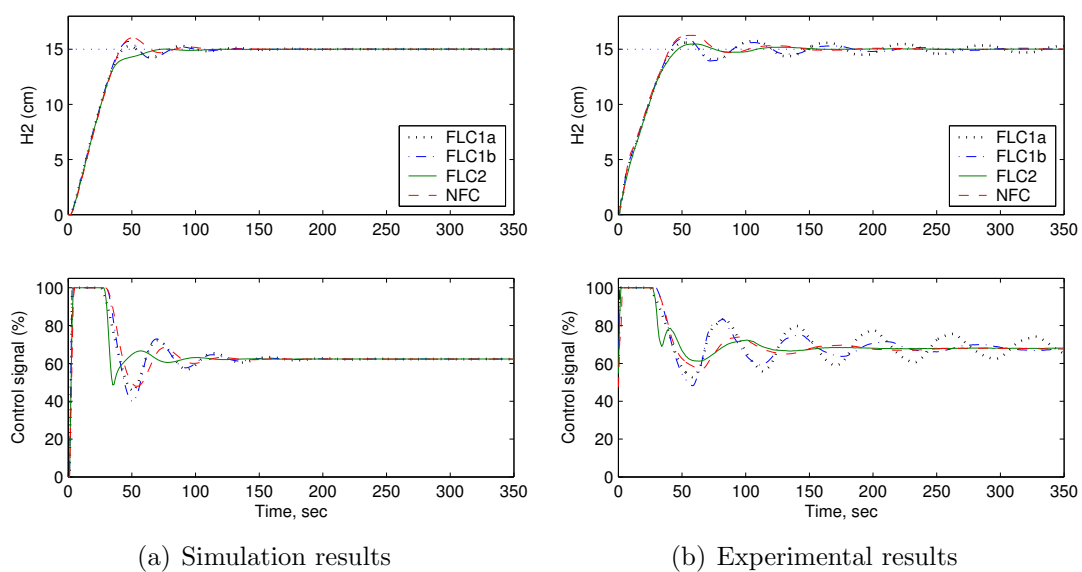
Figure 3.7: Step responses with a 2 sec transport delay

Next, the ability of the FLCs to cope with variations in the system dynamics was investigated by lowering the baffle separating the two tanks. This change modified the discharge coefficient between the two tanks (α_3) and gave rise to a more sluggish system. In addition, the difference in liquid level between the two tanks was larger at steady state. First, the experimental rig was set up such that the discharge coefficient between the two tanks (α_3) was reduced from 10 to 8. Since simulation model indicates that the steady-state water level in tank #1 and tank #2 is 22.4 cm and 15 cm respectively when $\alpha_3 = 8$, the baffle was lowered until the liquid level in the two tanks are at the above-mentioned heights. The step responses and the control signal are shown in Figure 3.8. Figure 3.9 shows the step responses and the control signal when a 1-sec transport delay was added to the modified plant. From the step responses, it may be observed that all the FLCs were able to attenuate the oscillations when there were modeling uncertainties. However, the settling time was much shorter when FLC_2 or NFC was employed. FLC_{1a} gave the poorest control performance. Though the liquid level in the tank eventually reached the desired setpoint, the settling time was so long that it was inconvenient to plot the complete trajectory in the figures.

3.4   Discussions

From the results presented in the previous section, it may be concluded that all the four FLCs provide comparable performances for the nominal plant (Figure 3.5). However, FLC_2 and NFC outperform FLC_{1a} and FLC_{1b} when unmodelled dynamics are introduced (Figure 3.6–3.9). The better performance of FLC_2 arises from the extra degree of freedom provided by the FOU. In order to gain some

(a) Simulation results   (b) Experimental results
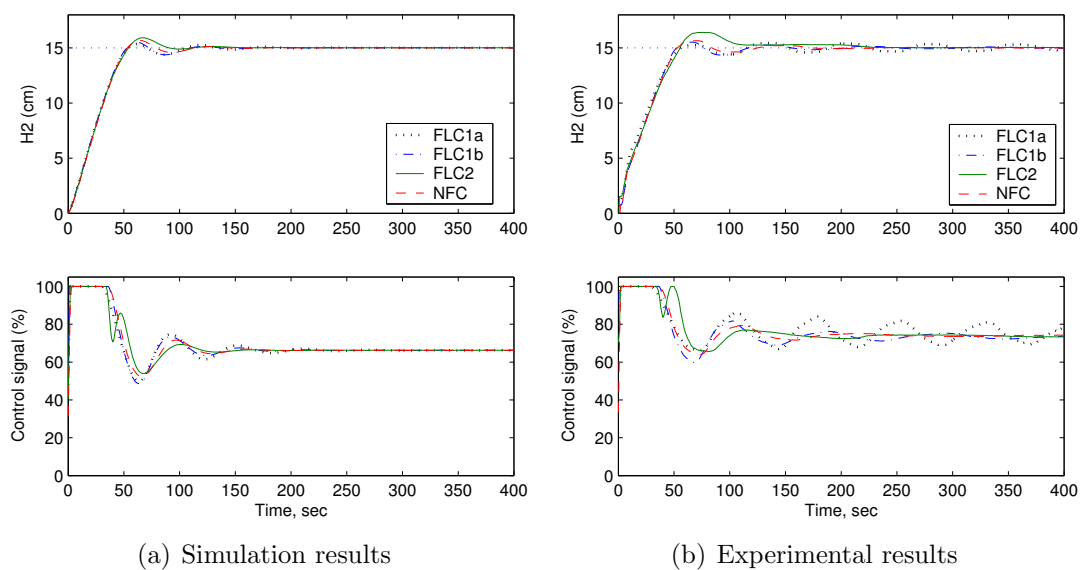
Figure 3.8: Step responses when the baffle was lowered

(a) Simulation results   (b) Experimental results
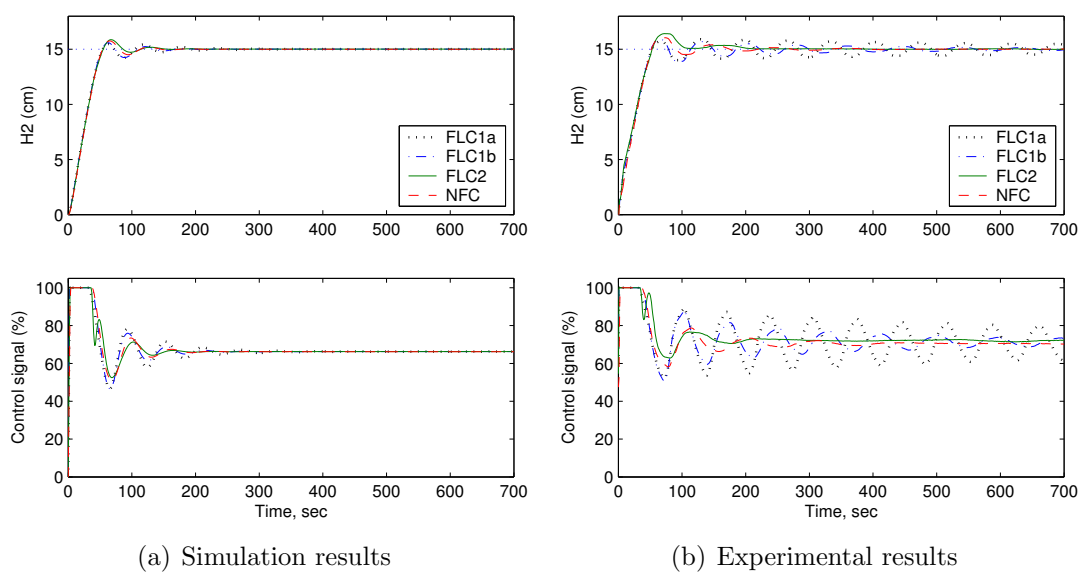
Figure 3.9: Step responses with the lowered baffle and a 1 sec transport delay

insights into why the type-2 FLC is able to achieve better control performances, the control surface of the four FLCs were plotted.
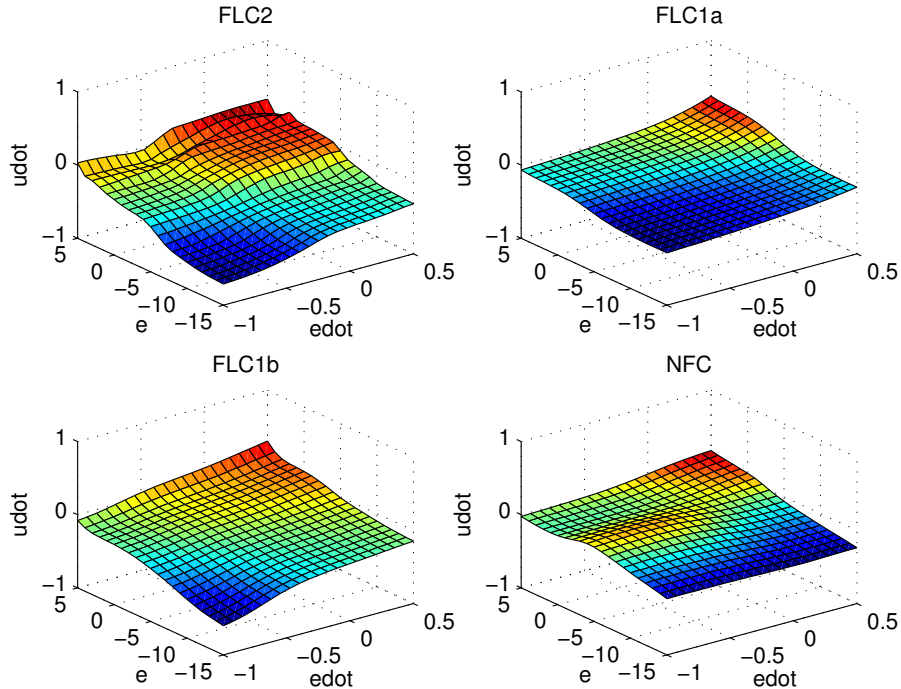
Figure 3.10: Control surfaces of the four FLCs

Figure 3.10 shows that the control surface of the type-2 FLC is more complex. It may be observed that the control surface of the type-2 FLC has a gentler gradient around the equilibrium point ($e = 0$, $\dot{e} = 0$). As a result, the changes in the output control signal are small in this area and small disturbances around the equilibrium point will not result in significant control signal change. This behaviour may help to explain why the type-2 FLC is better able to attenuate oscillations. To illustrate the idea more clearly, a slice of the control surface at $\dot{e} = 0$ is shown in Figure 3.11. It is observed that the outputs of the four FLCs are similar when $e \in [0, 0.5]$. However, when $e < 0$, the outputs of FLC_2 and NFC have much gentler slopes so the absolute values of $\dot{u}$ is much smaller compared to those of FLC_{1a} and FLC_{1b}. The implication is that an overshoot will decay away more gradually, and thus

reducing the amount of oscillations. This conclusion is consistent with the results in Figures 3.5–3.7, where there are much fewer oscillations when FLC_2 or NFC is employed. Unfortunately, the gentler gradient around the equilibrium point also means that more time is taken for an overshoot to die away. Figure 3.12 shows that FLC_2 takes a relatively longer time to recover from an overshoot.
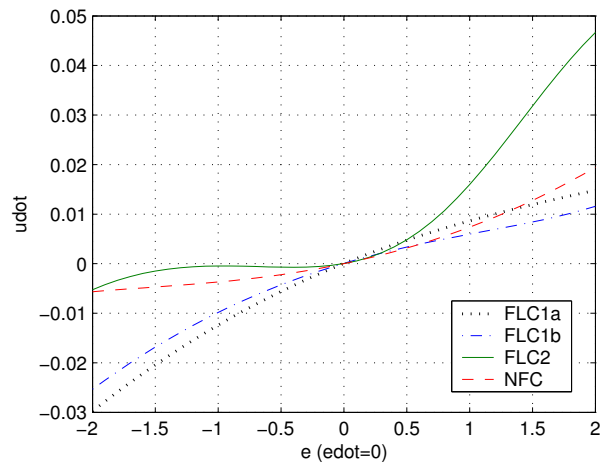
Figure 3.11: A slice of the control surfaces at $\dot{e} = 0$

(a) Simulation results

(b) Experiment results
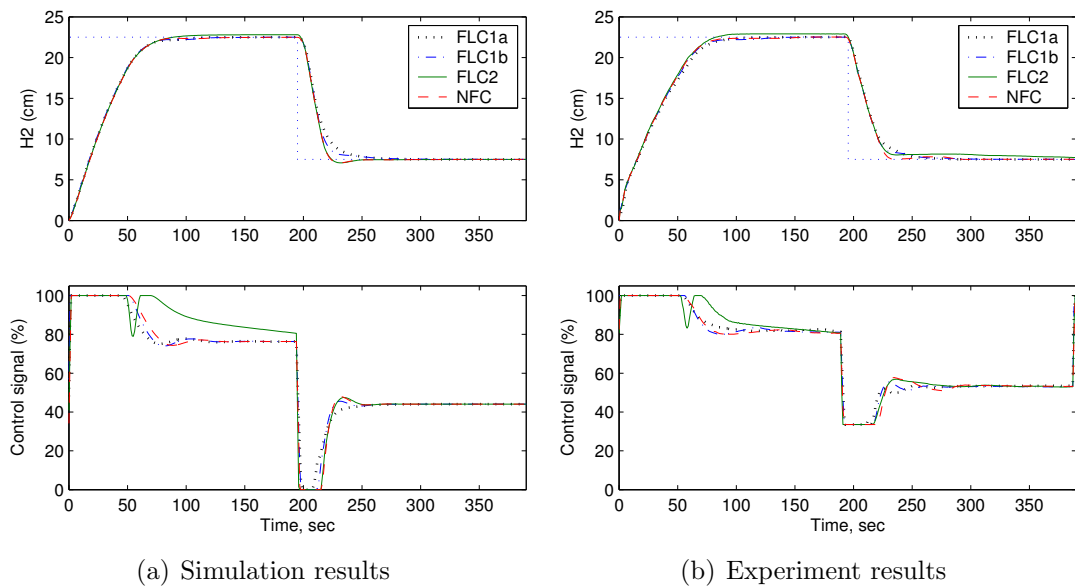
Figure 3.12: Step responses when setpoint is changed from $0 \rightarrow 22.5 \rightarrow 7.5$ cm

A consolidation of the simulation and experimental results obtained during the

comparative study are presented in Figures 3.13(a) and (b). The plots show the ITAEs for different plants in Table 3.3. As the deterioration in performances when the test platform is switched from simulation to the physical plant reflect the abilities of the four FLCs to handle modelling uncertainties, Figure 3.13(c) illustrates the difference in the ITAE values between the experimental and simulation results. The various ITAE values obtained via simulation (sim) and experimentally (exp) are also tabulated in Table 3.8. They are generated by integrating over the length of the responses shown in Figure 3.5–3.9 and Figure 3.12. From the data in Figure 3.13, it may be concluded that NFC provides the best performance, followed closely by FLC_2. Another finding is that FLC_2 generally outperforms FLC_{1b}, even though FLC_{1b} has 6 more parameters (degree of freedom) than FLC_2. However, a type-1 FLC with comparatively larger number of design parameters may be able to outperform a type-2 FLC. For example, NFC outperforms FLC_2 with the help of $45 - 23 = 22$ more parameters. The study suggests that a type-2 FLC can provide better performance with less MFs and a smaller rule base, making it is more appealing than its type-1 counterpart with regards to accuracy and interpretability.

Besides performance, the computational cost required to implement the FLCs is also an important consideration. The GAs used to tune the four FLCs were implemented as a Matlab 6.5 program and executed on an Intel Pentium III 996MHz computer with 256M RAM. The time needed by the four GAs to complete 100 generations of evolution was recorded and shown in Table 3.8. A 10000 time-step simulation (the setpoint is $15 + 10sin(i/50)$, where $i = 1, 2, \ldots, 10000$ is the time instant) using the evolved FLCs was also carried out on the same computer and
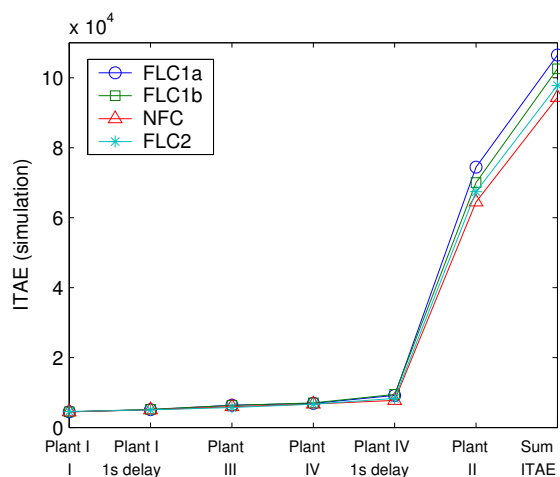
(a) ITAEs of the four FLCs on different plants: simulation results
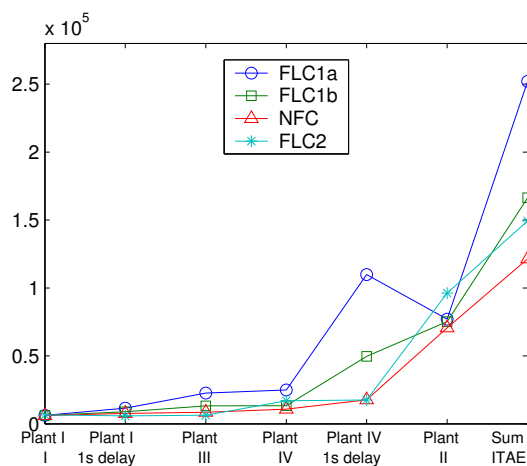
(b) ITAEs of the four FLCs on different plants: experimental results
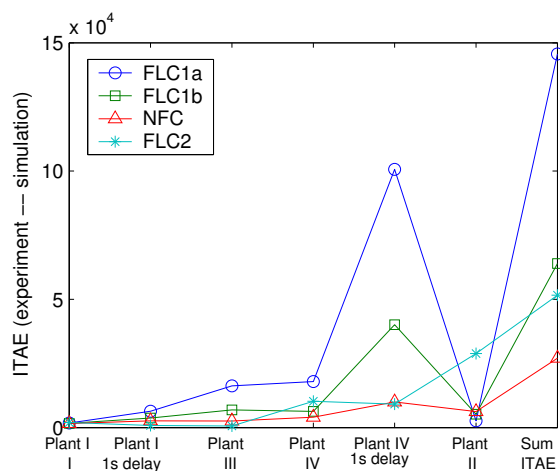
(c) ITAEs of the four FLCs on different plants: experimental results–simulation results

Figure 3.13: Comparisons of the ITAEs of the four FLCs on different plants

the computation time is tabulated in Table 3.8. The data indicate that the computational cost of FLC_2 is much higher than that of the three type-1 FLCs. Though the neurofuzzy controller (NFC) has $45 - 23 = 22$ more parameters than FLC_2, its computation time is only less than $\frac{1}{4}$ of that of FLC_2. The increase in computational burden is mainly due to the type-reducer, the main structural difference between a type-2 FLS and a type-1 FLS. If there are more MFs for each input, and consequently more rules, the difference in computational load may be more obvious [83]. While the need for large computing power is a hinderance to real-time implementation, efforts are being made to reduce the computational requirements of type-2 FLS [14, 83, 84].

3.5 Concluding Remarks

In this Chapter, a GA-based totally independent method is used to design a type-2 FLC for controlling a coupled-tank liquid-level control system. The performance of the type-2 FLC (23 parameters) is compared with that of three type-1 FLCs: a type-1 Mamdani FLC with 17 parameters, a type-1 Mamdani FLC with 29 parameters and a type-1 neuro-fuzzy controller with 45 parameters. The results demonstrate that a type-2 FLC can outperform type-1 FLCs that have more design parameters. In other words, a type-2 FLC with fewer MFs can achieve the similar performance as a type-2 FLC with much more MFs. Thus, the type-2 FLC is more appealing than its type-1 counterpart with regards to accuracy and interpretability. The main advantage of the type-2 FLC appears to be its ability to eliminate persistent oscillations, especially when unmodelled dynamics were introduced. This ability to handle modelling error is particularly useful when FLCs

Table 3.8: A comparison of the four FLCs

Item \ FLC			FLC_{1a}	FLC_{1b}	NFC	FLC_2
Structure	Type		Type-1	Type-1	Type-1	Type-2
	No. Input MFs		3	5	5	3
	No. Output MFs		5	9	25	5
	Total Parameters		17	29	45	23
Performance (ITAE)	Plant I	Sim (10^3)	4.4870	4.5010	4.4906	4.5766
		Exp (10^3)	6.2360	6.1768	6.0817	6.5160
	Plant I 1s delay	Sim (10^3)	5.0914	5.1833	5.0457	5.0475
		Exp (10^3)	11.488	8.9097	7.6360	5.8859
	Plant II	Sim (10^4)	7.4417	7.0015	6.4458	6.7426
		Exp (10^4)	7.7033	7.5202	7.0690	9.6253
	Plant III	Sim (10^3)	6.3906	6.3473	5.9437	5.7221
		Exp (10^3)	22.6450	13.2440	8.5271	6.3521
	Plant IV	Sim (10^3)	6.9179	7.0411	6.7093	6.6710
		Exp (10^3)	24.875	13.356	10.773	16.896
	Plant IV 1s delay	Sim (10^3)	9.1761	9.4582	7.7564	8.3341
		Exp (10^3)	109.820	49.584	17.731	17.511
	Sum of ITAEs	Sim (10^4)	10.6480	10.2550	9.4404	9.7777
		Exp (10^4)	25.2097	16.6470	12.1440	14.9414
Computation Time	GA tuning (sec)		950	1050	1300	5860
	Simulation (sec)		1.4070	1.5780	1.8120	8.1720

are tuned offline using GA and a model as the impact of unmodelled dynamics is reduced.

Chapter 4

Simplified Type-2 FLCs for Real-time Control

The results in the previous Chapter show that type-2 FLCs may be better able to eliminate persistent oscillations than their type-1 counterparts. The most likely explanation for this behavior is a type-2 FLC has a smoother control surface than that of a type-1 FLC, especially around the origin. Hence, small disturbances around steady state will not result in significant control signal changes so there are less oscillations. As the ability of type-2 FLCs to handle modeling uncertainties is superior, a type-2 FLC evolved using GA and the plant model is more likely to perform well in practice.

Despite the advantages offered by type-2 FLCs, one problem that may hinder the use of type-2 FLCs for real-time control is their high computational cost. Unlike a type-1 FLC, a type-reducer is needed to convert the type-2 fuzzy output sets into type-1 sets so that they can be processed by the defuzzifier to give a crisp output. Type-reduction is very computationally intensive, especially when there are many MFs and the rule base is large.

To reduce the computational burden while preserving the advantages of type-2 FLCs, two approaches may be considered : 1) faster type-reduction methods, such as the uncertainty bound concept in [14] and new type-reducers proposed in [84]; and 2) a simpler architecture. The second approach is studied in this Chapter. A procedure to obtain a type-2 FLC that is robust enough to cope

well with the uncertainties while having minimum computational cost is proposed. This Chapter also presents experimental study that establishes the feasibility of the proposed simplified type-2 structure.

The rest of this Chapter is organized as follows: Section 4.1 presents the simplified type-2 FLC as well as a computational costs comparison. Two type-1 FLCs and two type-2 FLCs with degrees of freedom are designed in Section 4.2 and their abilities to handle modeling uncertainties are compared using a coupled-tank liquid-level control system. Section 4.3 discusses the performances of the proposed architecture. Finally, conclusions are drawn in Section 4.4.

4.1 Simplified Type-2 FLCs

The simplified interval singleton type-2 FLC uses type-2 fuzzy sets only for the fuzzy partition governing behavior around the setpoint (steady-state). All other fuzzy sets are type-1. Figure 4.1(c)–(d) show the MFs of typical simplified type-2 FLCs. The structure is motivated by the observation that the main advantage of type-2 FLC is its ability to provide more damping as the output approaches the set-point. It is conjectured that the degradation in the ability of a type-2 FLC to handle modeling uncertainties will be insignificant if type-1 fuzzy sets are used to describe the fuzzy rules that govern the transient response. Such a simplified structure and a FLC where all the fuzzy sets used to partition the input domains are type-2 may have similar control surfaces around the origin. As the control surfaces are comparable, it is likely that these two kinds of FLCs may have similar performances. As the simplified architecture utilizes fewer type-2 sets, the computational cost can be reduced.

(a) MFs of e, which are all type-1

(b) MFs of $\dot{e}$, which are all type-1

(c) MFs of e. The middle one (the mth MF) is type-2 while all the others are type-1

(d) MFs of $\dot{e}$. The middle one (the mth MF) is type-2 while all the others are type-1
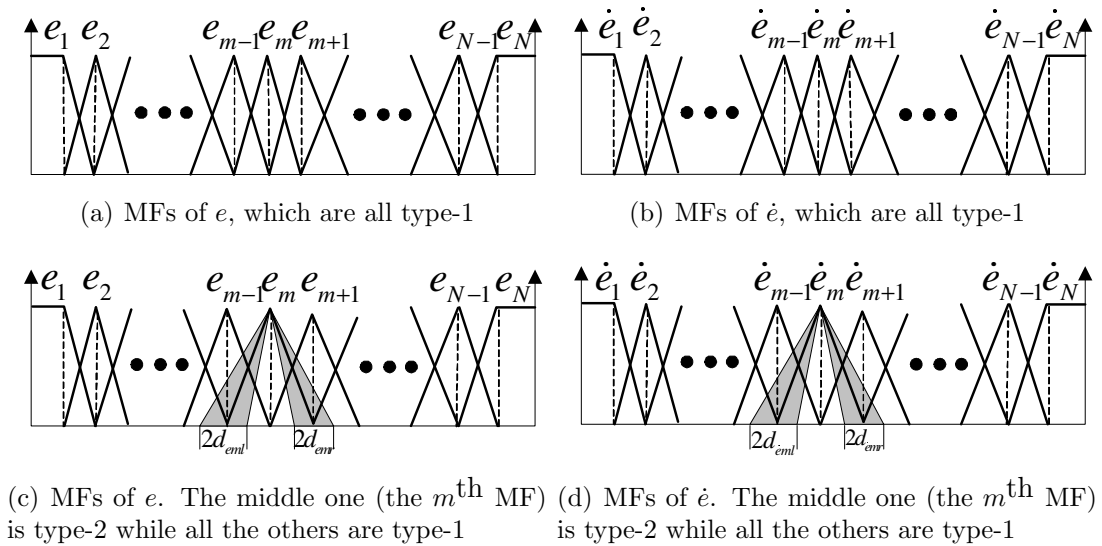
Figure 4.1: Example MFs of the FLCs

A simplified type-2 FLC may be designed by gradually replacing type-1 fuzzy sets by their type-2 counterparts until the resulting FLC meets the robustness requirements, starting with the fuzzy sets that characterize the region around steady-state. Since the computational cost will increase significantly when the number of type-2 MFs increases, as few type-2 MFs as possible introduced. For a PI-like FLC, the response near steady-state is determined mainly by the area around the origin, which is governed by the middle MFs of each input. Hence, the procedure for designing a simplified type-2 FLC is as follows :

Step 1 : *The type-1 FLC is designed through simulation on a nominal model.*

Step 2 : *Change the most important input MF to type-2. For the two inputs of a PI-like FLC, $\dot{e}$ is more susceptible to noises. The fuzzy set corresponding to zero $\dot{e}$ is changed to type-2, as illustrated in Figure 4.1(d).*

Step 3 : *If the type-2 FLC designed in Step 2 cannot cope well with the actual plant, the fuzzy set associated with zero e is changed to type-2, as illustrated*

in Figure 4.1(c).

Step 4 : *If the resulting type-2 FLC is still not robust enough, more type-2 MFs may be introduced starting from the middle of each input domain and gradually moving towards the limits of the domain. Another criteria is to use type-2 fuzzy sets to characterize the operating region that needs a smoother control surface.*

A FLC designed by the proposed procedure has two parts — a type-1 part and a type-2 part. Different portions will be activated when the state of the plant is in different operating region. During the transient stage, the FLC behaves like a type-1 FLC since no type-2 MFs are fired. When the output approaches the setpoint, type-2 MFs will be fired and the plant is controlled by a type-2 fuzzy logic system. Smoother control signals will be generated, which help to eliminate oscillations. Next, an analysis is performed in order to establish the computational savings provided by the simplified type-2 FLC.

4.1.1 Computational Cost Comparison

The reduction in computational requirement comes about mainly because the simplified structure enables type-reduction algorithm to be simplified. Consider a simplified type-2 FLC where M out of the N rules contain only type-1 MF in the antecedent. The remaining $N - M$ rules have at least one type-2 fuzzy set in the antecedent. There will, therefore, be M crisp firing strengths (f^i, $i = 1, 2, \ldots, M$) and $N - M$ interval firing strengths ($\tilde{f}^j$, $j = M + 1, M + 2, \ldots, N$). In this case,

Equation (2.4) reduces to :

$$Y_{cos}(\mathbf{x}) = \int_{y^1 \in Y^i} \cdots \int_{y^N \in Y^i} \int_{f^1 \in F^i(\mathbf{x})} \cdots \int_{f^N \in F^i(\mathbf{x})} 1 \left/ \frac{\sum_{i=1}^{N} f^i y^i}{\sum_{i=1}^{N} f^i} \right. = [y_l, \ y_r] \quad (4.1)$$

$$
\begin{aligned}
Y_{cos} &= \frac{\sum_{i=1}^{M} f^i y^i + \sum_{j=M+1}^{N} \tilde{f}^j y^j}{\sum_{i=1}^{M} f^i + \sum_{j=M+1}^{N} \tilde{f}^j} \\
&= \frac{\beta + \sum_{j=M+1}^{N} \tilde{f}^j y^j}{\alpha + \sum_{j=M+1}^{N} \tilde{f}^j} \\
&= \frac{\beta}{\alpha} + \frac{\sum_{j=M+1}^{N} \tilde{f}^j y^j - \frac{\beta}{\alpha} \sum_{j=M+1}^{N} \tilde{f}^j}{\alpha + \sum_{j=M+1}^{N} \tilde{f}^j} \\
&= \frac{\beta}{\alpha} + \frac{\sum_{j=M+1}^{N} \tilde{f}^j (y^j - \frac{\beta}{\alpha})}{\alpha + \sum_{j=M+1}^{N} \tilde{f}^j} \quad\quad (4.2)
\end{aligned}
$$

where $\alpha = \sum_{i=1}^{M} f^i$, $\beta = \sum_{i=1}^{M} f^i y^i$.

Defining y'^j and $\tilde{f}^{N+1}$ as :

$$
y'^j = \begin{cases} y^j - \frac{\beta}{\alpha}, & j = M+1, M+2, \ldots, N \\ \\ 0, & j = N+1 \end{cases}
$$

$$\tilde{f}^{N+1} = \alpha$$

Equation (4.2) can be further simplified to :

$$Y_{cos} = \frac{\beta}{\alpha} + \frac{\sum_{j=M+1}^{N+1} y'^j \tilde{f}^j}{\sum_{j=M+1}^{N+1} \tilde{f}^j} \quad\quad (4.3)$$

The second term in the right hand side of Equation (4.3), $\frac{\sum_{j=M+1}^{N+1} y'^j \tilde{f}^j}{\sum_{j=M+1}^{N+1} \tilde{f}^j}$ can be calculated by the Karnik-Mendel iterative method. Once α and β are calculated, the Karnik-Mendel type-reducer will converge in at most $(N + 1 - M)$ iterations because the number of interval firing strengths has been reduced from N to $(N + 1 - M)$.

To further investigate the savings in computational cost provided by the simplified type-2 FLCs, the computing requirements of one type-1 FLC (FLC_1) and three different type-2 FLCs ($FLC_{2s}, FLC_{2m}, FLC_{2f}$) are compared qualitatively. The FLCs have two input signals (e and $\dot{e}$). Each input domain is characterized by n fuzzy sets that are equally spaced and the consequent part is n^2 distinct fuzzy sets. FLC_{2s} is a type-2 FLC where only the middle MF of $\dot{e}$ is type-2 (corresponds to **Step 2** of the design procedure). Its input MFs are shown in Figure 4.1(a) and Figure 4.1(d). The FOU of the type-2 set is determined by two length $d_{e_{ml}}$ and $d_{e_{mr}}$. FLC_{2m} is one where the middle MF of both e and $\dot{e}$ are type-2. This FLC is the result of **Step 3** of the design procedure and its input MFs are shown in Figure 4.1(c) and Figure 4.1(d). All the input MFs of FLC_{2f} are type-2. The FOU of each type-2 MF is defined by $d = \frac{1}{n-1}$. The performances of the three type-2 FLCs are compared with a type-1 FLC, whose MFs are shown in Figure 4.1(a) and Figure 4.1(b).

The comparative study was performed by first dividing the domain of e, $[-1, 1]$, into 101 equally distributed points e_i, where $e_i = 2(i-1)/100 - 1$ ($i = 1, 2, \ldots, 101$). 101 $\dot{e}_i$ are generated in the same way. Thus, all possible combinations of e_i and $\dot{e}_i$ yielded 10201 input pairs. Computational cost is evaluated by comparing the time needed to find outputs for these 10201 inputs. All the experiments are done by Matlab on a 996 MHz computer with 256 MB of RAM and Windows XP. The Karnik-Mendel iterative type-reduction method used is standard routine downloaded from the web [85]. Table 4.1 shows the results for different values of n. The data indicate that the computations for the proposed structure is completed in less than half the time required for a full type-2 FLC. Computational savings is also

much larger when n is small. Having shown that the computing requirements of the simplified type-2 FLC is less, the control performance of the proposed structure is examined in the following section.

Table 4.1: Computational cost of the four FLCs

n \ FLC	FLC_1	FLC_{2s}	FLC_{2m}	FLC_{2f}
3	1.2 secs	2.0 secs	6.7 secs	10.4 secs
5	1.6 secs	2.5 secs	5.1 secs	10.3 secs
7	2.3 secs	3.7 secs	5.0 secs	12.0 secs
9	3.3 secs	5.6 secs	6.6 secs	15.0 secs
11	4.6 secs	8.6 secs	9.5 secs	19.6 secs

4.2   Liquid Level Control Experiments

In this section, the GA-based strategy that was employed to tune the parameters of FLCs are described. Four FLCs (FLC_{13}, FLC_{15}, FLC_{2s} and FLC_{2f}) are tested on the coupled-tank system introduced in the previous Chapter.

4.2.1   Structure of the FLCs

To provide a common basis for comparison, FLC_{13}, FLC_{2s} and FLC_{2f} have essentially the same architecture. The only difference is that the input domains of FLC_{13} (e and $\dot{e}$) are partitioned by type-1 sets, while that of the type-2 FLCs are partitioned by at least one type-2 set. Each input domain is partitioned by three fuzzy MFs that are labeled as **N**, **Z** and **P**. The output space ($\dot{u}$) has five MFs labeled as **NB**, **NS**, **Z**, **PS** and **PB**. As illustrated in Figure 2.1, a type-2 fuzzy set can be obtained by blurring the MF of a baseline type-1 set. For a triangular type-1 MF, there are at least two ways of blurring to obtain a type-2 MF. The first is to keep the apex fixed while blurring the width of the triangle, as shown

in Figure 2.1(a). The other way is to keep the width of the triangle fixed while blurring the apex, as shown in Figure 2.1(b). The first approach is employed here. Table 4.2 shows the fuzzy rule base used by the four FLCs. It is commonly used to construct FLCs. The various fuzzy set operations adopted in this Chapter are the sum-product inference engine, center-of-sets type-reducer and height defuzzifier.

Table 4.2: Rule base of FLC_{13}, FLC_{2s} and FLC_{2f}

e \ $\dot{e}$	$N_{\dot{e}}$	$Z_{\dot{e}}$	$P_{\dot{e}}$
N_e	NB	NS	Z
Z_e	NS	Z	PS
P_e	Z	PS	PB

Since each type-2 set provides an extra mathematical dimension, the type-2 FLCs have more degrees of freedom than FLC_{13}. To further study whether a type-1 FLC with a similar number of design parameters will have similar performance as a type-2 FLC, another type-1 FLC, FLC_{15}, is introduced. It has five MFs in each input domain. The rule base is shown in Table 4.3.

Table 4.3: Rule base of FLC_{15}

e \ $\dot{e}$	$\dot{e}_1$	$\dot{e}_2$	$\dot{e}_3$	$\dot{e}_4$	$\dot{e}_5$
e_1	$\dot{u}_1$	$\dot{u}_2$	$\dot{u}_3$	$\dot{u}_4$	$\dot{u}_5$
e_2	$\dot{u}_2$	$\dot{u}_3$	$\dot{u}_4$	$\dot{u}_5$	$\dot{u}_6$
e_3	$\dot{u}_3$	$\dot{u}_4$	$\dot{u}_5$	$\dot{u}_6$	$\dot{u}_7$
e_4	$\dot{u}_4$	$\dot{u}_5$	$\dot{u}_6$	$\dot{u}_7$	$\dot{u}_8$
e_5	$\dot{u}_5$	$\dot{u}_6$	$\dot{u}_7$	$\dot{u}_8$	$\dot{u}_9$

4.2.2 GA Coding Scheme and Parameters

In this section GAs are used to tune type-2 FLCs. First, the chromosome coding scheme is described. Since the input domain of FLC_{13} is partitioned by three MFs, three points are needed to determine the MFs of each input. The three points for the e domain are N_e, Z_e and P_e, as illustrated in Figure 4.2. Similarly, the three

points that define the three sets for the $\dot{e}$ domain are $N_{\dot{e}}$, $Z_{\dot{e}}$ and $P_{\dot{e}}$. Another five points are needed to determine the MFs of the output domain, $\dot{u}$. Consequently, there is a total of 11 parameters which need to be optimized by the GA.

Figure 4.3 shows the chromosome used by the GA, where the first 11 genes are parameters of FLC_{13}. The next two genes in the chromosome determine the FOU of the only type-2 set used to partition the $\dot{e}$ domain of FLC_{2s}. They define the amount by which the type-1 set is shifted ($d_{\dot{e}2l}$ and $d_{\dot{e}2r}$) to generate the FOU of the type-2 fuzzy set. In the case of FLC_{2f}, the input domains are partitioned by 6 type-2 sets so the chromosome has 19 genes, as shown in Figure 4.3. Finally for FLC_{15}, 5 parameters are needed to determine the MFs for each input and 9 parameters for the consequences. Thus each chromosome consists of $5 \times 2 + 9 = 19$ genes, the same as that of FLC_{2f}.
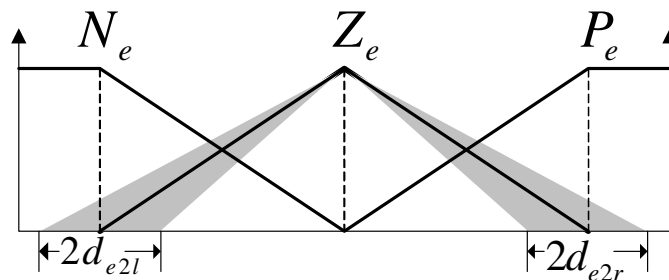
Figure 4.2: Example MFs of e

1	2	3	4	5	6	7	8	9	10	11	12	13	14	15	16	17	18
Ne	Ze	Pe	$N\dot{e}$	$Z\dot{e}$	$P\dot{e}$	NB	NS	Z	PS	PB	$d_{\dot{e}2l}$	$d_{\dot{e}2r}$	d_{e2l}	$d_{\dot{e}2r}$	$d_{\dot{e}1r}$	$d_{\dot{e}3l}$	d_{e1r}
Sub-chromosome of e			Sub-chromosome of $\dot{e}$			Sub-chromosome of $\dot{u}$											

Figure 4.3: GA coding scheme of the FLCs

The fitness of each chromosome in the GA population is assessed by subjecting the simulation model of the liquid level process described in the previous Chapter to step inputs. The GA parameters and fitness function are the same as those in

Chapter 3. The MFs of FLC_{13}, FLC_{15}, FLC_{2s} and FLC_{2f} evolved by GA are shown in Figure 4.4 respectively from the top to the bottom. The parameters are listed in Table 4.4.
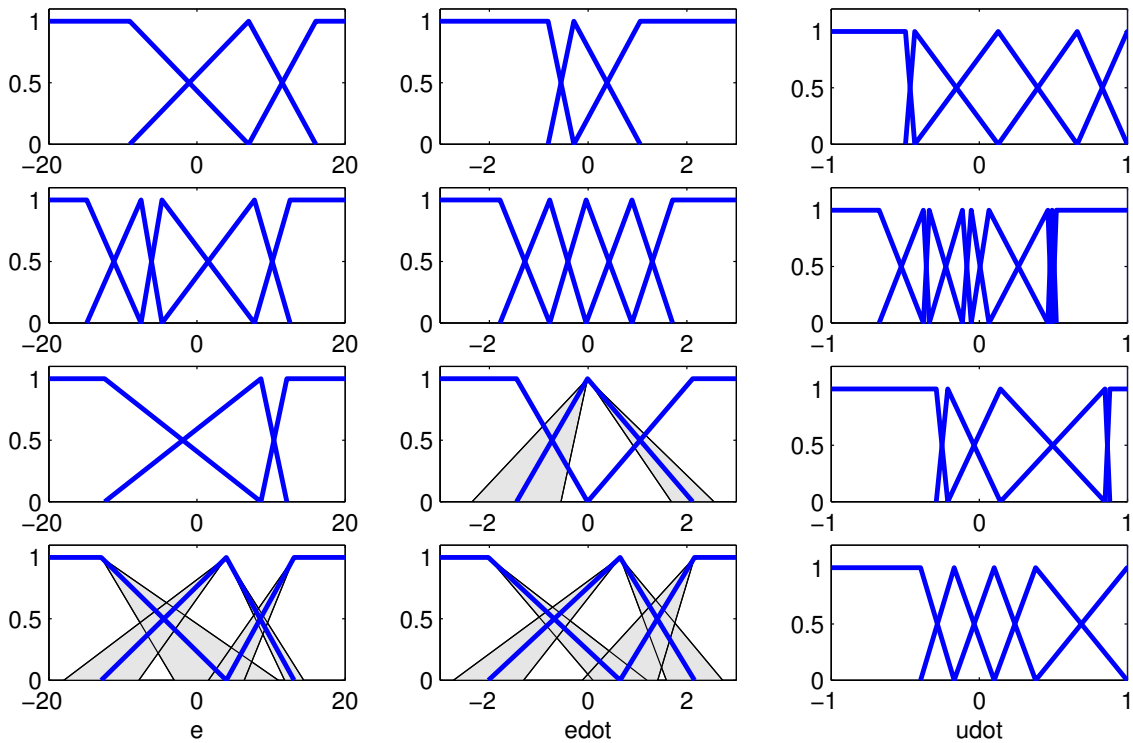
Figure 4.4: MFs of the four FLCs

4.2.3 Experimental Results

The results from the simulation and experimental study that was conducted to assess the performance of the type-1 and type-2 FLCs evolved by GA are presented here. The experiment configurations were the same as those in Chapter 3. The responses are shown in Figures 4.5-4.8. Generally, all the type-2 FLCs outperform their type-1 counterpart. It is also observed that the performances of the three type-2 FLCs are similar, though they have different number of type-2 MFs. The results suggest that some type-2 MFs are not necessary and the computational

Table 4.4: MFs of FLC_{13}, FLC_{2s} and FLC_{2f}

(a) MFs of e

	N_e	Z_e	P_e
FLC_1	-9.0611	6.9846	16.0539
FLC_{2s}	-12.4578	8.6232	12.1405
FLC_{2f}	-12.9137	3.9722	13.1283
	$d_{e_{1r}} = 7.0388$	$d_{e_{2l}} = 5.0656, d_{e_{2r}} = 1.2868$	$d_{e_{3l}} = 2.4127$

(b) MFs of $\dot{e}$

	$N_{\dot{e}}$	$Z_{\dot{e}}$	$P_{\dot{e}}$
FLC_1	-0.8093	-0.2884	1.0538
FLC_{2s}	-1.4505	-0.0119	2.1192
		$d_{\dot{e}_{2l}} = 0.9002, d_{\dot{e}_{2r}} = 0.4327$	
FLC_{2f}	-2.0186	0.6459	2.1534
	$d_{\dot{e}_{1r}} = 0.5479$	$d_{\dot{e}_{2l}} = 0.7091, d_{\dot{e}_{2r}} = 0.5697$	$d_{\dot{e}_{3l}} = 0.7644$

(c) MFs of $\dot{u}$

	NB	**NS**	**Z**	**PS**	**PB**
FLC_1	-0.4985	-0.4362	0.1282	0.6613	0.9998
FLC_{2s}	-0.2906	-0.2130	0.1422	0.8490	0.8817
FLC_{2f}	-0.3967	-0.1702	0.1002	0.3802	0.9978
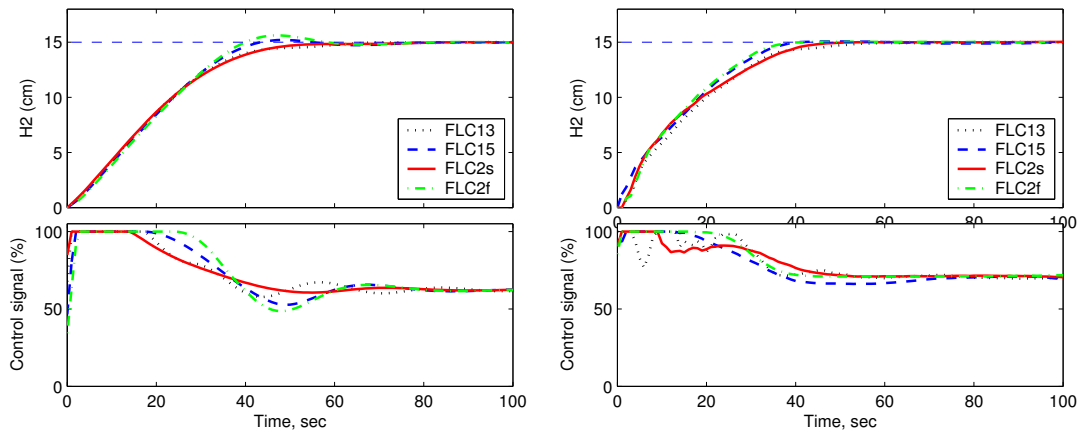
(a) Simulation results   (b) Experiment results

Figure 4.5: Step responses when the setpoint was 15 cm

Table 4.5: MFs of FLC_{15}

(a) MFs of e

e_1	e_2	e_3	e_4	e_5
-14.8778	-7.5460	-4.7217	7.7783	12.5710

(b) MFs of $\dot{e}$

$\dot{e}_1$	$\dot{e}_2$	$\dot{e}_3$	$\dot{e}_4$	$\dot{e}_5$
-1.7824	-0.7799	-0.0387	0.8896	1.7115

(c) MFs of $\dot{u}$

$\dot{u}_1$	$\dot{u}_2$	$\dot{u}_3$	$\dot{u}_4$	$\dot{u}_5$	$\dot{u}_6$	$\dot{u}_7$	$\dot{u}_8$	$\dot{u}_9$
-0.6755	-0.3771	-0.3381	-0.1142	-0.0543	0.0645	0.4632	0.4921	0.5194

cost can be reduced without sacrificing robustness by using type-1 MFs in place of some type-2 MFs.

(a) Simulation results   (b) Experiment results
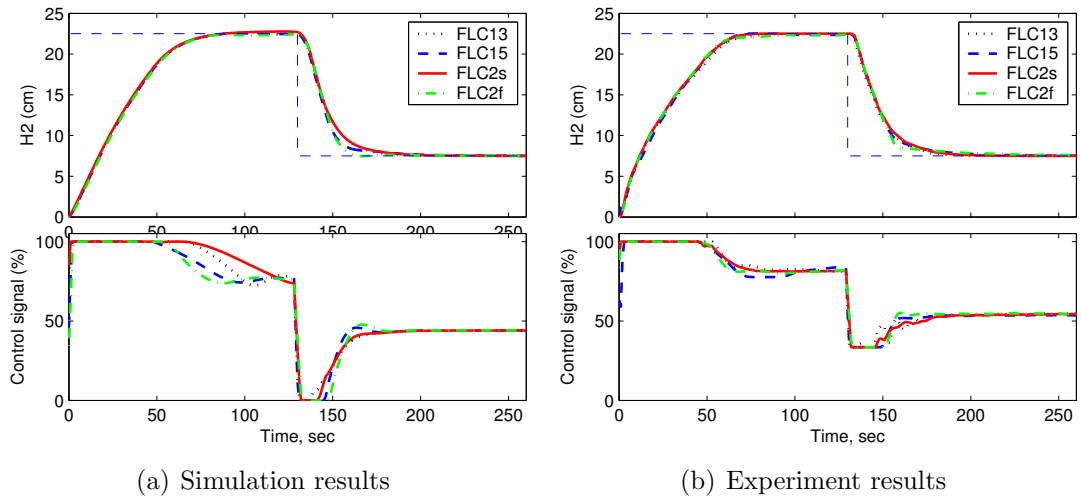
Figure 4.6: Step responses when the setpoint was changed

(a) Simulation results   (b) Experiment results
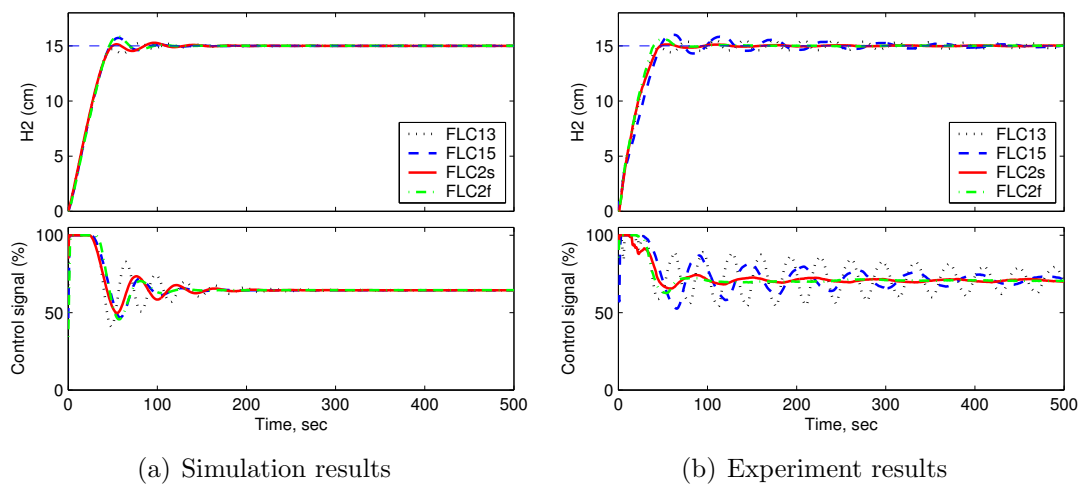
Figure 4.7: Step responses when the baffle was lowered

(a) Simulation results   (b) Experiment results
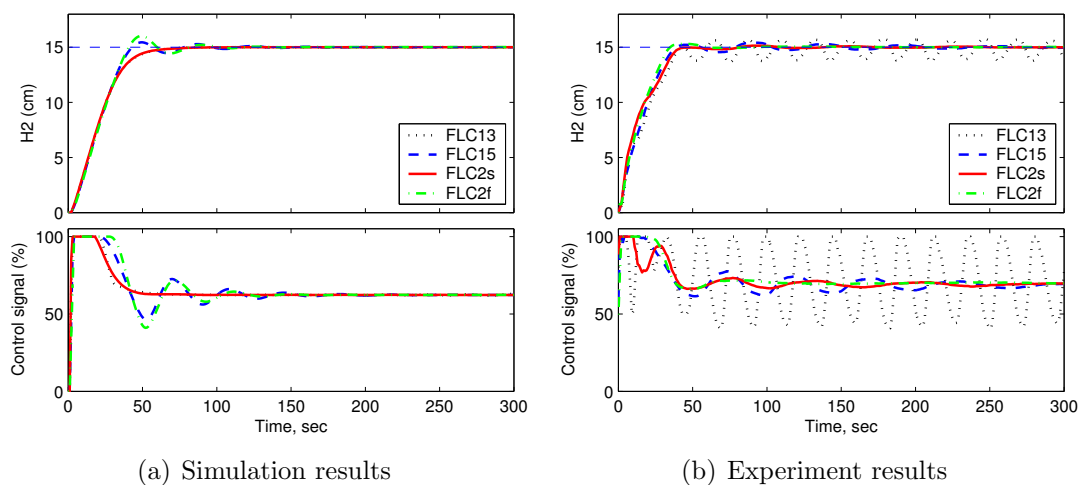
Figure 4.8: Step responses when there was a 2 sec transport delay

4.3 Discussions

From Figures 4.5-4.8, it may be concluded that the simulation results of the four FLCs are similar. However, the experimental results obtained using the type-2 FLCs generally coincide more than that of the type-1 FLCs. To provide quantitative measure of the performances of the four FLCs, the ITAEs in Figures 4.5-4.8 are calculated and plotted in Figure 4.9. I, II, III and IV in horizontal axis stands for Plant I, Plant II, Plant III and Plant IV in Table 3.3, respectively. Sum means the sum of the ITAEs on the four plants. Note the ITAEs of FLC_{13} on the four plants are considered as 100 per cent. The ITAEs of the other three FLCs are calculated accordingly. Thus a smaller number in Figure 4.9 means a better performance. It may be observed that the performances of the two type-2 FLCs are much better than these of type-1 FLCs in the experiments. Especially, FLC_{2s} outperforms FLC_{15} even though FLC_{15} has 6 more design parameters. In fact, five type-1 FLCs were optimized by GA and tested on the practical plant. Most of them performed poorly. The responses either had long settling time or exhibited persistent oscillations. FLC_{13} and FLC_{15} presented in the previous section are the best ones chosen from these type-1 FLCs. Several type-2 FLCs from different runs were also tested on the actual plant. The experimental results did not differ significantly from the simulation results. The trait is indicative of the superior ability of type-2 FLCs to tolerate more modeling uncertainties. When a simulation model is used to evaluate the GA candidate solutions, the type-2 FLCs will have a higher probability of performing well on the actual plant.

Figure 4.10 shows the control surfaces of the four FLCs. The control surfaces of the two type-2 FLCs are smoother than that of FLC_{13} around the origin ($e =$

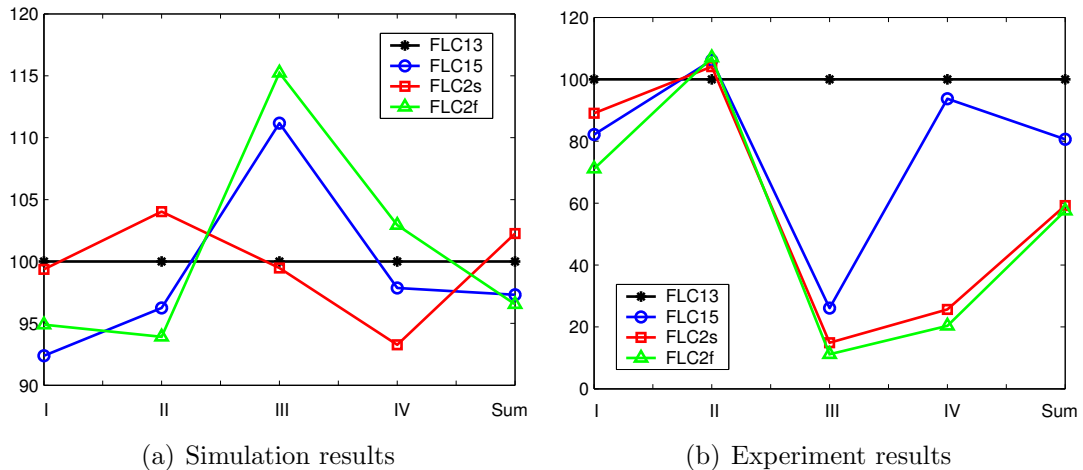(a) Simulation results   (b) Experiment results

Figure 4.9: Comparison of the four FLCs on the four plants

0, $\dot{e} = 0$). The smoother control surface, especially around the origin, is the reason why the type-2 FLCs are more robust (refer to Section 4.3). Note that the control surface of FLC_{2s} is similar to that of FLC_{2f}, even though FLC_{2f} has more type-2 MFs. The control surfaces provide further evidence that there will not be significant performance deterioration when the proposed simplified type-2 FLC is used in place of a traditional type-2 FLC where all the input sets are type-2 MFs.

With the simplified architecture, the computational cost of resulting simplified type-2 FLCs is much lower than a traditional type-2 FLC. The time taken by the GA to evolve the four FLCs is shown in Table 4.6. The data was obtained using a 996 MHz computer with 256 MB of RAM. A 10000-step simulation (the setpoint is $15 + 10sin(i/50)$, where $i = 1, 2, \ldots, 10000$ is the time instant) using the evolved FLCs was also run on the same computer and the computation time is shown in Table 4.6. The results indicate that the computational cost of FLC_{2s} is much lower when compared with that of FLC_{2f}. The experimental results presented in this paper suggest that the simplified type-2 structure is suitable for real-time implementation. It enables computational cost to be reduced without a degradation
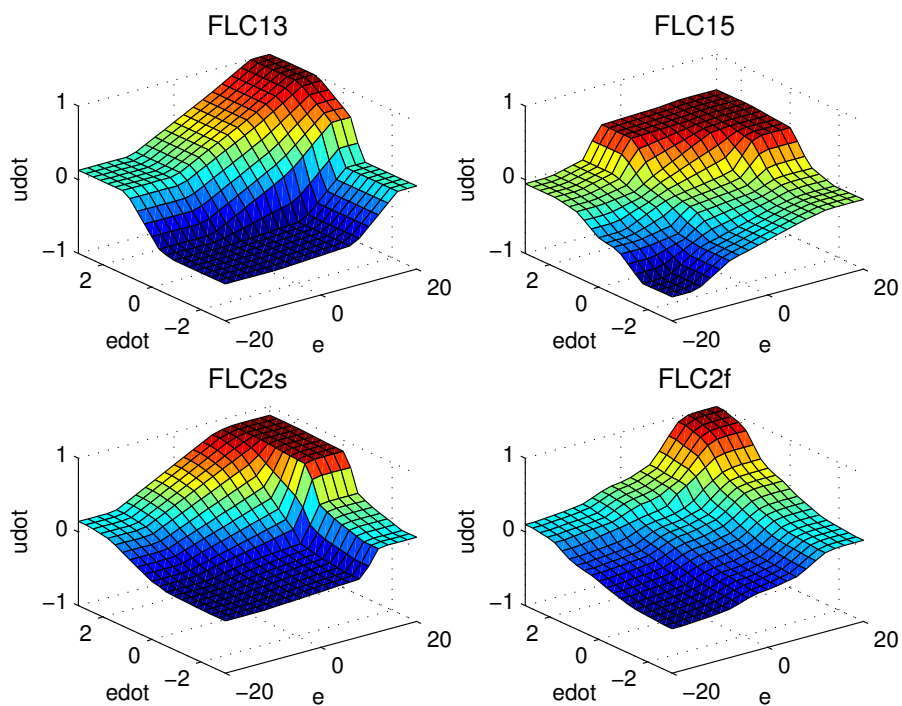
(a) Complete control surface
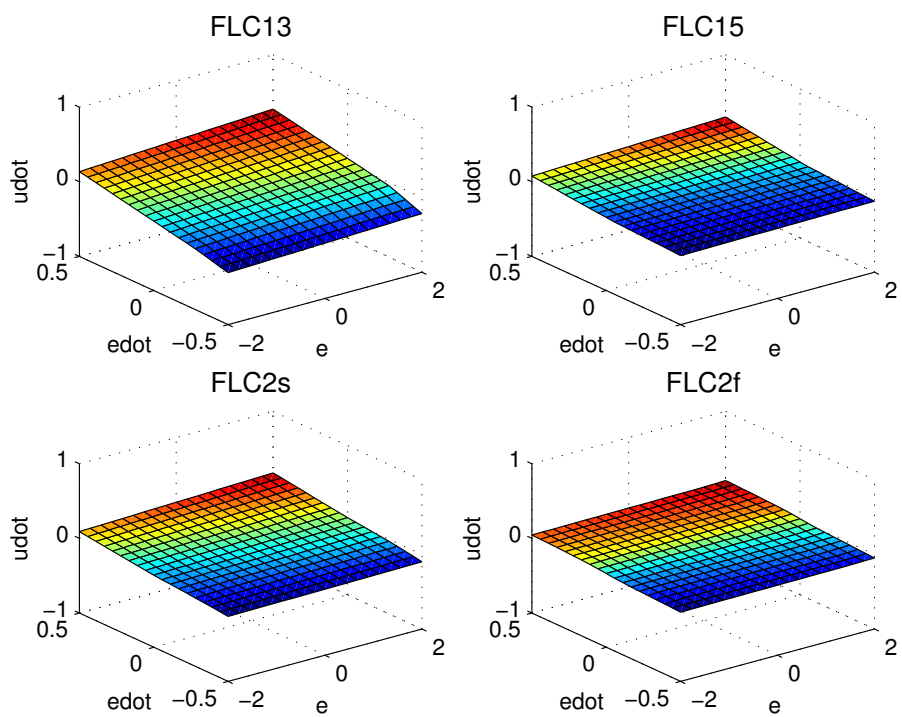
(b) Control surface near the origin

Figure 4.10: Control surface of the four FLCs

in the control performance and the ability to handle modeling uncertainties.

Table 4.6: Comparison of computational cost

Item \ FLC	FLC_{13}	FLC_{15}	FLC_{2s}	FLC_{2f}
GA tuning (sec)	500	550	1200	4500
Simulation (sec)	1.28	1.40	3.19	11.70

4.4   Concluding Remarks

In this Chapter, a simplified type-2 FLC that is more suitable for real-time control is proposed. A type-2 FLCs with simplified structure are designed for a coupled-tank liquid level control process. It performance is compared with two type-1 FLCs and a traditional type-2 FLC. Experimental results show that the simplified type-2 FLC outperforms the type-1 FLCs and has similar performance as the traditional type-2 FLC. Analysis also indicates there will be at least 50% reduction in computational cost if the simplified type-2 FLC is used in place of a traditional type-2 FLC. It may, therefore, be concluded that the simplified type-2 FLC is able to bring about computational savings without sacrificing the ability to handle modeling uncertainties.

Chapter 5

Theory of Equivalent Type-1 FLSs (ET1FLSs)

Chapters 3 and 4 show that the FOUs provide type-2 FLSs with the potential to outperform type-1 FLSs. However, how to choose the best FOU is still an open question. Several researchers have demonstrated that GAs can be used to evolve the FOU [64, 69, 71, 86, 87]. Unfortunately, there are no guidelines for designing the FOU theoretically and it is unclear how the FOU enables type-2 FLSs to differentiate themselves from their type-1 counterparts.

This Chapter aims at investigating how the extra degree of freedom provided by the FOU enables type-2 FLSs to model more complex input-output relationships than type-1 FLSs with the same number of MFs (resolution). The key idea is that a type-2 FLS may be viewed as being equivalent to a group of type-1 FLSs, referred to as *equivalent type-1 fuzzy logic systems* (ET1FLSs), as long as both systems have identical input-output relationships. To identify the ET1FLSs that can be used in place of a type-2 FLS, the FOU is first reduced into a group of *equivalent type-1 sets* (ET1Ss). By analyzing the characteristics of the ET1Ss and ET1FLSs, conclusions about the contributions of the extra mathematical dimension provided by the FOU can be drawn.

The rest of this Chapter is organized as follows: Section 5.1 introduces the definitions of ET1Ss and ET1FLSs. The algorithms for identifying ET1Ss and

ET1FLSs for a type-2 FLS is also provided. The ET1Ss and ET1FLSs of different type-2 fuzzy logic controllers (FLCs) are presented in Section 5.2. Section 5.3 discusses the relationships between ET1Ss (ET1FLSs) and the input-output relationships of type-2 FLCs. Finally, conclusions are drawn in Section 5.4.

5.1 ET1FLSs: Concepts and Identification

In the following sub-sections, the concepts of ET1FLSs and ET1Ss as well as the identification procedures are described.

5.1.1 Concepts

Type-2 fuzzy sets are characterized by three-dimensional MFs. The third dimension is the FOU that models the uncertainties in the shape and position of the fuzzy sets. A type-2 fuzzy set, $\widetilde{A}$, can be thought of as a collection of embedded type-2 fuzzy sets, $\widetilde{A}_e$. Associated with each $\widetilde{A}_e$ is an embedded type-1 set A_e [?]. The ability of type-2 FLSs to produce more complex input-output maps than their type-1 counterparts may be attributed to the extra degree of freedom provided by the FOU. Unlike type-1 FLSs which utilize certain MFs, the output of a type-2 FLS may be obtained via different embedded type-1 sets as the input vector varies. Despite the additional flexibility, the input-output relationship of a type-2 FLS is fixed once the system parameters, type reducer and defuzzifier are selected. This characteristics is shared by a type-1 FLS, suggesting that it is possible to use type-1 fuzzy logic theory to construct a system that has the same input-output map as a type-2 FLS. The resulting ET1FLSs provide a platform from which the relationship between the FOU shape and the modeling capability of type-2 FLSs can be analyzed.

The operation of using type-1 fuzzy theory to duplicate the input-output map of a type-2 FLS may be interpreted as identifying the appropriate embedded type-1 sets from among the countless such sets associated with the type-2 fuzzy sets that partition the input and output domains. While the limitless number of embedded type-1 sets enables a type-2 FLS to model more complex systems, it also makes the job of identifying suitable embedded type-1 fuzzy sets more daunting. The proposed methodology for deriving the ET1FLSs utilizes the following measures to make the problem more amenable :

- The universes of discourses are discretized. This step will reduce the number of embedded type-2 sets, and their embedded type-1 sets, to a finite number.

- A type-2 fuzzy set that is used in the rule base is selected and replaced by an embedded type-1 set chosen arbitrarily from the collection associated to the particular type-2 set. The process is repeated until all but one of the type-2 sets appearing in the fuzzy inference has been replaced.

Since embedded type-1 sets are pre-assigned to all but one type-2 set, ET1FLSs can be derived by identifying type-1 MFs that can be used, in place of the last type-2 fuzzy set, to maintain the input-output relationship of the type-2 FLS. The technique of designating the embedded type-1 set for all but one type-2 set is akin to amassing in one set, the degrees of freedom provided by all the type-2 sets. Multiple type-1 MFs will, therefore, be needed in order to maintain the same level of flexibility. The ensuing collection of type-1 sets is referred to collectively as ET1Ss. Having introduced the concepts qualitatively, the terms ET1FLSs and ET1Ss are formally defined in Definition 1 and 2 respectively.

Definition 1 *Equivalent type-1 fuzzy logic systems is the group of type-1 FLSs that, together, has the same input-output relationship as a type-2 FLS. For a type-2 FLS that has N type-2 fuzzy sets, an ET1FLS comprises of $N-1$ embedded type-1 set and one equivalent type-1 set.*

Definition 2 *The concept of equivalent type-1 sets is defined as the collection of type-1 sets that can be used in place of the FOUs in a type-2 FLS.*

To illustrate the idea more clearly, consider a two-inputs (x_1 and x_2) single-output (y) type-2 FLS. The inputs and output domains are each partitioned by N triangular interval type-2 fuzzy sets, as shown in Figure 5.1(a). Although triangular MFs are used in this example, the same procedure can be applied to type-2 FLSs with different MF shapes and thus the conclusions drawn herein can be generalized. Figure 5.1(b) shows the ET1FLSs. The pre-specified embedded type-1 fuzzy sets are shown as the thick bold lines and the remaining lines are the ET1Ss. The procedure for identifying ET1Ss, and consequently the ET1FLSs, is delineated in the next sub-section.

5.1.2 Procedure for Identifying ET1FLSs

Consider a n-inputs single-output type-2 FLS. Each input domain is partitioned by N_j ($j = 1, 2, \ldots, n$) type-2 fuzzy sets. Suppose the rule base has $\prod_{j=1}^{n} N_j$ rules (all possible combinations of input sets) and the consequent part of each rule is a distinct type-2 fuzzy set. The first step in deriving ET1FLSs is to select the type-2 fuzzy set that will be reduced to ET1Ss and replacing all other type-2 fuzzy sets by embedded type-1 sets. Assume that ET1Ss are to be found to replace $\widetilde{A}_{kl}$, the
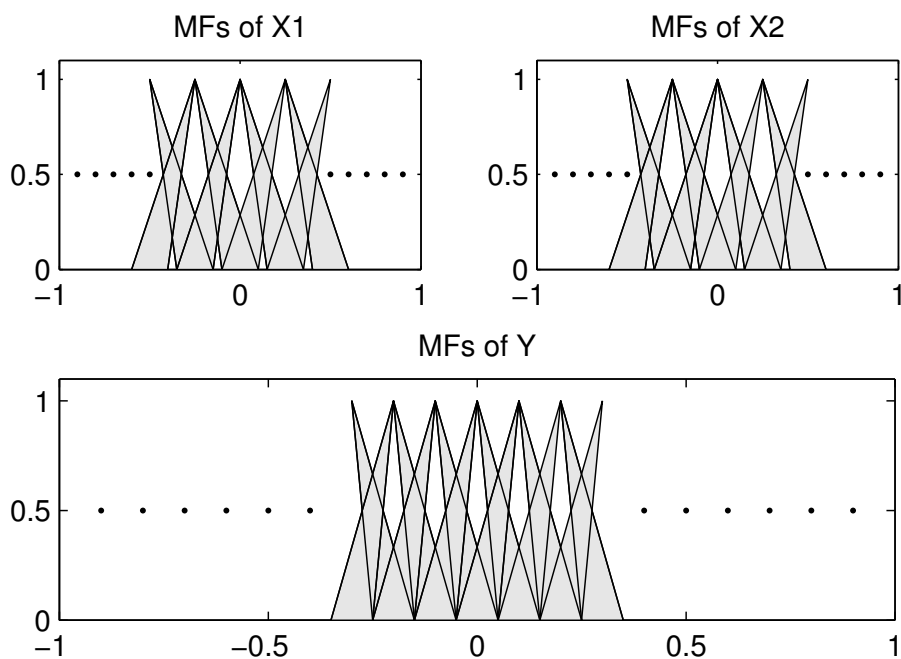
(a) The original type-2 FLS
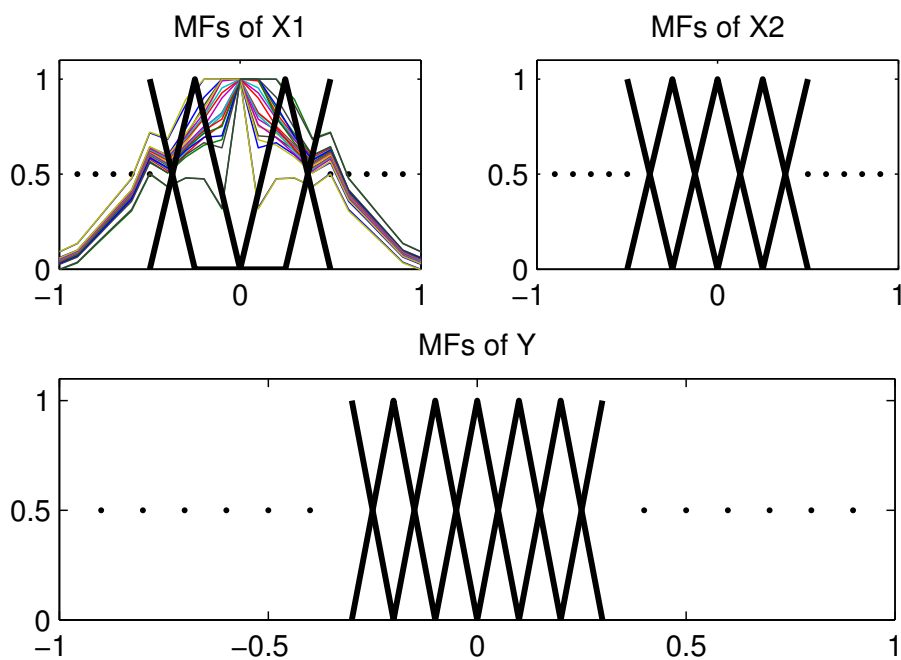
(b) $(3N-1)$ type-2 sets are replaced by $(3N-1)$ embedded type-1 sets, respectively. The remaining type-2 set is replaced by the ET1Ss of the type-2 FLS. Thus the ET1FLSs of the type-2 FLS are found. Each ET1FLS has $(3N-1)$ embedded type-1 sets and one of the ET1Ss as its MFs

Figure 5.1: The procedure for identifying ET1FLSs for a type-2 FLS

lth type-2 set in the kth input domain. The $\displaystyle\prod_{j=1(j\neq k)}^{n} N_j$ rules in the rule-base that

contain $\widetilde{A}_{kl}$ become

$R^{i_1 i_2 \ldots l \ldots i_n}$:   If x_1 is $A_{e,1i_1}$, x_2 is $A_{e,2i_2}$, ..., x_k is $A_{ET1S,kl}$ ..., and x_n is

A_{e,ni_n}, then y is $Y_{i_1 i_2 \ldots l \ldots i_n}$.

while the remaining rules in the rule-base may be expressed as

$R^{i_1 i_2 \ldots i_k \ldots i_n}$:   IF x_1 is $A_{e,1i_1}$, ..., x_k is A_{e,ki_k}, ..., and x_n is A_{e,ni_n},

THEN y is $Y_{i_1 i_2 \ldots i_k \ldots i_n}$.

where A_{e,ji_j} is the embedded type-1 set selected to replace $\widetilde{A}_{ji_j}$ ($j = 1, \ldots, k, \ldots, n$,

$i_j = 1, \ldots, N_j$, $i_k \neq l$) and $Y_{i_1 i_2 \ldots i_n}$ is a singleton located at the mid-point of the

generalized centroid (an internal type-1 set) for the corresponding type-2 conse-

quent set. Using sum-product inference and height defuzzification, the output of

the ET1FLS may be expressed as

$$y_E = \frac{\displaystyle\sum_{i_1=1}^{N_1} \cdots \sum_{i_k=1(i_k\neq l)}^{N_k} \cdots \sum_{i_n=1}^{N_n} f_{1i_1} \cdots f_{ki_k} \cdots f_{ni_n} Y_{i_1 \ldots i_k \ldots i_n}}{\displaystyle\sum_{i_1=1}^{N_1} \cdots \sum_{i_k=1(i_k\neq l)}^{N_k} \cdots \sum_{i_n=1}^{N_n} f_{1i_1} \cdots f_{ki_k} \cdots f_{ni_n} + \sum_{i_1=1}^{N_1} \cdots \sum_{i_{k-1}=1}^{N_{k-1}} \sum_{i_{k+1}=1}^{N_{k+1}} \cdots \sum_{i_n=1}^{N_n} f_{1i_1} \cdots f_{(k-1)i_{k-1}} f_{kl} f_{(k+1)i_{k+1}} \cdots f_{ni_n}}$$

$$+ \frac{\displaystyle\sum_{i_1=1}^{N_1} \cdots \sum_{i_{k-1}=1}^{N_{k-1}} \sum_{i_{k+1}=1}^{N_{k+1}} \cdots \sum_{i_n=1}^{N_n} f_{1i_1} \cdots f_{(k-1)i_{k-1}} f_{kl} f_{(k+1)i_{k+1}} \cdots f_{ni_n} Y_{i_1 \ldots i_{k-1} l i_{k+1} \ldots in}}{\displaystyle\sum_{i_1=1}^{N_1} \cdots \sum_{i_k=1(i_k\neq l)}^{N_k} \cdots \sum_{i_n=1}^{N_n} f_{1i_1} \cdots f_{i_k} \cdots f_{ni_n} + \sum_{i_1=1}^{N_1} \cdots \sum_{i_{k-1}=1}^{N_{k-1}} \sum_{i_{k+1}=1}^{N_{k+1}} \cdots \sum_{i_n=1}^{N_n} f_{1i_1} \cdots f_{(k-1)i_{k-1}} f_{kl} f_{(k+1)i_{k+1}} \cdots f_{ni_n}}$$

$$(5.1)$$

where f_{ji_j} is the firing level of the i_jth embedded type-1 set in the jth input

domain and f_{kl} is the firing level of the ET1S. As shown in Figure 5.2, the task

of identifying ET1Ss essentially boils down to identifying a point on the MF of

the ET1S $f_{kl} = f_{eq}$, referred to as *equivalent type-1 membership grade* (ET1MG).

Suppose the crisp output of the n-inputs single-output type-2 FLS corresponding

to the input vector $[x_1, x_2, \ldots x_n]$ is y. Since the output should not be affected

when the type-2 FLS is switched to its ET1S, $f_{kl} = f_{eq}$ must be selected such that

$y_{ET1FLS} = y$. Consequently, the mathematical expression for calculating $f_{kl} = f_{eq}$ can be derived by substituting y_E by y in Equation (5.1) and then solving for f_{eq}. The resulting expression is

$$f_{eq} = \frac{\sum_{i_1=1}^{N_1} \cdots \sum_{i_k=1, i_k \neq l}^{N_k} \cdots \sum_{i_n=1}^{N_n} f_{1i_1} \cdots f_{ni_n}(y - Y_{i_1 \dots i_k \dots i_n})}{\sum_{i_1=1}^{N_1} \cdots \sum_{i_{k-1}=1}^{N_{k-1}} \sum_{i_{k+1}=1}^{N_{k+1}} \cdots \sum_{i_n=1}^{N_n} f_{1i_1} \cdots f_{(k-1)i_{k-1}} f_{(k+1)i_{k+1}} \cdots f_{ni_n}(Y_{i_1 \dots i_{k-1} l i_{k+1} \dots i_n} - y)}$$

$$(5.2)$$
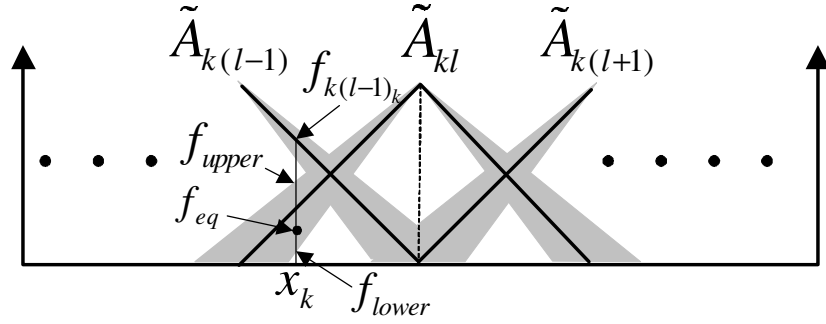
Figure 5.2: Illustration of f_{eq}, the ET1MG

Each ET1MG, f_{eq}, re-produces a point on the input-output map. A ET1S is identified by applying Equation (5.2) repeatedly for all discrete points in the kth input domain, assuming that x_i $(i = 1, \dots, n, i \neq k)$ are constants. Geometrically, a ET1S generates a plane on the input-output map of a type-2 FLS where x_i $(i = 1, \dots, n, i \neq k)$ are constants. By repeating the procedure for other planes in the input-output map the complete group of ET1Ss can be obtained. In summary, the procedure for finding ET1FLSs of a n-inputs single output type-2 FLS is as follows :-

1. Discretize each input domain into N_j $(j = 1, 2, \dots, n)$ points.

2. Equate $Y_{i_1 i_2 \ldots i_n}$ $(i_j = 1, 2, \ldots, N_j)$, the singleton output sets of the ET1FLSs, to the mid-point of the interval type-1 set that is the generalized centroid of the type-2 sets that partition the output domain.

3. Replace all but one (assume it is the lth input set in kth input domain) type-2 sets used to characterize the input domains with embedded type-1 sets. The embedded type-1 sets can be arbitrarily selected from the collection associated with the type-2 fuzzy set.

4. Apply Equation (5.2) recurrently to generate the ET1S corresponding to a plane of the input-output map where x_i $(i = 1, \ldots, n, i \neq k)$ are constants.

5. An ET1FLS is obtained by using the embedded type-1 sets and one of the ET1Ss as its MFs. Repeat step (4) for other planes in the input-output map of the type-2 FLS.

5.2   ET1FLSs of Type-2 FLCs

Having introduced the concepts of ET1Ss and ET1FLSs, they will be used to analyze the characteristics of type-2 FLSs. Fuzzy logic controllers (FLCs) are selected for this study because fuzzy control is one of the most common applications of FLSs. First, a baseline type-1 FLC is introduced. Type-2 FLCs are then obtained by introducing FOU to the baseline type-1 fuzzy sets.

Consider the baseline type-1 Proportional plus Integral (PI) FLC that has two inputs (e and $\dot{e}$) and one output ($\dot{u}$). It is assumed that each input domain consists of three type-1 MFs, shown as the dark thick lines in Figure 5.3. The rule base has 9 rules and assumes the following form :

$$R^{ij}: \quad \text{If } e \text{ is } e_i \text{ and } \dot{e} \text{ is } \dot{e}_j, \text{ then } \dot{u} \text{ is } \dot{u}_{ij}. \qquad i, j = 1, 2, 3$$

where

$$\dot{u}_{ij} = K_I \cdot P_{1i} + K_P \cdot P_{2j} \qquad i, j = 1, 2, 3 \tag{5.3}$$

P_{1i} is the apex of MF e_i, and P_{2j} is the apex of MF $\dot{e}_j$, as illustrated in Figure 5.3. The baseline type-1 FLC realizes the PI control law $\dot{u} = K_I \cdot e + K_P \cdot \dot{e}$ [88], where K_I and K_P are the integral and proportional gains respectively.

(a) MFs of e (b) MFs of $\dot{e}$
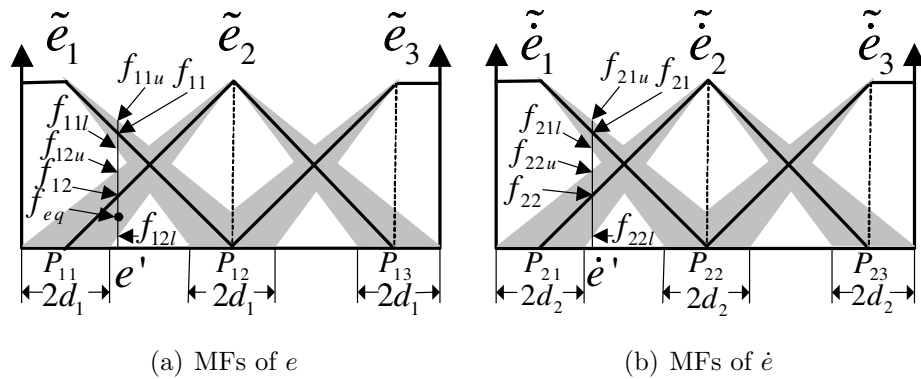
Figure 5.3: Input MFs of the baseline type-1 FLC and a type-2 FLC where all the MFs are type-2

The results presented in this section were obtained when the FLC parameters assume the values listed in Table 5.1. Table 5.2(a)-(c) contains the rule-bases for the various PI configurations. Using product-sum inference and height defuzzification, the output of the baseline type-1 FLC may be expressed as :

$$\dot{u}_{type-1} = \frac{\displaystyle\sum_{i=1}^{3}\sum_{j=1}^{3} f_{1i} f_{2j} \dot{u}_{ij}}{\displaystyle\sum_{i=1}^{3}\sum_{j=1}^{3} f_{1i} f_{2j}} \tag{5.4}$$

where f_{li} (f_{lj}) is the firing level of the ith (jth) fuzzy set in the lth ($l = 1, 2$) input domain.

A type-2 FLC is obtained by equipping the six fuzzy sets used to partition the

Table 5.1: Parameters of the FLCs used in the analysis.

$P_{11} = -1,$	$P_{12} = 0,$	$P_{13} = 1$
$P_{21} = -1,$	$P_{22} = 0,$	$P_{23} = 1$
$K_P = 1,$	$K_I = \{0.5,\ 1,\ 2\}$	

Table 5.2: The different rule bases when K_I changes

(a) $K_I = 0.5$

e \ $\dot{e}$	$\dot{e}_1$	$\dot{e}_2$	$\dot{e}_3$
e_1	-1.5	-0.5	0.5
e_2	-1	0	1
e_3	-0.5	0.5	1.5

(b) $K_I = 1$

e \ $\dot{e}$	$\dot{e}_1$	$\dot{e}_2$	$\dot{e}_3$
e_1	-2	-1	0
e_2	-1	0	1
e_3	0	1	2

(c) $K_I = 2$

e \ $\dot{e}$	$\dot{e}_1$	$\dot{e}_2$	$\dot{e}_3$
e_1	-3	-2	-1
e_2	-1	0	1
e_3	1	2	3

input domains of the baseline type-1 FLC with FOUs, shown as the shaded areas

in Figure 5.3. The output sets are defined in Table 5.2. By first reducing all type-2

sets, with the exception of $\tilde{e}_2$, to embedded type-1 sets that have the same shape

as the baseline type-1 fuzzy sets, the ET1FLSs associated with the type-2 FLC are

identified. $\tilde{e}_2$ is then replaced by ET1Ss that are found by calculating the ET1MGs

(f_{eq}) using Equation (5.5), which is derived by setting $f_{eq} = f_{12}$, $\dot{u}_{type-1} = \dot{u}_{type-2}$

and re-arranging Equation (5.4).

$$f_{eq} = \frac{\displaystyle\sum_{j=1}^{3} f_{11}f_{2j}(\dot{u}_{type-2} - \dot{u}_{1j}) + \sum_{j=1}^{3} f_{13}f_{2j}(\dot{u}_{type-2} - \dot{u}_{3j})}{\displaystyle\sum_{j=1}^{3} f_{2j}(\dot{u}_{2j} - \dot{u}_{type-2})} \tag{5.5}$$

where f_{ij} $(i = 1, 2, j = 1, 2, 3)$ is the amount by which the embedded type-1 fuzzy

sets are fired and $\dot{u}_{type-2}$ is the output of the type-2 FLC. Each ET1S reproduces the

slice of the input-output map where $\dot{e}$ is constant. Figure 5.4 shows the ET1FLSs of

the type-2 FLC when $K_I = 2$ and $d_1 = d_2 = 0.1$. When $K_I = 2$ and $d_1 = d_2 = 0.2$,

the ET1FLSs are plotted in Figure 5.5. The rule base used here is shown in

Table 5.2(c).

In order to examine how the ET1Ss shapes vary with the number of type-2

fuzzy sets used to construct the FLC, the simplest form of type-2 FLC comprising

of only one type-2 fuzzy set is analyzed. Figure 5.6 shows the antecedent fuzzy sets

of the type-2 FLC. The output sets remain unchanged. As there is only one type-2

fuzzy set, the step where embedded type-1 sets are specified may be skipped. The

ET1Ss are still calculated using Equation (5.5), where f_{ij} $(i = 1, 2, j = 1, 2, 3)$ is

now the membership grades of type-1 fuzzy sets shown in Figure 5.6. ET1FLSs

of the simplified type-2 FLC when different K_I values are used to set up the
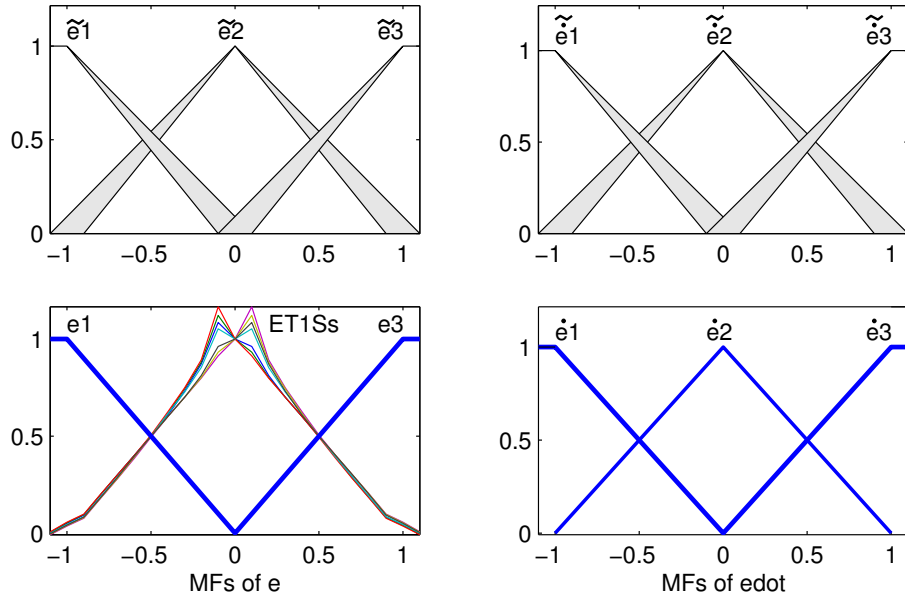
Figure 5.4: ET1FLSs of a type-2 FLC whose MFs are all type-2. $K_I = 2$, $d_1 = d_2 = 0.1$.
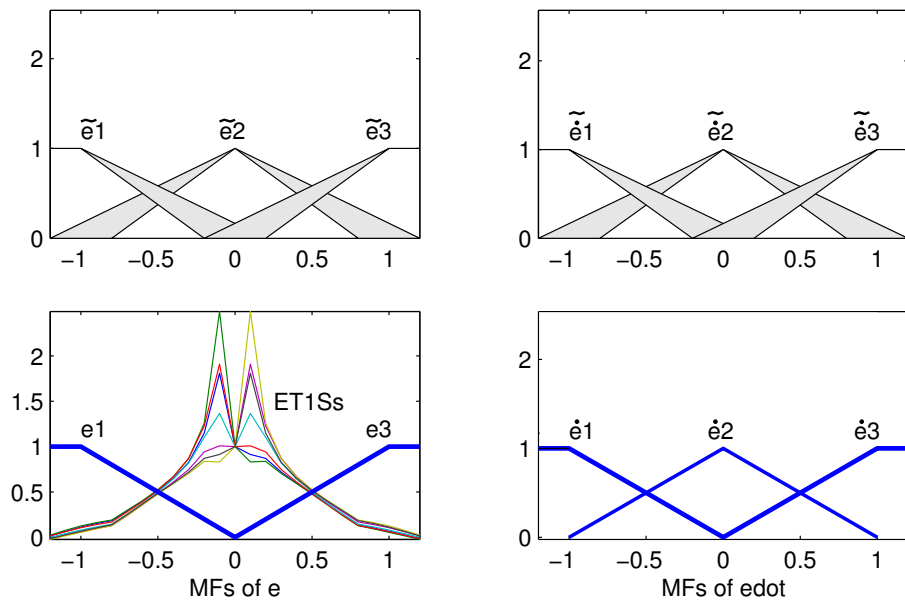
Figure 5.5: ET1Ss of a type-2 FLC whose MFs are all type-2. $K_I = 2$, $d_1 = d_2 = 0.2$.

consequent fuzzy sets are shown in Figure 5.7. Only the MFs of the e domain are plotted because the MFs of $\dot{e}$ are those shown in Figure 5.6(b). Both the FOU and the ET1Ss are plotted to better illustrate their relationships. The corresponding input-output maps of the various FLCs are shown in Figure 5.8.

(a) MFs of e (b) MFs of $\dot{e}$
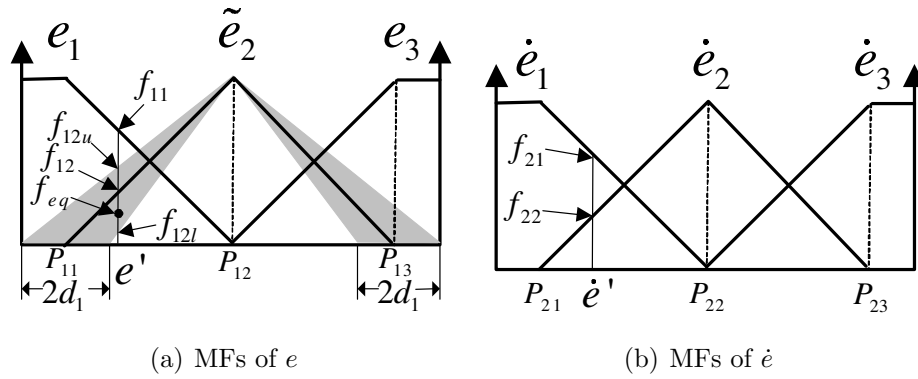
Figure 5.6: Input MFs of the simplified type-2 FLC

(a) $K_I = 0.5$

(b) $K_I = 1$

(c) $K_I = 2$

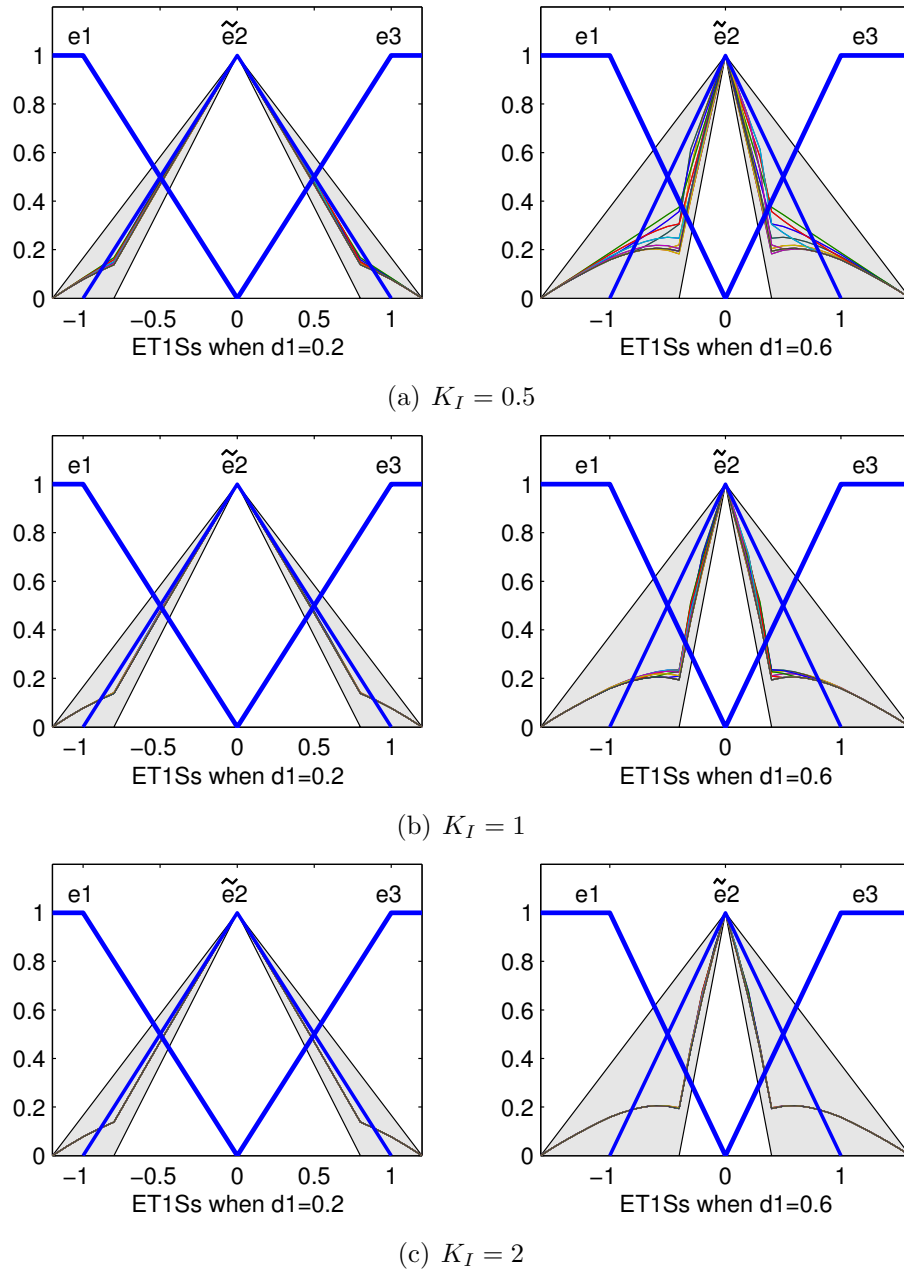Figure 5.7: ET1Ss of the simplified type-2 FLC shown in Figure 5.6 with different consequents.
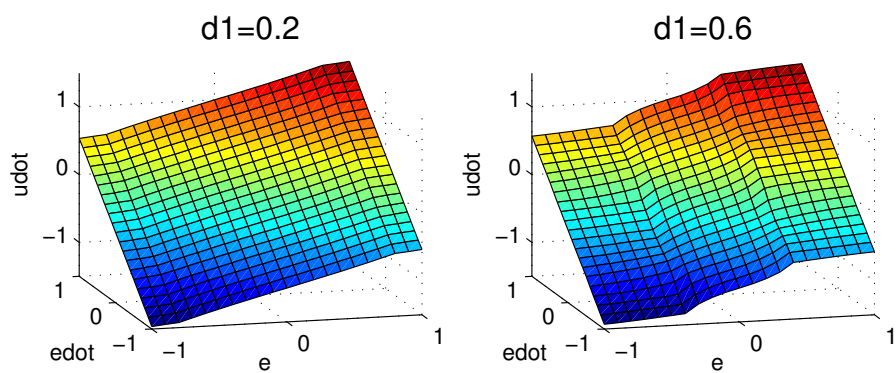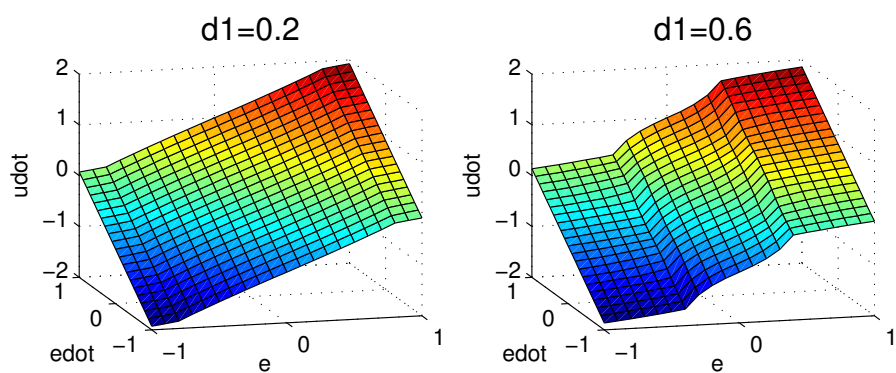
(a) $K_I = 0.5$

(b) $K_I = 1$

(c) $K_I = 2$

Figure 5.8: Input-output map of the simplified type-2 FLC shown in Figure 5.6 with different consequents

Lastly, the relationship between the ET1Ss characteristics and the shape of the FOU is examined via FLCs that partition the input domains using the fuzzy sets shown in Figure 5.9. In this case, the ET1FLSs and the input-output maps of various type-2 FLCs with the output sets tabulated in Table 5.2 are shown in Figure 5.10 and Figure 5.11.

(a) MFs of input e (b) MFs of input $\dot{e}$
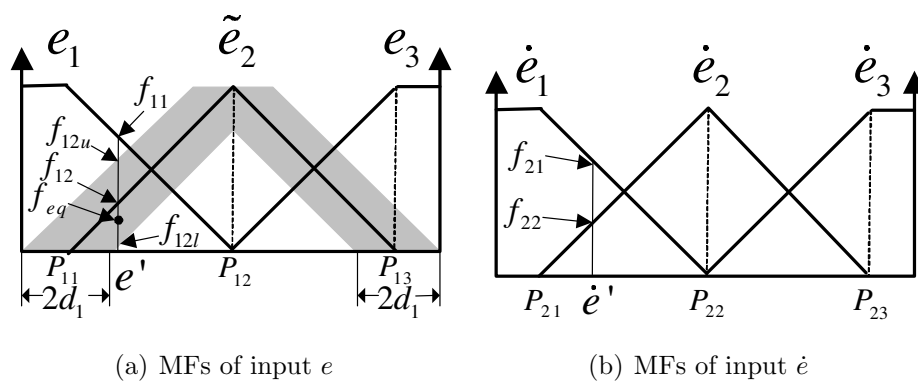
Figure 5.9: Input MFs of the simplified type-2 FLC with different shape of FOU

5.3 Analysis and Discussions

This section aims at analyzing the properties of type-2 FLS using the ET1FLSs and ET1Ss shown in Figs. 5.7 and 5.10.

5.3.1 Relationship between ET1MG and the Type-2 FLC Output

The input-output maps of type-2 FLSs shown in Figs. 5.8 and 5.11 are clearly nonlinear and more complex than a type-1 FLC that is equivalent to a PI controller. To analyze the relationship between the ET1MG, f_{eq}, and the output of the type-2 FLC shown in Figure 5.6, consider the following equation obtained by re-arranging

Equation (5.5) :

$$\dot{u}_{type-2} = \frac{f_{11} \sum\limits_{j=1}^{3} f_{2j} \dot{u}_{1j} + f_{eq} \sum\limits_{j=1}^{3} f_{2j} \dot{u}_{2j} + f_{13} \sum\limits_{j=1}^{3} f_{2j} \dot{u}_{3j}}{(f_{11} + f_{eq} + f_{13}) \cdot (f_{21} + f_{22} + f_{23})} \qquad (5.6)$$

where $\dot{u}_{type-2}$ is the output of the type-2 FLC, f_{ij} $(i = 1, 2, j = 1, 2, 3)$ is the firing level of the jth type-1 fuzzy sets in the ith input domain and f_{eq} is the ET1MG for the set $\tilde{e}_2$.

(a) $K_I = 0.5$

(b) $K_I = 1$

(c) $K_I = 2$

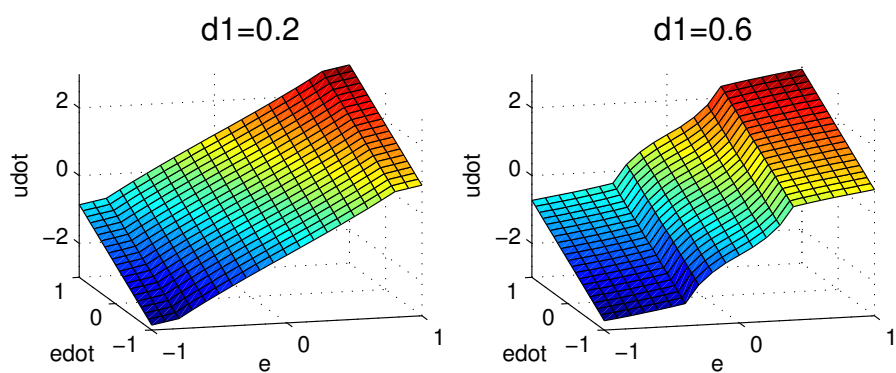Figure 5.10: ET1Ss of the simplified type-2 FLC shown in Figure 5.9 with different consequents

(a) $K_I = 0.5$

(b) $K_I = 1$

(c) $K_I = 2$

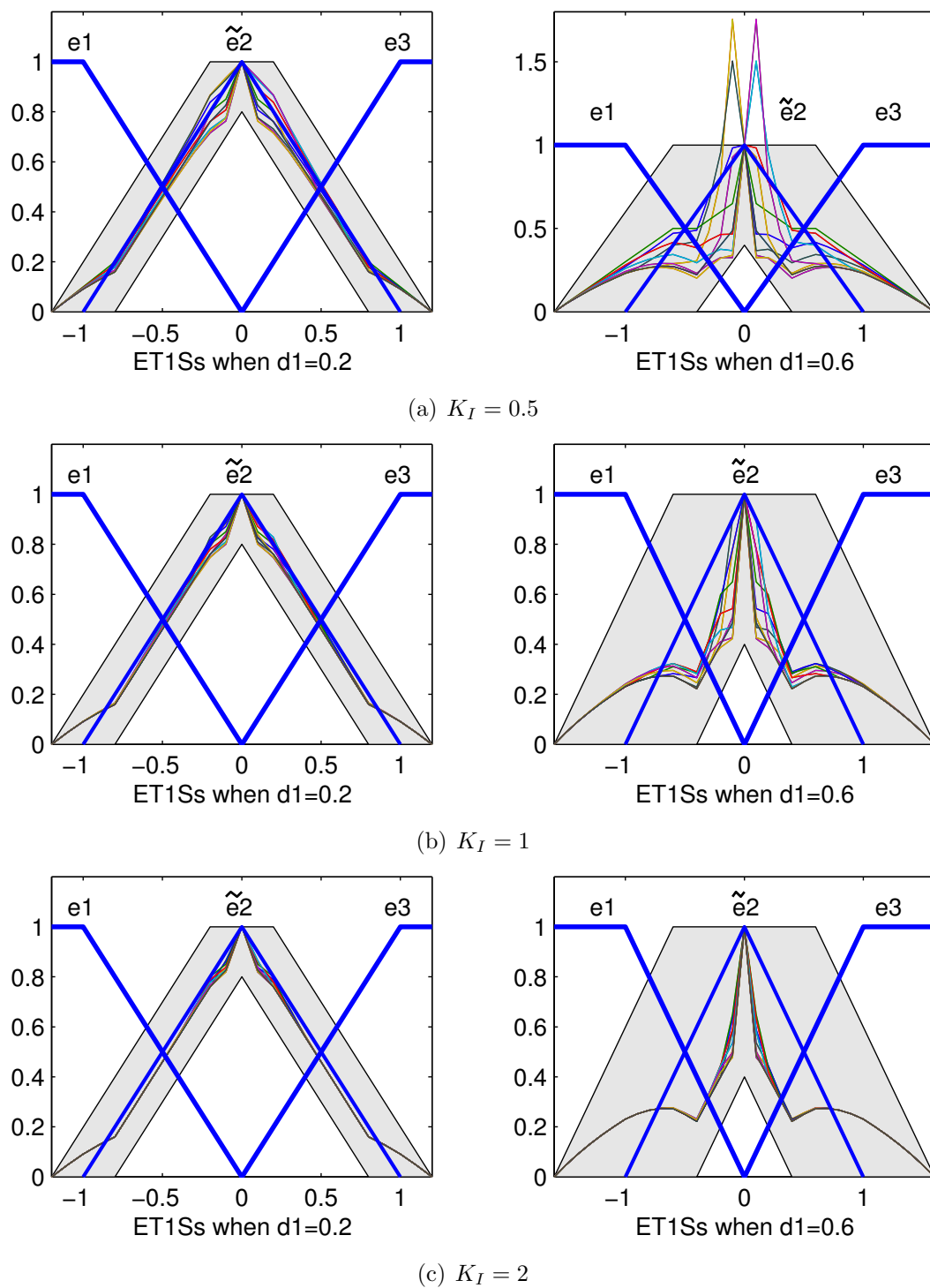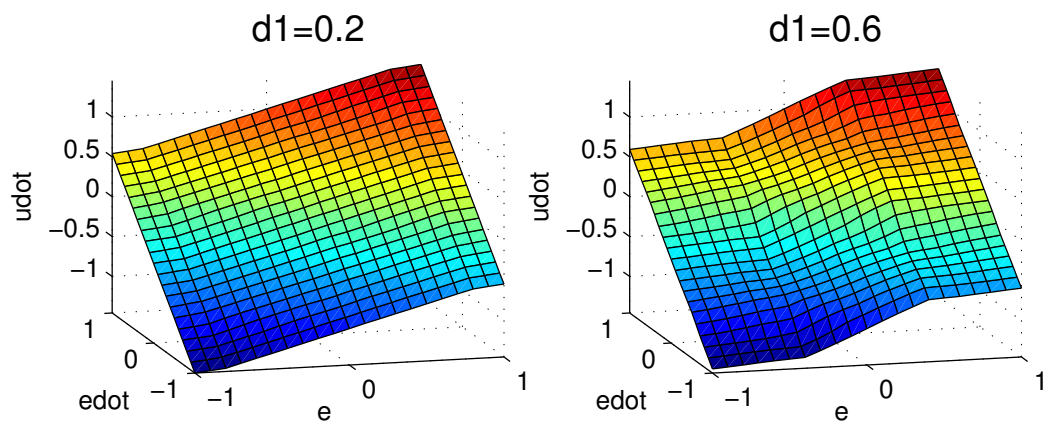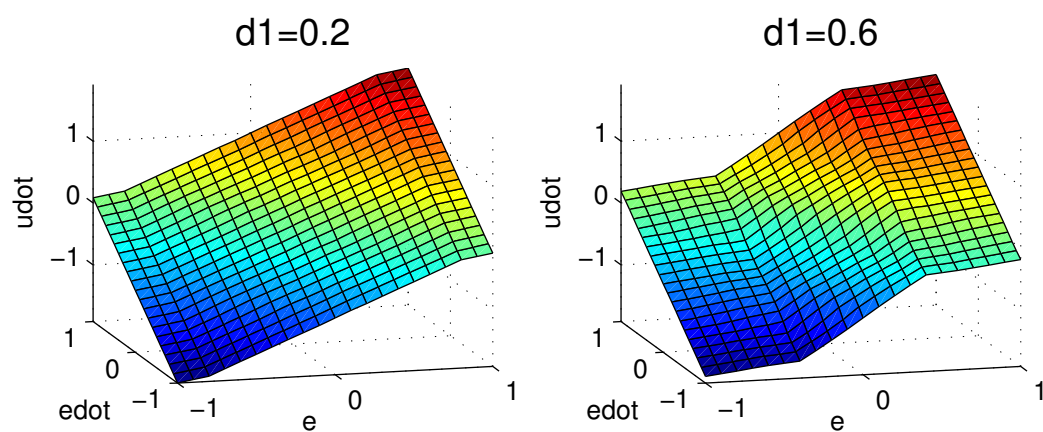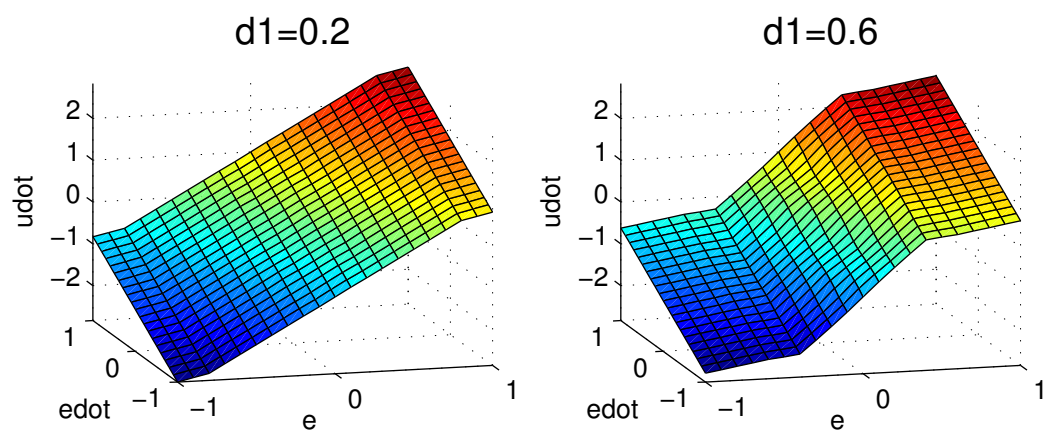Figure 5.11: Input-output map of the simplified type-2 FLC shown in Figure 5.9 with different consequents

Substituting u_{ij} by Equation (5.3), the derivative of $\dot{u}_{type-2}$ (slope of the type-2 FLS) with respect to f_{eq} can be expressed as :

$$\ddot{u}_{type-2} = \frac{K_I[f_{11}(P_{12} - P_{11}) + f_{13}(P_{13} - P_{12})]}{(f_{11} + f_{eq} + f_{13})^2} \tag{5.7}$$

Equation (5.7) indicates that $|\ddot{u}|$ is inversely proportional to f_{eq}. Hence, the slope of $\dot{u}_{type-2}$ will be steeper than the baseline type-1 FLC when f_{eq} is smaller than the amount by which the type-1 set is activated. As the membership grades of the ET1Ss can be bigger or smaller than that of the baseline type-1 MF, the input-output map of a type-2 FLC may have slopes that are steeper or gentler. This conclusion is in-line with the findings drawn from Figure 5.12. The diagram shows two slices of the input-output maps corresponding to different $\dot{e}$ and K_I. When $K_I = 2$, $d_1 = 0.6$ and $e \in (0, 0.8)$, the slice of the input-output map of the type-2 FLC is above that of the baseline type-1 FLC in Figure 5.12. Analogously, the ET1Ss are below the baseline type-1 set (Refer to Figure 5.7(c)). Another observation is the ET1Ss intersect the baseline type-1 set at three points $e = \{0, \pm 0.8\}$ in Figure 5.7. The two slices of the input-output map of the corresponding FLCs, in Figure 5.12, also intersect at these 3 points.

Furthermore, the ET1Ss in Figs. 5.7 and 5.10 illustrate that a larger FOU gives rise to a more complex input-output relationship. This observation is consistent with intuitions. When the FOU is bigger, the difference between f_{12u} and f_{12l} is larger (refer to Figure 5.6), which may result in more diverse output and hence more complex input-output map. The various ET1Ss will also be more diverse.

(a) $K_I = 2$, $\dot{e} = 0$ (b) $K_I = 0.5$, $\dot{e} = 0$
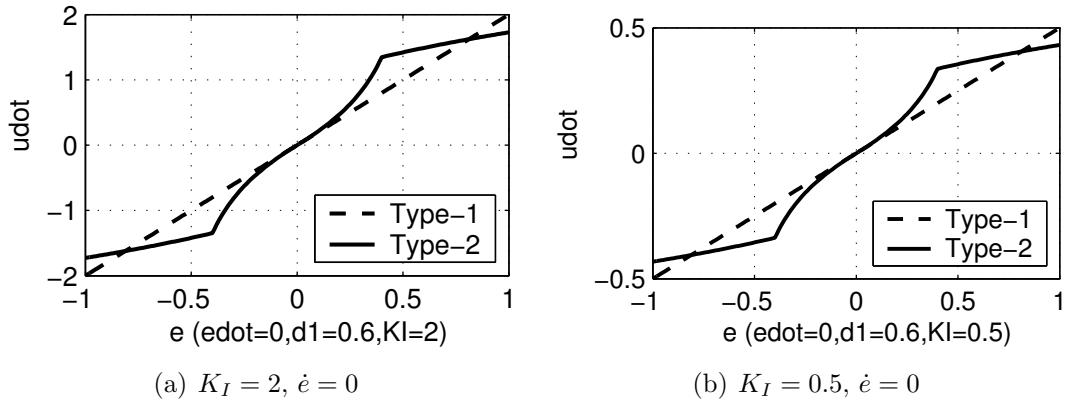
Figure 5.12: Illustration of the slope of the input-output map

5.3.2 Properties of the ET1Ss

The MFs of the type-2 FLCs studied in this Chapter is symmetric. When $K_P = 1$, $K_I = 0.11$ and $d_1 = 0.5$, as shown in Figure 5.13, the ET1S for $\dot{e} = 0$ is also symmetric. However, the ET1S when $\dot{e} = -0.2$ is symmetric to the one when $\dot{e} = 0.2$. It may be concluded that, taken as a group, ET1Ss are symmetric if the corresponding type-2 set is symmetric. Otherwise, the ET1Ss will not be symmetric.

Another important property is the ET1Ss may not lie within the FOU of the corresponding type-2 set. Moreover, the ET1MGs of the ET1Ss may be larger than 1 or smaller than 0. ET1Ss with some ET1MGs that are larger than the upper membership grade are illustrated in Figure 5.13. More interesting ET1Ss are presented in Figure 5.14(a), where some of the ET1MGs of the ET1Ss are negative. To provide insights into why ET1MGs may assume negative values, consider the input pair $e = -0.2$, $\dot{e} = 0.2$. The slice of the input-output map where $\dot{e} = 0.2$ is shown in Figure 5.14(b). The point of interest is labelled by a square. In this case, the input vector fires the sets e_1, $\tilde{e}_2$, $\dot{e}_2$ and $\dot{e}_3$ by the following
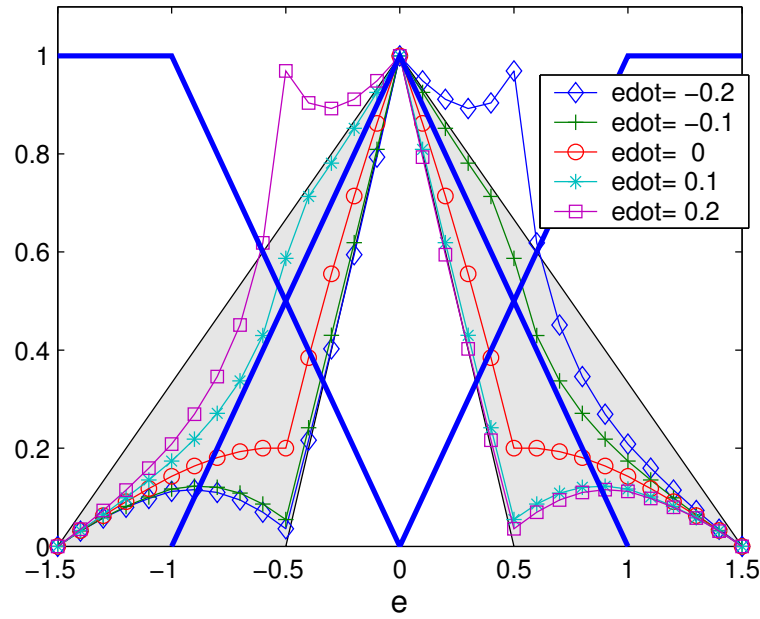
Figure 5.13: Illustration of symmetry

amounts :

$$
\begin{aligned}
e_1 : \quad f_{11} &= 0.2 \\
\tilde{e}_2 : \quad \tilde{f}_{12} &= [0, 0.8889] \\
\dot{e}_2 : \quad f_{22} &= 0.8 \\
\dot{e}_3 : \quad f_{23} &= 0.2
\end{aligned}
$$

Thus, rules in the rule base are activated with the following strengths :

Rule No:	Firing Strength	$\rightarrow$	Consequent
R^{12} :	$f_{11} \times f_{22} = 0.16$	$\rightarrow$	-0.2
R^{13} :	$f_{11} \times f_{23} = 0.04$	$\rightarrow$	0.8
R^{22} :	$\tilde{f}_{12} \times f_{22} = [0, 0.7111]$	$\rightarrow$	0
R^{23} :	$\tilde{f}_{12} \times f_{23} = [0, 0.1778]$	$\rightarrow$	1

For the type-2 FLS, the bounds of the type-reduced interval type-1 set obtained
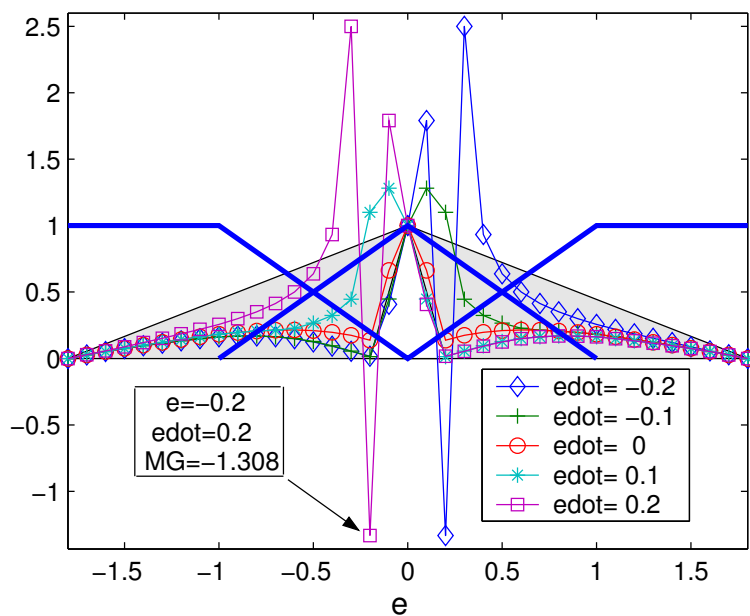
(a) Example where ET1Ss are not within FOU ($K_I = 0.2$, $d_1 = 0.8$)
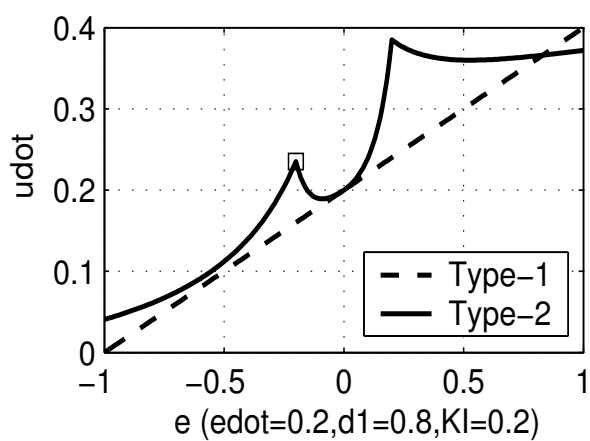
(b) A slice when $\dot{e} = 0.2$

Figure 5.14: Illustration of ET1Ss outside the FOU

using the Karnik-Mendel type-reducer [?] and the resulting crisp output are :

$$y_l = \frac{-0.16 \times 0.2 + 0.04 \times 0.8 + 0 \times 0 + 0 \times 1}{0.04 + 0.16 + 0 + 0} = 0$$

$$y_r = \frac{-0.16 \times 0.2 + 0.04 \times 0.8 + 0 \times 0 + 0.1778 \times 1}{0.04 + 0.16 + 0 + 0.1778} = 0.4722$$

$$\dot{u} = \frac{y_l + y_r}{2} = 0.2361 \tag{5.8}$$

Suppose the ET1MG of the interval firing strength $\tilde{f}_{e_2} = [0, 0.8889]$ is f_{eq}. Then, the rules in the ET1FLS are activated by the following amount :

Rule No:	Firing Strength	$\rightarrow$	Consequence
R^{12} :	$f_{11} \times f_{22} = 0.16$	$\rightarrow$	-0.2
R^{13} :	$f_{11} \times f_{23} = 0.04$	$\rightarrow$	0.8
R^{22} :	$f_{eq} \times f_{22} = 0.8 f_{eq}$	$\rightarrow$	0
R^{23} :	$f_{eq} \times f_{23} = 0.2 f_{eq}$	$\rightarrow$	1

The expression governing the output of the ET1FLS is :

$$\dot{u}_{ET1FLS} = \frac{0.16 \times -0.2 + 0.04 \times 0.8 + 0.8 f_{eq} \times 0 + 0.2 f_{eq} \times 1}{0.16 + 0.04 + 0.8 f_{eq} + 0.2 f_{eq}}$$

$$= \frac{0.2 f_{eq}}{0.2 + f_{eq}} \tag{5.9}$$

When f_{eq} is positive, the output of the ET1FLS, $\dot{u}_{ET1FLS}$, will increase and tend towards 0.2 as $f_{eq} \rightarrow +\infty$ i.e.

$$\lim_{f_{eq} \rightarrow +\infty} \frac{0.2 f_{eq}}{0.2 + f_{eq}} = 0.2$$

Since the maximum $\dot{u}_{ET1FLS}$ value is 0.2 if f_{eq} is constrained to be positive, the resulting ET1FLS will not be able to replicate the crisp output of the type-2 FLC which is 0.2361 (Equation (5.8)). The only way for the outputs of the ET1FLS and the type-2 FLS to match is for f_{eq} to take on the negative value -1.3080. This

analysis indicates that the extra dimension provided by the FOU enables a type-2 FLC to produce outputs that cannot be achieved by traditional type-1 FLCs.

From the above analysis, there are two main differences between type-1 and type-2 FLCs. Firstly, a type-2 FLC can be viewed as a combination of many different ET1FLSs. A different ET1FLS is utilized when the input is changed. Secondly, a type-2 FLC may give rise to an ET1MG that is negative or larger than unity. These two characteristics of a type-2 FLC enable it to model more complex input-output relationships than its type-1 counterpart. The input-output map of a type-2 FLC may not be achieved by a type-1 FLC with the same number of MFs.

5.3.3 Discontinuities in the Input-Output Map of Type-2 FLCs

Unlike the input-output map of a type-1 FLC, which is always piecewise continuous, the input-output map of a type-2 FLC may have discontinuities under certain circumstances. A detailed input-output map of the type-2 FLC shown in Figure 5.3 with $d_1 = d_2 = 0.6$ and $K_I = K_P = 1$ is illustrated in Figure 5.15(a). From the slice of input-output map when $\dot{e} = 0$ shown in Figure 5.15(b), it may be observed that discontinuities occur when $\dot{e} = 0$ and $e = \pm 0.6$.

To establish the condition under which discontinuities occur, the discontinuity that occurs at $(e, \dot{e}) = (-0.6, 0)$ is examined. Consider input pairs of the form $(e, \dot{e}) = (-0.6 + \omega, 0)$, where $\omega \in [0, 0.2]$. This range of ω is chosen because the analysis is simpler as the firing level of the lower MF of $\tilde{e}_2$ is always 0. The firing
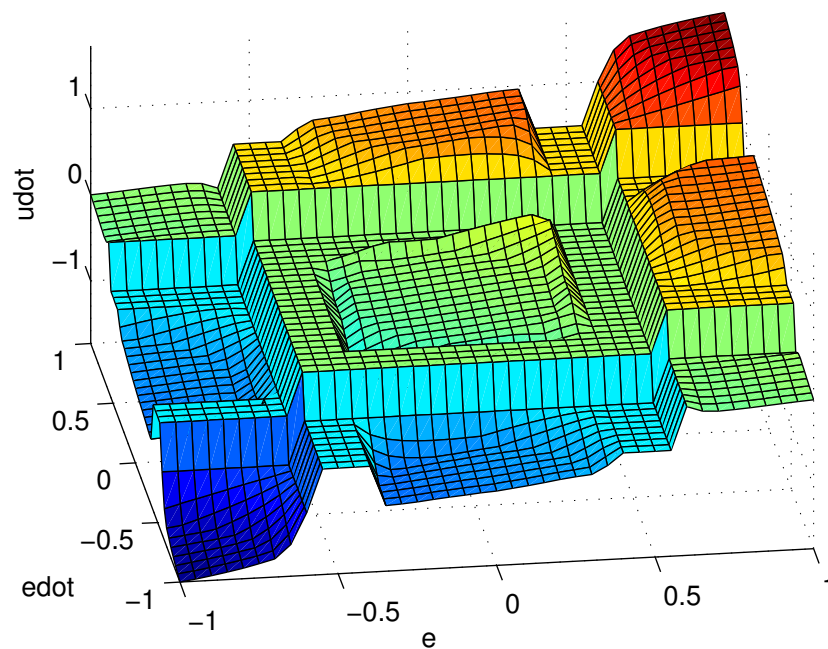
(a) The input-output map of the type-2 FLS shown in Figure 5.3 with $d_1 = d_2 = 0.6$ and $K_I = K_P = 1$
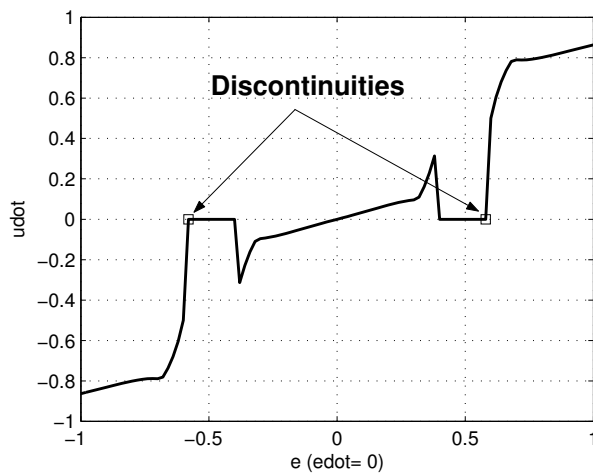
(b) A slice of the input-output map when $\dot{e} = 0$

Figure 5.15: Discontinuities in the input-output map of a type-2 FLC

levels of the MFs shown in Figure 5.16 are :

$$
\begin{array}{llll}
\tilde{f}_{11} & = & [0, \frac{1.2-\omega}{1.6}] & \quad \tilde{f}_{21} & = & [0, 0.3750] \\
\tilde{f}_{12} & = & [0, \frac{1+\omega}{1.6}] & \quad \tilde{f}_{22} & = & [1, 1] \\
\tilde{f}_{13} & = & [0, \frac{\omega}{1.6}] & \quad \tilde{f}_{23} & = & [0, 0.3750]
\end{array}
\tag{5.10}
$$
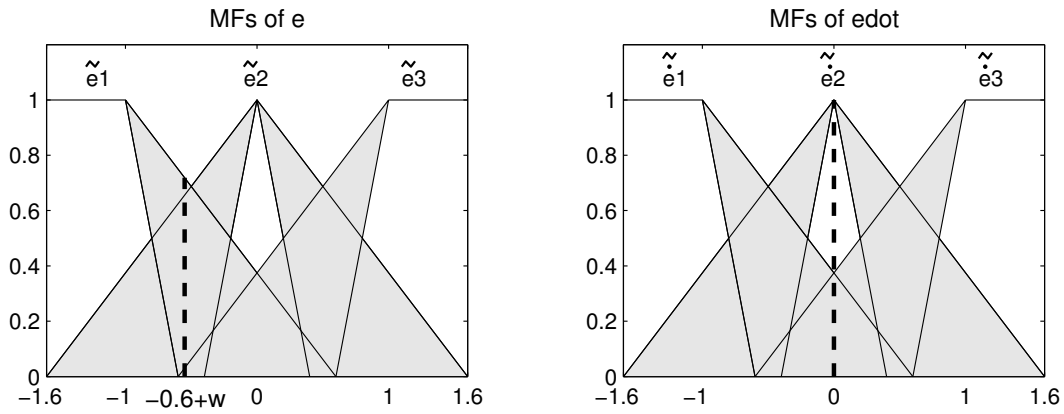
Figure 5.16: Input MFs of the type-2 FLC shown in Figure 5.6 with $d_1 = d_2 = 0.6$

Although the rule base given in Table 5.2(b) consists of 9 rules, there are only 5 distinct consequent sets. Since fuzzy union is implemented as mathematical addition, the firing levels of the rules with the same consequence can be summed. Therefore, the activation levels of the 5 consequents are as follows :

Firing Strength	$\rightarrow$	Consequent
$\tilde{f}_{11} \times \tilde{f}_{21} = [0, \frac{0.3750(1.2-\omega)}{1.6}]$	$\rightarrow$	-2
$\tilde{f}_{11} \times \tilde{f}_{22} + \tilde{f}_{12} \times \tilde{f}_{21} = [0, \frac{1.5750-0.6250\omega}{1.6}]$	$\rightarrow$	-1
$\tilde{f}_{11} \times \tilde{f}_{23} + \tilde{f}_{12} \times \tilde{f}_{22} + \tilde{f}_{13} \times \tilde{f}_{21} = [0, \frac{1.45+\omega}{1.6}]$	$\rightarrow$	0
$\tilde{f}_{12} \times \tilde{f}_{23} + \tilde{f}_{13} \times \tilde{f}_{22} = [0, \frac{0.3750+1.3750\omega}{1.6}]$	$\rightarrow$	1
$\tilde{f}_{13} \times \tilde{f}_{23} = [0, \frac{0.3750\omega}{1.6}]$	$\rightarrow$	2

$$\tag{5.11}$$

The output of the inference engine is :

$$
Y = \frac{-2 \times f_1 - 1 \times f_2 + 0 \times f_3 + 1 \times f_4 + 2 \times f_5}{f_1 + f_2 + f_3 + f_4 + f_5} = [y_l, \, y_r]
\tag{5.12}
$$

where y_l is the lower bound of the interval type-1 set Y, y_r is the upper bound of Y and

$$f_1 \in [0, \tfrac{0.3750(1.2-\omega)}{1.6}]$$

$$f_2 \in [0, \tfrac{1.5750-0.6250\omega}{1.6}]$$

$$f_3 \in [0, \tfrac{1.45+\omega}{1.6}]$$

$$f_4 \in [0, \tfrac{0.3750+1.3750\omega}{1.6}]$$

$$f_5 \in [0, \tfrac{0.3750\omega}{1.6}]$$

Equation (5.12) can be simplified to :

$$Y = \frac{-2f_1 - f_2 + f_4 + 2f_5}{f_1 + f_2 + f_3 + f_4 + f_5} = [y_l, \, y_r] \tag{5.13}$$

y_l and y_r are, respectively, the smallest and largest values in the set found by substituting all possible combinations of points in the firing sets into Equation (5.13). Since the lower bounds of the firing sets are all zeros, the smallest value in the set Y corresponds to the case where only the f_i corresponding to the smallest coefficient is non-zero and all other f_i are zeros. This may be understood as that only the rules with the smallest consequent are fired while the firing levels of all other rules are zero. In the numerator of Equation (5.13), f_1 has the smallest coefficient. Furthermore, $f_1 = \frac{0.3750(1.2-\omega)}{1.6} > 0$ when $\omega \in [0, 0.2]$ so the minimum value correspond to the case where only f_1 is non-zero and positive. Setting $f_2 = f_3 = f_4 = f_5 = 0$ in Equation (5.13), $y_l = \frac{-2f_1 - f_2 + f_4 + 2f_5}{f_1 + f_2 + f_3 + f_4 + f_5} = \frac{-2f_1}{f_1} = -2$.

Similar arguments can be made to deduce y_r. In this case the f_i corresponding to the largest coefficient should be non-zero while all other f_i are zeros. f_5 has the largest coefficient in the numerator of Equation (5.13). When $f_1 = f_2 = f_3 = f_4 = 0$ and $\omega \neq 0$ such that $f_5 = \frac{0.3750\omega}{1.6} > 0$, $y_r = \frac{-2f_1 - f_2 + f_4 + 2f_5}{f_1 + f_2 + f_3 + f_4 + f_5} = \frac{2f_5}{f_5} = 2$. However, the derivation fails when $\omega = 0$ because $f_5 = 0$. For the special case of $\omega = 0$,

the combination of f_i terms that produces y_r is $f_4 > 0$ and $f_1 = f_2 = f_3 = 0$ so $y_r = \frac{-2f_1 - f_2 + f_4 + 2f_5}{f_1 + f_2 + f_3 + f_4 + f_5} = \frac{f_4}{f_4} = 1$. In summary :

$$y_l = -2, \qquad w \in [0, 0.2] \tag{5.14}$$

and

$$y_r = \begin{cases} 1, & w = 0 \\ 2, & w \in (0, 0.2] \end{cases} \tag{5.15}$$

Consequently, the output $\dot{u}$ is :

$$\dot{u} = \frac{y_l + y_r}{2} = \begin{cases} \frac{-2+1}{2} = -0.5, & w = 0 \\ \frac{-2+2}{2} = 0, & w \in (0, 0.2] \end{cases} \tag{5.16}$$

Equation (5.16) indicates that there is a discontinuity at $\omega = 0$ or $e = -0.6 + \omega = -0.6$. The analytical result is consistent with the findings from the plots shown in Figure 5.15(b). This study indicates that the discontinuities in the input-output map may occur at the point where the lower bounds of all the firing sets are zeros and the upper bound of the firing set corresponding to the largest or smallest consequent changes from zero to a positive value.

5.4 Concluding Remarks

In this Chapter, the original concepts of ET1Ss and ET1FLSs are introduced and the procedures to identify them are proposed. ET1Ss and ET1FLSs are then used as a tool for analyzing the characteristics of type-2 FLS. The study demonstrated that the FOU may be viewed as a collection of ET1Ss. For a given input vector, the type-reducer chooses a corresponding ET1FLS. Since type-2 FLSs has the ability to switch between its ET1FLSs according to the input, more complex input-output map than that of a single type-1 FLS can be modeled. Results

reported herein may also help in determining the best FOU and designing new type-reducers to meet specific requirements. In addition, the concepts of ET1Ss and ET1FLSs provide a framework for extending the entire wealth of type-1 fuzzy control/identification/design/analysis techniques to type-2 systems.

Chapter 6

Analysis of Interval Type-2 Fuzzy PI Controllers

It has been shown in Chapters 3 and 4 that the control surface of a type-2 FLC may be smoother than its type-1 counterpart, especially in the area around the origin. This may be the reason why type-2 FLCs are generally better able to eliminate oscillations. Utilizing the concept of ET1Ss proposed in Chapter 5, the control surface of a type-2 FLC can be analyzed mathematically.

This Chapter focuses on using ET1Ss as a tool for analyzing the characteristics of a type-2 fuzzy Proportional plus Integral (PI) controller. The work is meaningful as control engineering is one of the most active and fruitful application of fuzzy set theory. The analysis is performed by first determining the equivalent PI gains in a fuzzy partition. By examining the equivalent PI gains, insights into why type-2 FLCs are better at handling modeling uncertainties are obtained.

The rest of this Chapter is organized as follows: Section 6.1 introduces the type-2 fuzzy PI controller used in this paper. A theorem on how shifting the consequent sets affect the output of a type-2 FLS is also introduced. Section 6.2 presents the equivalent Proportional and Integral gains of the type-2 fuzzy PI controller. The equivalent Proportional and Integral gains are then used to explain several traits of the type-2 fuzzy PI controller in Section 6.3. Finally, conclusions are drawn in Section 6.4.

6.1 Type-2 Fuzzy PI Controllers

The structure of the type-2 fuzzy PI controller analyzed in this Chapter is similar to the Mamdani FLC. The two inputs are also e and $\dot{e}$, and the output signal is $\dot{u}$. Instead of type-1 sets, the e and $\dot{e}$ domains are partitioned by interval type-2 fuzzy sets, as illustrated in Fig. 6.1. The consequent part of the fuzzy rules in the inference engine are type-1 fuzzy sets with centroid located at

$$\dot{u}_{ij} = K_I \cdot P_{e_i} + K_P \cdot P_{\dot{e}_j} \qquad i, j = 1, 2, \ldots, N \qquad (6.1)$$

where K_P and K_I are constants. P_{e_i} and $P_{\dot{e}_j}$ are the apexes of the embedded type-1 sets lying midway between the upper and lower MFs (the bold lines in Fig. 6.1). The architecture of the type-2 fuzzy PI controller is designed such that it reduces to a type-1 FLC, whose behavior is well-known, when the FOUs reduce to zero. In this case, the type-1 FLC obtained when $FOU = 0$ is equivalent to a PI controller, with proportional and integral gains of K_P and K_I respectively, under "Product-Sum-Gravity Method" inference. The type-1 FLC is used as a basis for studying the behavior of a type-2 fuzzy PI controller. Before presenting the main results, a theorem showing that the output of a type-2 FLS may be shifted is introduced.
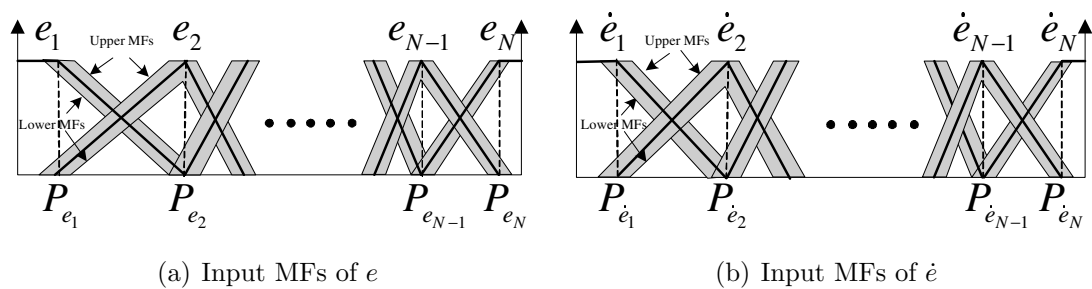

(a) Input MFs of e (b) Input MFs of $\dot{e}$

Figure 6.1: Input MFs of the fuzzy PI controllers

6.1.1 Shift Property

Theorem 1 *Let* $\widetilde{FLS}_1$ *be a N-inputs single-output type-2 FLS whose inference engine comprises q rules of the following form :*

$$\widetilde{R}_1^{i_1 i_2 \ldots i_N}(\widetilde{R}_1^k): \quad \text{If } x_1 \text{ is } \widetilde{X}_{i_1} \text{ and } x_2 \text{ is } \widetilde{X}_{i_2} \text{ and} \cdots \text{and } x_N \text{ is } \widetilde{X}_{i_N}$$

$$\text{then } y \text{ is } Y_{1,i_1 i_2 \ldots i_N}$$

$\widetilde{X}_{i_j}$ *($j = 1 \ldots N$) are interval type-2 fuzzy sets that partition the N input domains.* $Y_{1,i_1 i_2 \ldots i_N}$ *is a type-1 fuzzy set whose centroid is located at* Y_k *($k = 1, \ldots, q$). It is assumed that the rules are enumerated such that* $Y_1 < \ldots < Y_k < \ldots Y_q$.

Suppose $\widetilde{FLS}_2$ *is another type-2 FLS whose input spaces are characterized by exactly the same type-2 fuzzy sets as* $\widetilde{FLS}_1$. *The q consequent sets are the output sets for* $\widetilde{FLS}_1$ *shifted uniformly by a non-zero constant* γ *(γ may be positive or negative). In summary, the q rules of* $\widetilde{FLS}_2$ *assume the following form :*

$$\widetilde{R}_2^{i_1 i_2 \ldots i_N}(\widetilde{R}_2^k): \quad \text{If } x_1 \text{ is } \widetilde{X}_{i_1} \text{ and } x_2 \text{ is } \widetilde{X}_{i_2} \text{ and} \cdots \text{and } x_N \text{ is } \widetilde{X}_{i_N}$$

$$\text{then } y \text{ is } Y_{2,i_1 i_2 \ldots i_N}$$

The centroids for $Y_{2,i_1 i_2 \ldots i_N}$ *are located at* $Y_k - \gamma$.

Then, for the same input vector $(x_1, x_2, \ldots, x_N)$, *the output of* $\widetilde{FLS}_2$ *($y_{\widetilde{FLS}_2}$) is equal to* $y_{\widetilde{FLS}_1} - \gamma$, *where* $y_{\widetilde{FLS}_1}$ *is the output of* $\widetilde{FLS}_1$.

Proof : Suppose the input vector is $(x_1, x_2, \ldots, x_N)$. Then, the firing set associated with the kth ($\widetilde{R}_1^{i_1 i_2 \ldots i_N}$) rule of $\widetilde{FLS}_1$ is the interval type-1 set

$$\tilde{f}_k = [\underline{f}_k(x_1, x_2, \ldots, x_N), \overline{f}_k(x_1, x_2, \ldots, x_N)] \equiv [\underline{f}_k, \overline{f}_k] \tag{6.2}$$

where $\underline{f}_k = \underline{\mu}_{\widetilde{X}_{i_1}}(x_1) \star \ldots \star \underline{\mu}_{\widetilde{X}_{i_N}}(x_N)$ and $\overline{f}_k = \overline{\mu}_{\widetilde{X}_{i_1}}(x_1) \star \ldots \star \overline{\mu}_{\widetilde{X}_{i_N}}(x_N)$. Using center-of-sets type reduction, the type-reduced output set of $\widetilde{FLS}_1$ is the following

interval type-1 set :

$$[y_{\widehat{FLS}_1,l}, y_{\widehat{FLS}_1,r}] = \int_{f_1 \in [\underline{f}_1, \overline{f}_1]} \cdots \int_{f_q \in [\underline{f}_q, \overline{f}_q]} 1 \left| \frac{\sum_{k=1}^q f_k Y_k}{\sum_{k=1}^q f_k} \right. \tag{6.3}$$

The Karnik-Mendel iterative method is usually used to determine the bounds. $y_{\widehat{FLS}_1,l}$ and $y_{\widehat{FLS}_1,r}$ are, respectively, the smallest and largest centroid of all the embedded type-1 sets associated with the type-2 output set. It has been proved that the embedded type-1 sets that lead to $y_{\widehat{FLS}_1,l}$ and $y_{\widehat{FLS}_1,r}$ only involve the lower and upper MFs, and there is only one switch between them [89, 90]. Hence, $y_{\widehat{FLS}_1,l}$ and $y_{\widehat{FLS}_1,r}$ can be expressed mathematically as follows :

$$y_{\widehat{FLS}_1,l} = \min_{L \in 1,\ldots,q} \left(\frac{\sum_{k=1}^L \overline{f}_k Y_k + \sum_{k=L+1}^q \underline{f}_k Y_k}{\sum_{k=1}^L \overline{f}_k + \sum_{k=L+1}^q \underline{f}_k} \right) \tag{6.4a}$$

$$y_{\widehat{FLS}_1,r} = \max_{R \in 1,\ldots,q} \left(\frac{\sum_{k=1}^R \underline{f}_k Y_k + \sum_{k=R+1}^q \overline{f}_k Y_k}{\sum_{k=1}^R \underline{f}_k + \sum_{k=R+1}^q \overline{f}_k} \right) \tag{6.4b}$$

The defuzzified output of $\widehat{FLS}_1$ is then

$$y_{\widehat{FLS}_1} = \frac{y_{\widehat{FLS}_1,l} + y_{\widehat{FLS}_1,r}}{2} \tag{6.5}$$

Since the antecedents for both FLSs are identical, the firing set associated with the kth ($\widetilde{R}_2^{i_1 i_2 \ldots i_N}$) rule of $\widehat{FLS}_2$ is the expression in Equation (6.2). The centroids of the consequent type-1 sets are uniformly shifted by γ so the bounds of the

type-reduced output set is :

$$
\begin{aligned}
y_{\widetilde{FLS}_2,l} &= \min_{L \in 1,\ldots,q} \left(\frac{\sum_{k=1}^{L} \overline{f}_k(Y_k - \gamma) + \sum_{k=L+1}^{q} \underline{f}_k(Y_k - \gamma)}{\sum_{k=1}^{L} \overline{f}_k + \sum_{k=L+1}^{q} \underline{f}_k} \right) \\
&= \min_{L \in 1,\ldots,q} \left(\frac{\sum_{k=1}^{L} \overline{f}_k Y_k + \sum_{k=L+1}^{q} \underline{f}_k Y_k}{\sum_{k=1}^{L} \overline{f}_k + \sum_{k=L+1}^{q} \underline{f}_k} - \gamma \right) \\
&= \min_{L \in 1,\ldots,q} \left(\frac{\sum_{k=1}^{L} \overline{f}_k Y_k + \sum_{k=L+1}^{q} \underline{f}_k Y_k}{\sum_{k=1}^{L} \overline{f}_k + \sum_{k=L+1}^{q} \underline{f}_k} \right) - \gamma \\
&= y_{\widetilde{FLS}_1,l} - \gamma \qquad\qquad\qquad\qquad\qquad (6.6a) \\
y_{\widetilde{FLS}_2,r} &= \max_{R \in 1,\ldots,q} \left(\frac{\sum_{k=1}^{R} \underline{f}_k(Y_k - \gamma) + \sum_{k=R+1}^{q} \overline{f}_k(Y_k - \gamma)}{\sum_{k=1}^{R} \underline{f}_k + \sum_{k=R+1}^{q} \overline{f}_k} \right) \\
&= y_{\widetilde{FLS}_1,r} - \gamma \qquad\qquad\qquad\qquad\qquad (6.6b)
\end{aligned}
$$

Thus, the output of $\widetilde{FLS}_2$ is :

$$
y_{\widetilde{FLS}_2} = \frac{y_{\widetilde{FLS}_2,l} + y_{\widetilde{FLS}_2,r}}{2} = \frac{y_{\widetilde{FLS}_1,l} - \gamma + y_{\widetilde{FLS}_1,r} - \gamma}{2} = \frac{y_{\widetilde{FLS}_1,l} + y_{\widetilde{FLS}_1,r}}{2} - \gamma = y_{\widetilde{FLS}_1} - \gamma
$$

$$(6.7)$$

which is the output of $\widetilde{FLS}_1$ shifted by γ.

The theorem is useful because the input-output relationship corresponding to a particular fuzzy partition of a FLS may be analyzed by shifting the input sets to a more convenient point i.e.

$$
y_{\widetilde{FLS}_1}(x_1, \ldots x_N) = y_{\widetilde{FLS}_2}(x'_1, \ldots x'_N) - \gamma \qquad\qquad (6.8)
$$

where $x_i = x'_i - \Gamma_i$ $(i = 1, \ldots, N)$ and Γ_i is a constant.

Consider the type-2 fuzzy PI controller described in Section 6.1, and denoting it as $\widetilde{FLC}_1$. Suppose the input vector $(e, \dot{e})$, where $P_{e_i} \leq e \leq P_{e_{i+1}}$ and $P_{\dot{e}_j} \leq \dot{e} \leq P_{\dot{e}_{j+1}}$, fires the four type-2 sets labeled as $\tilde{e}_i$, $\tilde{e}_{i+1}$, $\tilde{\dot{e}}_j$ and $\tilde{\dot{e}}_{j+1}$ in Fig. 6.2(a). The shaded regions are the FOU, while the dark thick lines are the MFs of type-1 sets when FOU is reduced to zero. As defined by Equation (6.1), the consequent sets

are type-1 fuzzy sets whose centroids are located at :

$$\dot{u}_{i,j} = K_I P_{e_i} + K_P P_{\dot{e}_j}$$

$$\dot{u}_{i+1,j} = K_I P_{e_{i+1}} + K_P P_{\dot{e}_j}$$

$$\dot{u}_{i,j+1} = K_I P_{e_i} + K_P P_{\dot{e}_{j+1}}$$

$$\dot{u}_{i+1,j+1} = K_I P_{e_{i+1}} + K_P P_{\dot{e}_{j+1}}$$

Consider another type-2 fuzzy PI controller ($\widetilde{FLC}_2$) with antecedent sets shown in Fig. 6.2(b). The type-2 sets are generated by shifting the input sets of $\widetilde{FLC}_1$ ($\tilde{e}_i$, $\tilde{e}_{i+1}$, $\tilde{\dot{e}}_j$ and $\tilde{\dot{e}}_{j+1}$) such that the resulting fuzzy partition is centered at the origin. Let the centroids of the consequent sets for $\widetilde{FLC}_2$ be :

$$\dot{u}'_{i,j} = K_I P'_{e_i} + K_P P'_{\dot{e}_j} = K_I(P_{e_i} - d_e) + K_P(P_{\dot{e}_j} - d_{\dot{e}}) = \dot{u}_{i,j} - \gamma$$

$$\dot{u}'_{i+1,j} = K_I P'_{e_{i+1}} + K_P P'_{\dot{e}_j} = K_I(P_{e_{i+1}} - d_e) + K_P(P_{\dot{e}_j} - d_{\dot{e}}) = \dot{u}_{i+1,j} - \gamma$$

$$\dot{u}'_{i,j+1} = K_I P'_{e_i} + K_P P'_{\dot{e}_{j+1}} = K_I(P_{e_i} - d_e) + K_P(P_{\dot{e}_{j+1}} - d_{\dot{e}}) = \dot{u}_{i,j+1} - \gamma$$

$$\dot{u}'_{i+1,j+1} = K_I P'_{e_{i+1}} + K_P P'_{\dot{e}_{j+1}} = K_I(P_{e_{i+1}} - d_e) + K_P(P_{\dot{e}_{j+1}} - d_{\dot{e}}) = \dot{u}_{i+1,j+1} - \gamma$$

where $\gamma = (K_I d_e + K_P d_{\dot{e}})$, $d_e = \frac{P_{e_i} + P_{e_{i+1}}}{2}$ and $d_{\dot{e}} = \frac{P_{\dot{e}_j} + P_{\dot{e}_{j+1}}}{2}$. According to the theorem, the output of $\widetilde{FLC}_2$ is smaller than that of $\widetilde{FLC}_1$ by γ if the input vector is $(e', \dot{e}') = (e - d_e, \dot{e} - d_{\dot{e}})$. This relationship between $\widetilde{FLC}_1$ and $\widetilde{FLC}_2$ implies that any results derived for the antecedent sets shown in Fig. 6.2(b) can be extended to fuzzy partitions that are not symmetrical about zero. For this reason, the remaining sections of this Chapter only focuses on input spaces that are centered on the origin.
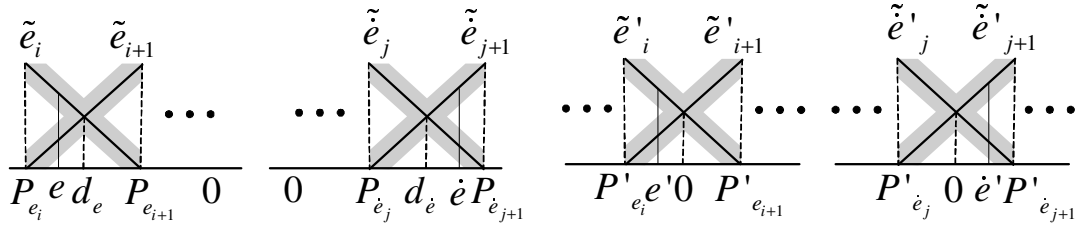
(a) Fuzzy sets that are not centered around the origin (b) Fuzzy sets that are symmetrical about the origin

Figure 6.2: Illustration of shift invariant property

6.2 Equivalent Proportional and Integral Gains of a Type-2 FLC

This section aims at providing insights into the characteristics of a type-2 fuzzy PI controller. The type-2 fuzzy PI controller is essentially a non-linear PI controller that reduces to the classical PI controller when FOU is zero. As its behavior can be analyzed by examining how the equivalent proportional and integral gains vary with input and FOU sizes, the first step is to derive expressions for the equivalent proportional and integral gains. Fig. 6.3 shows the symmetric type-2 sets used in this study, where $P_{e_1} = P_{\dot{e}_1} = -D$ and $P_{e_2} = P_{\dot{e}_2} = D$. As defined in Equation (6.1), the centroids of the type-1 consequent sets are placed at :

$$\dot{u}_{11} = -K_I D - K_P D \tag{6.9a}$$

$$\dot{u}_{12} = -K_I D + K_P D \tag{6.9b}$$

$$\dot{u}_{21} = K_I D - K_P D \tag{6.9c}$$

$$\dot{u}_{22} = K_I D + K_P D \tag{6.9d}$$

First, consider the input space that is bounded by the following inequalities :

$$|e| \leq D - d \tag{6.10}$$

$$|\dot{e}| \leq D - d \tag{6.11}$$

(a) Input MFs of e (b) Input MFs of $\dot{e}$
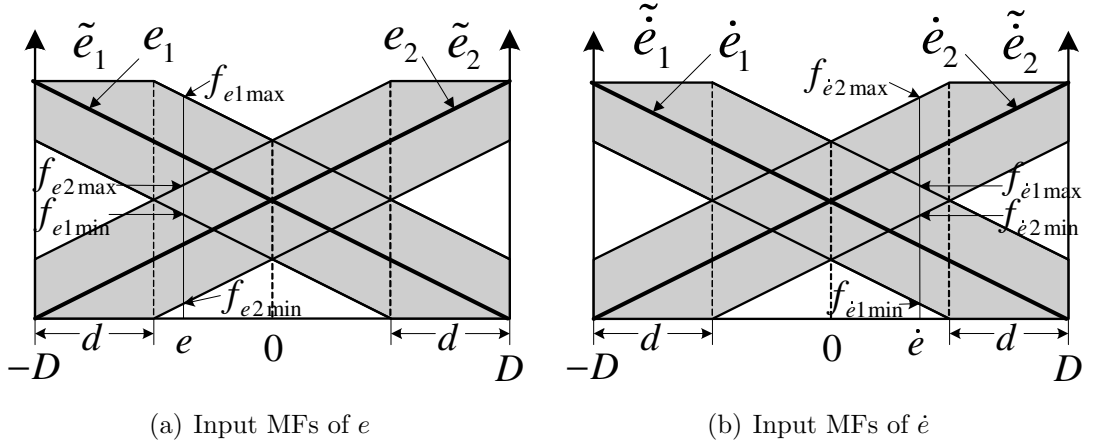
Figure 6.3: Input MFs of the type-2 fuzzy PI controller

A graphical illustration of the region is shown in Fig. 6.4. In this domain, the firing levels corresponding to the input vector $(e, \dot{e})$ are as follows:

$$
\begin{aligned}
f_{\tilde{e}_1} = [f_{e_{1min}}, f_{e_{1max}}] &= \left[\frac{D - d - e}{2D}, \frac{D + d - e}{2D} \right] \\
f_{\tilde{e}_2} = [f_{e_{2min}}, f_{e_{2max}}] &= \left[\frac{e + D - d}{2D}, \frac{e + D + d}{2D} \right] \\
f_{\tilde{\dot{e}}_1} = [f_{\dot{e}_{1min}}, f_{\dot{e}_{1max}}] &= \left[\frac{D - d - \dot{e}}{2D}, \frac{D + d - \dot{e}}{2D} \right] \\
f_{\tilde{\dot{e}}_2} = [f_{\dot{e}_{2min}}, f_{\dot{e}_{2max}}] &= \left[\frac{\dot{e} + D - d}{2D}, \frac{\dot{e} + D + d}{2D} \right]
\end{aligned}
\tag{6.12}
$$

Figure 6.4: The region of the input domain determined by Inequalities (6.10) and (6.11)

The firing set associated with the four rules are :

$$\tilde{f}_{11} = f_{\tilde{e}_1} \star f_{\dot{\tilde{e}}_1} = [\underline{f}_{11}, \overline{f}_{11}] \tag{6.13a}$$

$$= \left[\frac{(D-d-e)(D-d-\dot{e})}{4D^2}, \frac{(D+d-e)(D+d-\dot{e})}{4D^2} \right] \tag{6.13b}$$

$$\tilde{f}_{12} = f_{\tilde{e}_1} \star f_{\dot{\tilde{e}}_2} = [\underline{f}_{12}, \overline{f}_{12}] \tag{6.13c}$$

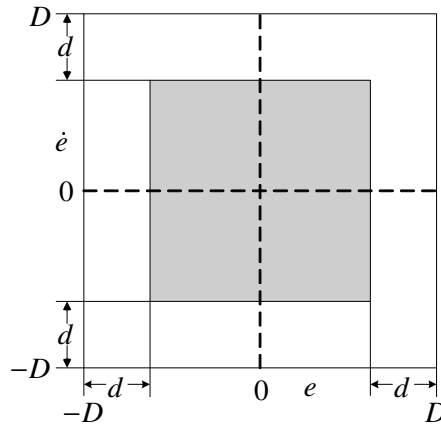$$= \left[\frac{(D-d-e)(D-d+\dot{e})}{4D^2}, \frac{(D+d-e)(D+d+\dot{e})}{4D^2} \right] \tag{6.13d}$$

$$\tilde{f}_{21} = f_{\tilde{e}_2} \star f_{\dot{\tilde{e}}_1} = [\underline{f}_{21}, \overline{f}_{21}] \tag{6.13e}$$

$$= \left[\frac{(D-d+e)(D-d-\dot{e})}{4D^2}, \frac{(D+d+e)(D+d-\dot{e})}{4D^2} \right] \tag{6.13f}$$

$$\tilde{f}_{22} = f_{\tilde{e}_2} \star f_{\dot{\tilde{e}}_2} = [\underline{f}_{22}, \overline{f}_{22}] \tag{6.13g}$$

$$= \left[\frac{(D-d+e)(D-d+\dot{e})}{4D^2}, \frac{(D+d+e)(D+d+\dot{e})}{4D^2} \right] \tag{6.13h}$$

Using center-of-sets type reduction, the type-reduced output of the inference engine for the type-2 fuzzy PI controller is the following interval type-1 set :

$$\tilde{\dot{u}} = \frac{\tilde{f}_{11}\dot{u}_{11} + \tilde{f}_{12}\dot{u}_{12} + \tilde{f}_{21}\dot{u}_{21} + \tilde{f}_{22}\dot{u}_{22}}{\tilde{f}_{11} + \tilde{f}_{12} + \tilde{f}_{21} + \tilde{f}_{22}} = [\dot{u}_l, \ \dot{u}_r]$$

The bounds of the interval type-1 set, $\dot{u}_l$ and $\dot{u}_r$, may be found using the Karnik-Mendel iterative procedure. The algorithm first arranges the centroid of the consequent sets, $\dot{u}_{ij}$ (Equation (6.9)), in ascending/descending order. As the relative positions of the centroids depend on K_P and K_I, two cases need to be considered.

6.2.1   Case 1 : $K_P \geq K_I$

In this case, $\dot{u}_{11} \leq \dot{u}_{21} \leq \dot{u}_{12} \leq \dot{u}_{22}$. To derive closed-form solutions for the equivalent Proportional and Integral gains, it is necessary to express the Karnik-Mendel type reducer in closed-form. A closed-from expression cannot be derived for the general case. Nevertheless, the problem can be simplified by imposing the

following constraint :

$$\dot{u}_{21} \leq \dot{u}_l \leq \dot{u}_r \leq \dot{u}_{12} \tag{6.14}$$

Theorem 1 in [90] proves that the switch points that lead to the bounds of the type-reduced set $[\dot{u}_l, \dot{u}_r]$ coincides with the centroid of the corresponding embedded type-1 set. Hence, Equation (6.14) dictates that the switch points will occur between $\dot{u}_{12}$ and $\dot{u}_{21}$. Substituting $L = 2$ and $R = 2$ into Equations (6.4a) and (6.4b), the bounds of the type-reduced set may be expressed as :

$$\dot{u}_l = \frac{\overline{f}_{11}\dot{u}_{11} + \overline{f}_{21}\dot{u}_{21} + \underline{f}_{12}\dot{u}_{12} + \underline{f}_{22}\dot{u}_{22}}{\overline{f}_{11} + \overline{f}_{21} + \underline{f}_{12} + \underline{f}_{22}} \tag{6.15}$$

$$= \frac{-2D^2 dK_P + D^2 K_I e + D^2 K_P \dot{e}}{D^2 + d^2 - \dot{e}d} \tag{6.16}$$

$$\dot{u}_r = \frac{\underline{f}_{11}\dot{u}_{11} + \underline{f}_{21}\dot{u}_{21} + \overline{f}_{12}\dot{u}_{12} + \overline{f}_{22}\dot{u}_{22}}{\underline{f}_{11} + \underline{f}_{21} + \overline{f}_{12} + \overline{f}_{22}} \tag{6.17}$$

$$= \frac{2D^2 dK_P + D^2 K_I e + D^2 K_P \dot{e}}{D^2 + d^2 + \dot{e}d} \tag{6.18}$$

Hence, the output of the type-2 FLC is :

$$\begin{aligned}
\dot{u} &= \frac{\dot{u}_l + \dot{u}_r}{2} \\
&= \frac{D^2(D^2 - d^2)K_P \dot{e} + D^2(D^2 + d^2)K_I e}{(D^2 + d^2)^2 - d^2\dot{e}^2} \\
&= \frac{D^2(D^2 - d^2)K_P}{(D^2 + d^2)^2 - \dot{e}^2 d^2}\dot{e} + \frac{D^2(D^2 + d^2)K_I}{(D^2 + d^2)^2 - \dot{e}^2 d^2}e \\
&= \alpha K_P \dot{e} + \beta K_I e \tag{6.19}
\end{aligned}$$

where

$$\alpha = \frac{D^2(D^2 - d^2)}{(D^2 + d^2)^2 - \dot{e}^2 d^2} \tag{6.20}$$

$$\beta = \frac{D^2(D^2 + d^2)}{(D^2 + d^2)^2 - \dot{e}^2 d^2} \tag{6.21}$$

αK_p is the *equivalent Proportional gain* of the resulting type-2 FLC and βK_I is the *equivalent Integral gain*. Equations (6.20) and (6.21) show that the equivalent

Proportional and Integral gains will be smaller than those of the baseline type-1 fuzzy PI controller when $|\dot{e}| \leq \sqrt{D^2 + d^2}$ since both α and β are smaller than unity. The relationships between α, β and $\dot{e}$ for different FOU sizes (d) are shown in Fig. 6.7. Here $D = 1$. The plot indicates that the values of α and β, and consequently the equivalent Proportional and Integral gains, will become smaller as the input vector approaches the origin. Since smaller PI parameters give rise to more sluggish performances, the conclusion is consistent with experimental observations suggesting that a type-2 fuzzy PI controller is better able to eliminate steady-state oscillations [70, 83, 91, 92].
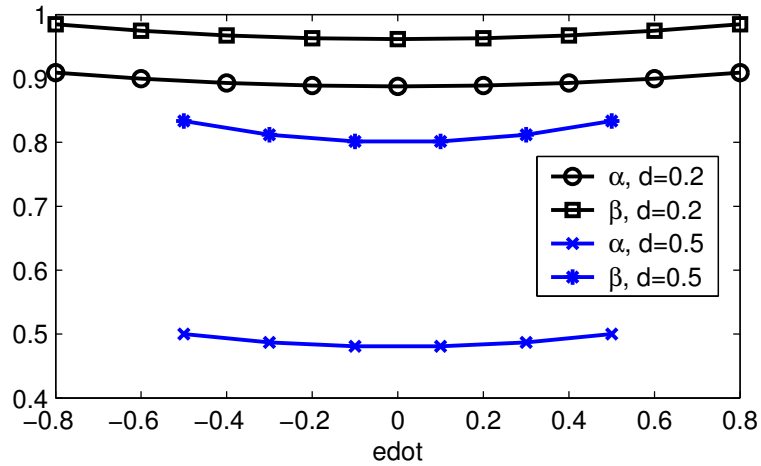
Figure 6.5: Relationship between α, β and $\dot{e}$

6.2.2 Case 2 : $K_I \geq K_P$

When $K_I > K_P$, then $\dot{u}_{11} \leq \dot{u}_{12} \leq \dot{u}_{21} \leq \dot{u}_{22}$. Under the assumption that $\dot{u}_{12} \leq \dot{u}_l \leq \dot{u}_r \leq \dot{u}_{21}$, the bounds of the type-reduced set may be written as

$$\dot{u}_l = \frac{\overline{f}_{11}\dot{u}_{11} + \overline{f}_{12}\dot{u}_{12} + \underline{f}_{21}\dot{u}_{21} + \underline{f}_{22}\dot{u}_{22}}{\overline{f}_{11} + \overline{f}_{12} + \underline{f}_{21} + \underline{f}_{22}} \quad (6.22)$$

$$\dot{u}_r = \frac{\underline{f}_{11}\dot{u}_{11} + \underline{f}_{12}\dot{u}_{12} + \overline{f}_{21}\dot{u}_{21} + \overline{f}_{22}\dot{u}_{22}}{\underline{f}_{11} + \underline{f}_{12} + \overline{f}_{21} + \overline{f}_{22}} \quad (6.23)$$

By repeating the mathematical manipulations described in the previous sub-section, the output of the type-2 fuzzy PI controller is found to be :

$$\dot{u} = \alpha' K_P \dot{e} + \beta' K_I e \tag{6.24}$$

where

$$\alpha' = \frac{D^2(D^2 + d^2)}{(D^2 + d^2)^2 - e^2 d^2} \tag{6.25}$$

$$\beta' = \frac{D^2(D^2 - d^2)}{(D^2 + d^2)^2 - e^2 d^2} \tag{6.26}$$

Again, $\alpha' K_p$ is the *equivalent Proportional gain* and $\beta' K_I$ is the *equivalent Integral gain*. It may be observed that there are the following differences between Equation (6.19) and Equation (6.24) :

1. $\dot{e}$ in the denominator of α and β is replaced by e in the denominator of α' and β'.

2. The numerators of Equation (6.24) are interchanged, compared with those in Equation (6.19).

Since the equivalent Proportional and Integral gains in Equation (6.19) and Equation (6.24) are similar, it is sufficient to focus only on one of the two cases.

6.2.3 Range Where Equivalent Gains Are Valid

In order to derive closed-form expressions for the equivalent Proportional and Integral gains, Equation (6.14) was introduced. The condition imposes a constrain on the input region where the equations for the equivalent Proportional and Integral gains are valid. This subsection presents the accurate input ranges where Equation (6.19) is applicable.

Consider the first part of Equation (6.14), which states that $\dot{u}_{21} \leq \dot{u}_l$. For the case where $K_P > K_I$, $\dot{u}_l = \frac{\overline{f}_{11}\dot{u}_{11}+\overline{f}_{21}\dot{u}_{21}+\underline{f}_{12}\dot{u}_{12}+\underline{f}_{22}\dot{u}_{22}}{\overline{f}_{11}+\overline{f}_{21}+\underline{f}_{12}+\underline{f}_{22}}$ (Equation (6.15)). Hence,

$$\frac{\overline{f}_{11}\dot{u}_{11} + \overline{f}_{21}\dot{u}_{21} + \underline{f}_{12}\dot{u}_{12} + \underline{f}_{22}\dot{u}_{22}}{\overline{f}_{11} + \overline{f}_{21} + \underline{f}_{12} + \underline{f}_{22}} \geq \dot{u}_{21}$$

$$\frac{\overline{f}_{11}\dot{u}_{11} + \underline{f}_{12}\dot{u}_{12} + \underline{f}_{22}\dot{u}_{22}}{\overline{f}_{11} + \underline{f}_{12} + \underline{f}_{22}} \geq \dot{u}_{21} \tag{6.27}$$

Replacing f_{ij} and $\dot{u}_{ij}$ $(i, j = 1, 2)$ by the expressions in Equations (6.13) and (6.9) and re-arranging, Equation (6.27) reduces to :

$$DK_I e + (dK_I + DK_P - dK_P)\dot{e} - (D^2 K_I + d^2 K_I - D^2 K_P - d^2 K_P + 2DdK_P) \geq 0 \tag{6.28}$$

Repeating the above steps for $\dot{u}_{12} \geq \dot{u}_r$, the second part of Equation (6.14), the following expression is obtained :

$$DK_I e + (dK_I + DK_P - dK_P)\dot{e} + (D^2 K_I + d^2 K_I - D^2 K_P - d^2 K_P + 2DdK_P) \leq 0 \tag{6.29}$$

Equations (6.28) and (6.29), together with Equations (6.10) and (6.11), completely define the range of e and $\dot{e}$ where the equivalent Proportional and Integral gains shown in Equation (6.19) are applicable. The corresponding constraints when $K_I > K_P$ (Equation (6.24)) are as follows :

$$DK_P\dot{e} + (DK_I + dK_P - dK_I)e + (D^2 K_I + d^2 K_I - D^2 K_P - d^2 K_P - 2DdK_I) \geq 0$$

$$DK_P\dot{e} + (DK_I + dK_P - dK_I)e - (D^2 K_I + d^2 K_I - D^2 K_P - d^2 K_P - 2DdK_I) \leq 0$$

6.3 Analysis of a Type-2 Fuzzy PI Controller

In this section, the objective is to analyze the traits of a type-2 fuzzy PI controller. As the focus is on understanding the controller characteristics and not its ability to control complex systems, the following simple first-order plus dead-time plant is

employed as the nominal system and used to design the type-2 fuzzy PI controller :

$$G(s) = \frac{K}{\tau s + 1} e^{-Ls} = \frac{1}{10s + 1} e^{-2.5s} \qquad (6.30)$$

Two sets are used to characterize each input domain, e and $\dot{e}$. The type-2 sets used are shown in Fig. 6.3, where $|D| = 1$. According to the ITAE setpoint tracking tuning rule [93], the PI parameters for $G(s)$ are as follows :

$$\dot{u} = 0.586K \left(\frac{L}{\tau}\right)^{-0.916} \left[\dot{e} + \frac{1.03 - 0.165\frac{L}{\tau}}{\tau} e\right] = 2.086\dot{e} + 0.2063e \qquad (6.31)$$

Hence, centroids of the four consequent sets for the type-2 fuzzy PI controller are generated by substituting $K_P = 2.086$ and $K_I = 0.2063$ into Equation (6.9).

As $K_P > K_I$, the equivalent Proportional and Integral gains are determined by Equation (6.24). The closed-form solutions of the equivalent Proportional and Integral gains are derived using the assumption shown in Equation (6.14). Using Equations (6.28) and (6.29), Equations (6.10) and (6.11), the range in which the equivalent Proportional and Integral gains are valid when $d = 0.2$ and 0.5 are plotted and shown in Fig. 6.6. The diagram indicates that the assumption may impose further restriction on the region where the equivalent gains are valid. Fig. 6.7 shows how α, β vary with $\dot{e}$ in the range where the equivalence is valid.

Fig. 6.7 demonstrates that the extra degree of freedom provided by the FOU results in varying equivalent Proportional and Integral gains. Unlike a type-1 FLC (triangular MFs) whose input-output relationship is linear within a fuzzy partition, a type-2 fuzzy PI controller realizes a non-linear PI controller within each fuzzy partition. As the values of α and β are both smaller than unity, the equivalent Proportional and Integral gains are smaller than the PI parameters used to place the centroid of the consequent sets. The deviation from the type-1 FLC becomes
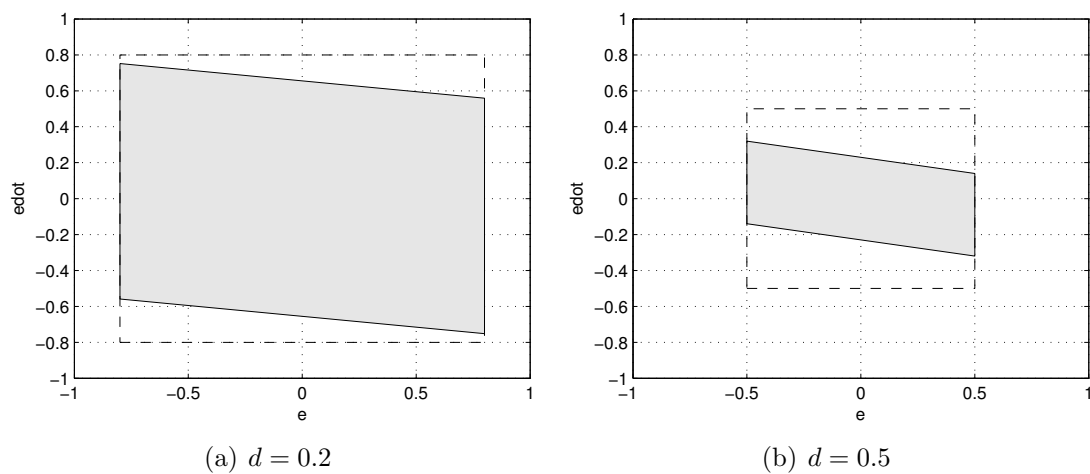
(a) $d = 0.2$ (b) $d = 0.5$

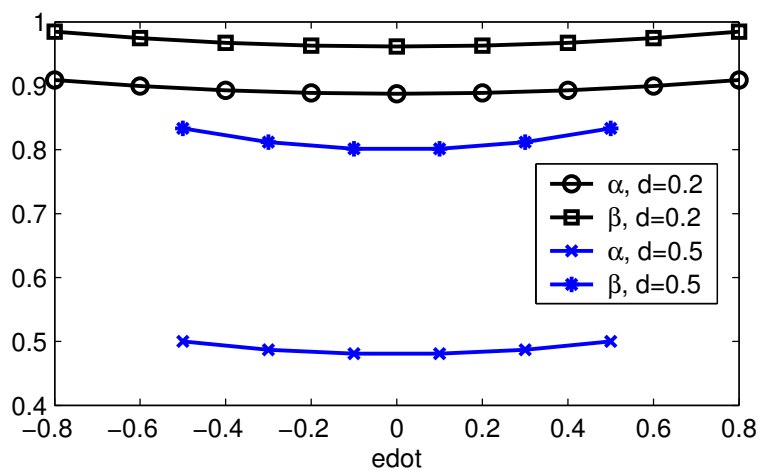Figure 6.6: The input regions where Equation (6.19) is applicable

Figure 6.7: Relationship between α, β and $\dot{e}$, where $D = 1$.

larger as d increases. This observation is supported by the partial derivative of α and β with respect to d :

$$\frac{\partial \alpha}{\partial d} = \frac{-2D^2d[(D^2+d^2)^2 + 2(D^4 - d^4) - D^2\dot{e}^2]}{[(D^2+d^2)^2 - d^2\dot{e}^2]^2} \qquad (6.32)$$

$$\frac{\partial \beta}{\partial d} = \frac{-2D^2d[(D^2+d^2)^2 - D^2\dot{e}^2]}{[(D^2+d^2)^2 - d^2\dot{e}^2]^2} \qquad (6.33)$$

$|\dot{e}| \leq D - d$ (Equation (6.10)) is a condition used to derive the equivalent Proportional and Integral gains. This condition, together with $D > 0$ mean that both $\dot{\alpha}$ and $\dot{\beta}$ are negative. Hence, an increase in d will cause the values of α and β to decrease, when the other variables are held constant.

Another interesting observation is $\alpha < \beta$. Dividing Equation (6.21) by Equation (6.20) yields

$$\frac{\beta}{\alpha} = \frac{D^2 + d^2}{D^2 - d^2} > 1 \qquad (6.34)$$

It indicates that the equivalent proportional gain decreases relatively faster, compared to the equivalent integral gain, as the FOU becomes larger. The reverse is true when $K_I > K_P$ because the following inequality may be deduced from Equations (6.25) and (6.26) :

$$\frac{\beta'}{\alpha'} = \frac{D^2 - d^2}{D^2 + d^2} < 1 \qquad (6.35)$$

In order to examine whether the equivalent gains correlate with control performances, step responses were obtained using type-2 fuzzy PI controllers for the nominal plant (Equation (6.30)) when $d = 0$ (type-1 fuzzy PI controller), $d = 0.2$ and $d = 0.5$. The plots are shown in Fig. 6.8. Fig. 6.9 contains step responses that illustrate how type-2 PI controllers ($d = 0, 0.2, 0.5$) copes with parameter uncertainty. From the diagrams, the following traits can be observed :

- The larger the FOU, the better the ability to eliminate oscillations about the setpoint (Figs 6.9(a) and 6.9(c)) [70, 83, 91, 92].

- The type-2 fuzzy PI controller cannot outperform its type-1 counterpart when the dynamics of the plant is slow (Figs. 6.9(b) and 6.9(d)).

Both characteristics may be attributed to more conservative PI parameters, which is consistent with the equivalent gains shown in Fig. 6.7. The step responses also show that differences in the control performances obtained using type-2 and type-1 fuzzy PI controllers may be small. This is because the factors that modulate the effective gains, α and β, are close to unity when d is small.
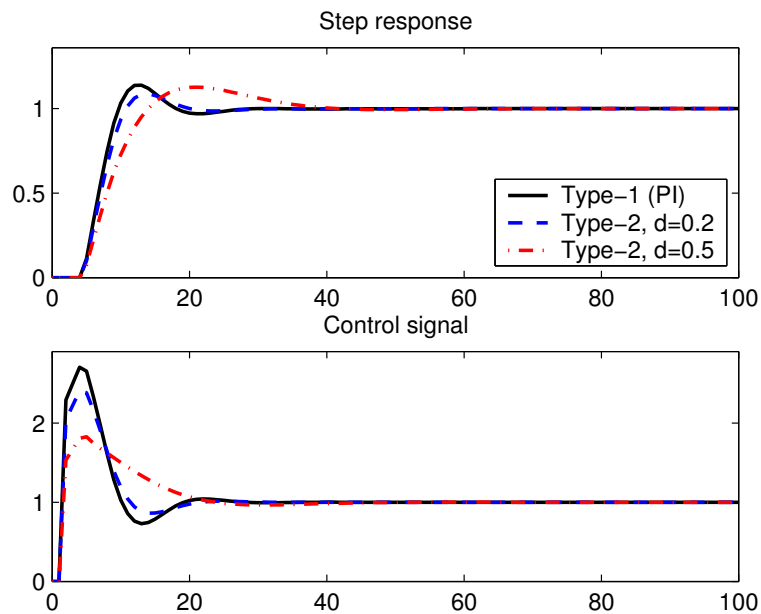
Figure 6.8: Control performances of the type-2 and type-1 fuzzy PI controllers on the nominal plant, $G(s) = \frac{Y(s)}{U(s)} = \frac{1}{10s+1}e^{-2.5s}$

6.4 Concluding Remarks

The type-2 fuzzy PI controller is introduced. By deriving and examining the equivalent Proportional and Integral gains, the impact of the additional degree of
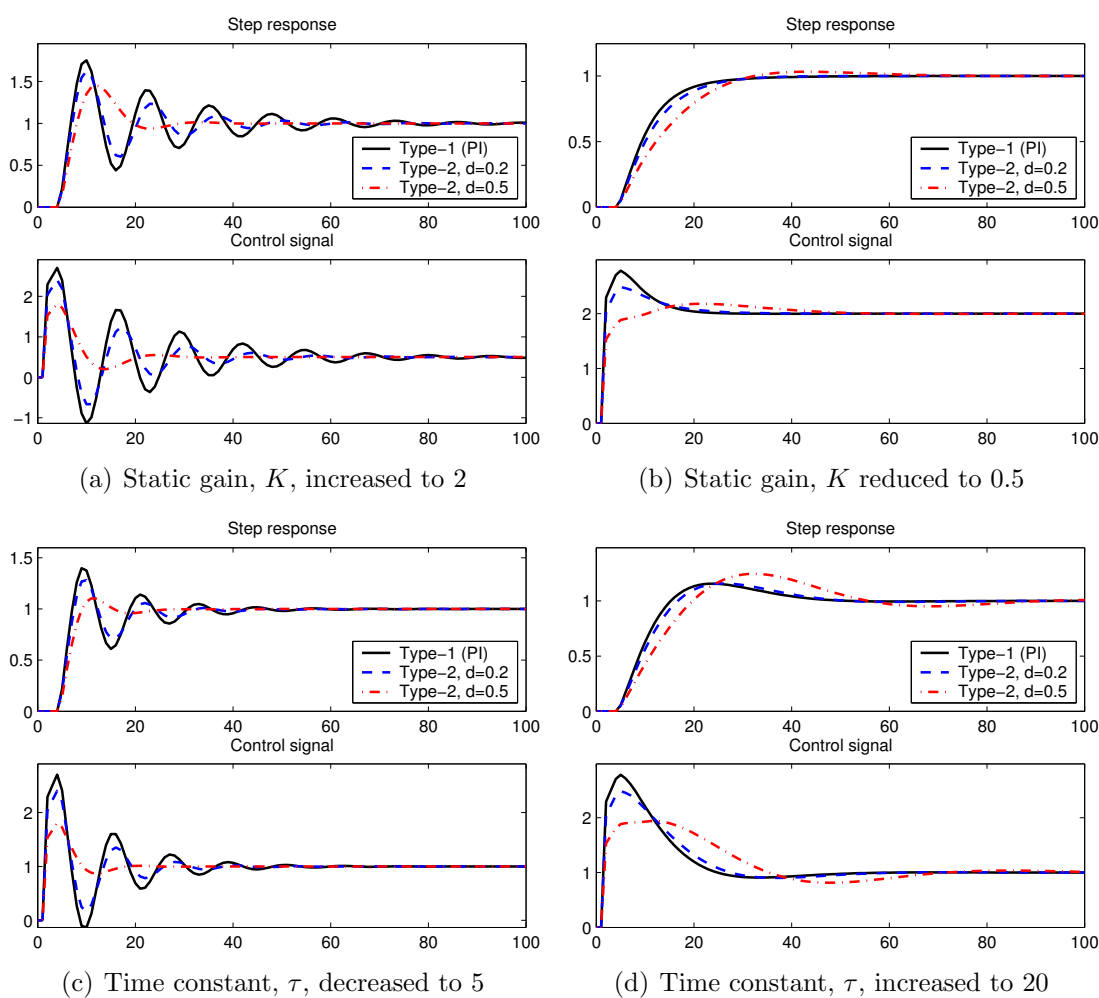
Figure 6.9: Control performances of the type-2 and type-1 fuzzy PI controllers for different plant

freedom provided by the FOU is studied. Results show that a type-2 fuzzy PI controller realizes a non-linear PI controller within each fuzzy partition. In addition, the equivalent Proportional and Integral gains of a type-2 fuzzy PI controller are smaller than the type-1 FLC obtained when the FOU is removed. Since smaller PI parameters gives rise to more sluggish performances, the findings provide theoretical explanation for the experimental observations suggesting that a type-2 fuzzy PI controller is better able to eliminate steady-state oscillations. The results presented in this Chapter is a step towards a better understanding of type-2 fuzzy PI controllers.

Chapter 7

Conclusions and Future Research Directions

In this Thesis, extensive simulations and experiments were conducted to study the properties of type-2 FLSs. The following conclusions are drawn :

1. A type-2 FLC may be able to outperform type-1 FLCs that have more design parameters. Thus, a type-2 FLC is more appealing than its type-1 counterparts with regards to accuracy and interpretability. The main advantage of a type-2 FLC appears to be its ability to eliminate persistent oscillations, especially when unmodelled dynamics were introduced. This ability to handle model uncertainties is particularly useful when FLCs are tuned offline using GA and a model as the impact of unmodelled dynamics is reduced.

2. The most important part of a type-2 PI-like FLC seems to be the MFs around the origin. Thus a simplified type-2 FLC where only the MFs near the origin are type-2 and all other MFs are type-1 may have the similar performance as a traditional type-2 FLS whose all MFs are type-2. Furthermore, the computational cost may be greatly saved. Experimental results in this Thesis verified that the simplified type-2 FLC is able to bring about computational savings without sacrificing the ability to handle modeling uncertainties.

3. The FOU of a type-2 set may be viewed as a collection of ET1Ss. For a given input vector, the type-reducer chooses a corresponding ET1FLS. Since

type-2 FLSs has the ability to switch between its ET1FLSs according to the input, more complex input-output map than that of a single type-1 FLS can be modeled. The concept of ET1S will also help in determining the best FOU and designing new type-reducers to meet specific requirements.

4. For a double-input single-output PI-like type-2 FLC, in each fuzzy partition there exists an area near the origin where the equivalent proportional and integral gains are smaller than these of the baseline type-1 FLC. Besides, the two gains will change with the change of inputs. This explains why type-2 FLCs generally have better ability to eliminate oscillations, and provide insights into how to evolve faster type-reducers theoretically.

Based on the results obtained in this Thesis, possible future research directions are :

1. The Karnik-Mendel type-reducer need further study in order to understand them better. It is noticed that when the FOUs are introduced to a baseline type-1 FLS which has a monotonic input-output map, the input-output map of the resulting type-2 FLS may become non-monotonic. Besides, discontinuities may occur in the input-output map. These may be disadvantages when type-2 FLSs are applied to control. Hence, it is interesting to study the conditions under which the non-monotonicity and discontinuities will occur.

2. The Karnik-Mendel type-reducer has very high computational cost besides the disadvantages pointed out above. It may be possible to find out faster and better type-reducers based on the concept of ET1Ss and ET1MGs.

3. Another interesting topic is to find a relationship between the appropriate FOUs for a type-2 FLC and the uncertainties in the plant parameters. If it is solved, the applications of type-2 FLCs will be greatly promoted.

Bibliography

[1] J. M. Mendel, *Rule-Based Fuzzy Logic Systems: Introduction and New Directions.* NJ: Prentice-Hall, 2001.

[2] L.-X. Wang, *A Course in Fuzzy Systems and Control.* Prentice Hall, 1997.

[3] L. Zadeh, "Fuzzy sets," *Inform. and Contr.*, vol. 8, pp. 338–353, 1965.

[4] I. Turksen, "Fuzzy data mining and expert system development," in *Proc. IEEE Int. Conf. Syst. Man, Cybern.*, Oct. 1998, pp. 2057–2061.

[5] D. Lee and M. Kim, "Database summarization using fuzzy ISA hierarchies," *IEEE Trans. Syst., Man, Cybern. B*, vol. 27, pp. 68–78, 1997.

[6] D. Chiang, L. Chow, and Y. Wang, "Mining time series data by a fuzzy linguistic summary system," *Fuzzy Sets Syst.*, vol. 112, pp. 419–432, 2000.

[7] W. Pedrycz, "Fuzzy set technology in knowledge discovery," *Fuzzy Sets Syst.*, vol. 98, pp. 279–290, 1998.

[8] R. Yager, "Database discovery using fuzzy sets," *Int. J. Intell. Syst.*, vol. 11, pp. 691–712, 1996.

[9] J. Baldwin, "Knowledge from data using fuzzy methods," *Pattern Recongnition Lett.*, vol. 17, pp. 593–600, 1996.

[10] L. Zadeh, "Toward a theory of fuzzy information granulation and its centrality in human reasoning and fuzzy logic," *Fuzzy Sets Syst.*, vol. 19, pp. 111–127, 1997.

[11] W. Melek, Z. Lu, A. Kapps, and W. Fraser, "Comparison of trend detection algorithms in the analysis of physiological time-series data," *IEEE Trans. Biomed. Eng.*, vol. 52, no. 4, pp. 639 – 651, 2005.

[12] S. Liao, T. Tang, and W.-Y. Liu, "Finding relevant sequences in time series containing crisp, interval, and fuzzy interval data," *IEEE Trans. Syst., Man, Cybern., B*, vol. 34, no. 5, pp. 2071 – 2079, 2004.

[13] M. Versaci and F. Morabito, "Fuzzy time series approach for disruption prediction in tokamak reactors," *IEEE Trans. Magn.*, vol. 39, no. 3, pp. 1503–1506, 2003.

[14] H. Wu and J. M. Mendel, "Uncertainty bounds and their use in the design of interval type-2 fuzzy logic systems," *IEEE Trans. Fuzzy Syst.*, vol. 10, no. 5, pp. 622–639, 2002.

[15] O. Castillo and P. Melin, "Hybrid intelligent systems for time series prediction using neural networks, fuzzy logic, and fractal theory," *IEEE Trans. Neural Networks*, vol. 13, no. 6, pp. 1395 – 1408, 2002.

[16] N. Kasabov and Q. Song, "DENFIS: Dynamic evolving neural-fuzzy inference system and its application for time-series prediction," *IEEE Trans. Fuzzy Syst.*, vol. 10, no. 2, pp. 144–154, 2002.

[17] J. Ye, X. Shen, and J. Mark, "Call admission control in wideband CDMA cellular networks by using fuzzy logic," *IEEE Trans. Mobile Comput.*, vol. 4, no. 2, pp. 129–141, 2005.

[18] S. Patchararungruang, S. Halgamuge, and N. Shenoy, "Optimized rule-based delay proportion adjustment for proportional differentiated services," *IEEE J. Select. Areas Commun.*, vol. 23, no. 2, pp. 261–276, 2005.

[19] S. Shen, C.-J. Chang, C. Huang, and Q. Bi, "Intelligent call admission control for wideband CDMA cellular systems," *IEEE Trans. Wireless Commun.*, vol. 3, no. 5, pp. 1810–1821, 2004.

[20] Q. Liang, N. Karnik, and J. Mendel, "Connection admission control in ATM networks using survey-based type-2 fuzzy logic systems," *IEEE Trans. Syst., Man, Cybern. C*, vol. 30, no. 3, pp. 329–339, 2000.

[21] Q. Liang, "Ad hoc wireless network traffic-self-similarity and forecasting," *IEEE Commun. Lett.*, vol. 5, no. 7, pp. 297 – 299, 2002.

[22] L.-X. Wang, *Adaptive Fuzzy Systems and Control: Design and Stability Analysis.*   NJ: Prentice Hall, 1994.

[23] T. Johansen, "Fuzzy model based control: Stability, robustness, and performance issues," *IEEE Trans. Fuzzy Syst.*, vol. 2, no. 3, pp. 221–234, 1994.

[24] W. Kickert, "Towards an analysis of linguistic modelling," *Fuzzy Sets Syst.*, vol. 2, pp. 293–307, 1979.

[25] W. C. Kim, S. C. Ahn, and W. H. Kwon, "Towards an analysis of linguistic modelling," *Fuzzy Sets Syst.*, vol. 71, pp. 131–142, 1995.

[26] R. Yager and P. Dimitar, *Essential on Fuzzy Modeling and Control.*   John Wiley & Son, 1994.

[27] H. Ying, W. Siler, and J. Buckley, "Fuzzy control theory: A nonlinear case," *Automatica*, vol. 26, no. 3, pp. 513–520, 1990.

[28] J. Bezdek, "Fuzzy models–what are they, and why?" *IEEE Trans. Fuzzy Syst.*, vol. 1, no. 1, pp. 1–5, 1993.

[29] J. Buckley and H. Ying, "Expert fuzzy controller," *Fuzzy Sets Syst.*, vol. 43, pp. 127–137, 1991.

[30] C. Bonivento, R. Rovatti, and C. Fantuzzi, *Fuzzy Logic Control: Advances in Methodology.* Italy: Proc. International Summer School, Ferrara, 16-20 , 1998.

[31] E. H. Mamdani, "Application of fuzzy algorithms for control of simple dynamic plant," *Proc. Inst. Elec. Eng.*, vol. 121, no. 12, pp. 1585–1588, 1974.

[32] E. H. Mamdani and S. Assilian, "An experiment in linguistic synthesis with a fuzzy logic controller," *Int. J. Man-machine Studies*, vol. 7, pp. 1–13, 1975.

[33] P. J. King and E. H. Mamdani, "The application of fuzzy controller systems to industrial processes," *Automatica*, vol. 13, pp. 235–242, 1977.

[34] E. Mamdani and B. Gaines, *Fuzzy Reasoning and its Applications.* Academic Press, NY, 1981.

[35] J. Buckley, "Universal fuzzy controllers," *Automatica*, vol. 28, pp. 1245–1248, 1992.

[36] T. Takagi and M. Sugeno, "Fuzzy identification of systems and its application to modeling and control," *IEEE Trans. Syst., Man, Cybern.*, vol. 15, pp. 116–132, 1985.

[37] W. Pedrycz, *Fuzzy Control and Fuzzy System (Second, Extended Edition)*. NY: John Willey & Sons, 1993.

[38] R. BabušKa and H. Verbruggen, "Fuzzy modeling and model-based control for nonlinear systems," in *Applications of Fuzzy Logic: Towards High Machine Intelligence Quotient Systems*, M. Jamshidi, A. Titli, S. Boveries, and L. Zadeh, Eds. Prentice Hall, NY, 1997, pp. 49–74.

[39] H. B. Verbruggen, H.-J. Zimmermann, and R. B. (Eds.), *Fuzzy Algorithms for Control*. Boston: Kluwer Academic, 1999.

[40] T. Terano, K. Asai, and M. Sugeno, *Applied Fuzzy Systems*. Academic Press, Boston, 1994.

[41] U. Kaymak, J. Sousa, and H. Verbruggen, "A comparative study of fuzzy and conventional criteria in model-based predictive control," in *FUZZ-IEEE*, vol. 2, July 1997, pp. 907 – 914.

[42] J.-H. Kim and U.-Y. Huh, "Fuzzy model based predictive control," in *FUZZ-IEEE*, vol. 1, May 1998, pp. 405 – 409.

[43] M. Hadjili, V. Wertz, and G. Scorletti, "Fuzzy model-based predictive control," in *37th IEEE Conference on Decision and Control*, vol. 3, Dec 1998, pp. 2927 – 2929.

[44] A. Flores, D. Saez, J. Araya, M. Berenguel, and A. Cipriano, "Fuzzy predictive control of a solar power plant," *IEEE Transactions on Fuzzy Systems*, vol. 13, no. 1, pp. 58 – 68, Feb 2005.

[45] J. Driankov, H. Hellendoorn, and M. Reinfrant, *An Introduction to Fuzzy Control*. Prentice Hall, NY, 1993.

[46] L. A. Zadeh, "The concept of a linguistic variable and its application to approximate reasoning-1," *Inform. Sci.*, vol. 8, pp. 199–249, 1975.

[47] Q. Liang and J. Mendel, "Interval type-2 fuzzy logic systems: theory and design," *IEEE Trans. Fuzzy Syst.*, vol. 8, no. 5, pp. 535–550, 2000.

[48] ——, "Equalization of nonlinear time-varying channels using type-2 fuzzy adaptive filters," *IEEE Trans. Fuzzy Syst.*, vol. 8, no. 5, pp. 551–563, 2000.

[49] ——, "Overcoming time-varying co-channel interference using type-2 fuzzy adaptive filters," *IEEE Trans. Circuits Syst. II*, vol. 47, no. 12, pp. 1419–1428, 2000.

[50] ——, "MPEG VBR video traffic modelling and classification using fuzzy technique," *IEEE Trans. Fuzzy Syst.*, vol. 9, no. 1, pp. 183–193, 2001.

[51] R. R. Yager, "Fuzzy subsets of type-2 in decisions," *J. Cybern.*, vol. 10, pp. 137–159, 1980.

[52] T. Ozen and J. Garibaldi, "Effect of type-2 fuzzy membership function shape on modelling variation in human decision making," in *Proceedings. FUZZ-IEEE*, vol. 2, July 2004, pp. 971–976.

[53] T. Ozen, J. Garibaldi, and S. Musikasuwan, "Modelling the variation in human decision making," in *Proc. FUZZ-IEEE*, vol. 2, July 2004, pp. 617 – 622.

[54] R. I. John, P. R. Innocent, and M. R. Barnes, "Neuro-fuzzy clustering of radiographic tibia images using type 2 fuzzy sets," *Inform. Sci.*, vol. 125, pp. 65–82, 2000.

[55] O. Castillo and P. Melin, "Adaptive noise cancellation using type-2 fuzzy logic and neural networks," in *Proc. FUZZ-IEEE*, vol. 2, 25-29 July 2004, pp. 1093–1098.

[56] J. Mendel, "Fuzzy sets for words: A new beginning," in *Proc. FUZZ-IEEE*, vol. 1, May 2003, pp. 37 – 42.

[57] H. Wu and J. Mendel, "Antecedent connector word models for interval type-2 fuzzy logic systems," in *Proc. FUZZ-IEEE*, vol. 2, July 2004, pp. 1099 – 1104.

[58] J. Zeng and Z.-Q. Liu, "Type-2 fuzzy hidden markov models to phoneme recognition," in *Proceedings of the 17th International Conference on Pattern Recognition*, vol. 1, Aug. 2004, pp. 192–195.

[59] O. Castillo and P. Melin, "A new hybrid approach for plant monitoring and diagnostics using type-2 fuzzy logic and fractal theory," in *Proc. FUZZ-IEEE*, vol. 1, May 2003, pp. 102 – 107.

[60] ——, "Fuzzy logic for plant monitoring and diagnostics," in *Proc. FUZZ-IEEE*, vol. 1, July 2004, pp. 61 – 66.

[61] W. W. Tan and J. Lai, "Development of a type-2 fuzzy proportional controller," in *Proceedings. FUZZ-IEEE*, vol. 3, July 2004, pp. 1305 – 1310.

[62] H. Hagras, "A hierarchical type-2 fuzzy logic control architecture for autonomous mobile robots," *IEEE Trans. Fuzzy Syst.*, vol. 12, no. 4, pp. 524–539, Aug. 2004.

[63] P. Melin and O. Castillo, "A new approach for quality control of sound speakers combining type-2 fuzzy logic and fractal theory," in *Proc. FUZZ-IEEE*, vol. 2, May 2002, pp. 625–630.

[64] C. H. Wang, C. S. Cheng, and T. T. Lee, "Dynamical optimal training for interval type-2 fuzzy neural network (T2FNN)," *IEEE Trans. Syst., Man, Cybern. B*, vol. 34, no. 3, pp. 1462– 1477, June 2004.

[65] P. Melin and O. Castillo, "A new method for adaptive model-based control of non-linear plants using type-2 fuzzy logic and neural networks," in *12th IEEE Int. Conf. on Fuzzy Syst.*, vol. 1, May 2003, pp. 420 – 425.

[66] C.-H. Lee and Y.-C. Lin, "Control of nonlinear uncertain systems using type-2 fuzzy neural network and adaptive filter," in *2004 IEEE International Conference on Networking, Sensing and Control*, vol. 2, 2004, pp. 1177–1182.

[67] W. W. Tan and S. N. Pall, "Performance study of type-2 fuzzy controllers," in *2nd Int. Conf. Comput. Intell., Robot. and Autonomous Syst.*, Singapore, Dec. 2003.

[68] J. Mendel and F. Liu, "Super-exponential convergence of the Karnik-Mendel algorithms for computing the centroid of an interval type-2 fuzzy set," 2005, accepted for publication in IEEE Trans. on Fuzzy Systems.

[69] P. Innocent, R. John, I. Belton, and D. Finlay, "Type 2 fuzzy representations of lung scans to predict pulmonary emboli," in *Proc. Joint 9th IFSA World Congress and 20th NAFIPS Int. Conf.*, vol. 4, Vancouver, BC, Canada, July 2001, pp. 1902 – 1907.

[70] D. R. Wu and W. W. Tan, "A type-2 fuzzy logic controller for the liquid-level process," in *Proc. FUZZ-IEEE*, vol. 2, Budapest, July 2004, pp. 953–958.

[71] S. Park and H. Lee-Kwang, "A designing method for type-2 fuzzy logic systems using genetic algorithms," in *Proc. Joint 9th IFSA World Congress and 20th NAFIPS Int. Conf.*, vol. 5, Vancouver, BC, Canada, July 2001, pp. 2567 – 2572.

[72] J. Holland, *Adaptation in Natural and Artificial Systems*. MI: University of Michigan Press, 1975.

[73] D. E. Goldberg, *Genetic Algorithms in Search, Optimization and Machine Learning*. Addison-Wesley, 1989.

[74] Z. Michalewicz, *Genetic Algorithms + Data Structures = Evolution Programs*. NY: Springer-Verlag, 1996.

[75] K. Man, K. Tang, S. Kwong, and W. Halang, *Genetic Algorithms for Control and Signal Processing*. NY: Springer, 1997.

[76] M. Sakawa, *Genetic Algorithms and Fuzzy Multiobjective Optimization*. Boston: Kluwer Academic, 2002.

[77] J. Kim, Y. Moon, and B. Zeigler, "Designing fuzzy net controllers using genetic algorithms," *IEEE Control Syst. Mag.*, vol. 15, no. 3, pp. 66–72, 1995.

[78] A. Homaifar and E. McCormick, "Simultaneous design of membership functions and rule sets for fuzzy controllers using genetic algorithms," *IEEE Trans. Fuzzy Syst.*, vol. 3, no. 2, pp. 129–138, May 1995.

[79] O. Cordon, F. Herrera, F. Hoffmann, and L. Magdalena, *Genetic Fuzzy System: Evolutionary Tuning and Learning of Fuzzy Knowledge Bases.* Singapore: World Scientific, 2001.

[80] O. Cordon, F. Herrera, F. Gomide, F. Hoffmann, and L. M. (Edts), "Genetic fuzzy systems: New developments," *Special Issue Fuzzy Sets Syst.*, vol. 141, no. 1, pp. 1–163, Jan. 2004.

[81] L. Teo, M. Khalid, and R. Yusof, "Self-tuning neuro-fuzzy control by genetic algorithms with an application to a coupled-tank liquid-level control system," *Int. J. Eng. Applicat. of Artificial Intell.*, vol. 11, pp. 517–529, 1998.

[82] K. Lim and K. Sin, "Teaching with the KRi coupled-tank control apparatus model PP-100," KentRidge Instruments Pte Ltd, Tech. Rep., 1995.

[83] D. R. Wu and W. W. Tan, "A simplified architecture for type-2 FLSs and its application to nonlinear control," in *Proc. IEEE Conf. Cybern. and Intell. Syst.*, Singapore, Dec. 2004, pp. 485–490.

[84] ——, "Computationally efficient type-reduction strategies for a type-2 fuzzy logic controller," in *FUZZ-IEEE*, Reno, USA, May 2005, pp. 353–358.

[85] N. N. Karnik, Q. Liang, and J. M. Mendel, "Type-2 fuzzy logic software," 2000, http://sipi.usc.edu/ mendel/software/.

[86] D. R. Wu and W. W. Tan, "A simplified type-2 fuzzy controller for real-time control," *ISA Transactions*, 2005, accepted for publication.

[87] ——, "Genetic learning and performance evaluation of type-2 fuzzy logic controllers," *Int. J. Eng. Applicat. of Artificial Intell.*, 2005, accepted for publication.

[88] M. Mizumoto, "Realization of PID controls by fuzzy control methods," *Fuzzy Sets Syst.*, vol. 70, pp. 171–182, 1995.

[89] N. N. Karnik and J. M. Mendel, "Centroid of a type-2 fuzzy set," *Information Sciences*, vol. 132, pp. 195–220, 2001.

[90] J. Mendel and H. Wu, "Properties of the centroid of an interval type-2 fuzzy set, including the centroid of a fuzzy granule," in *Proc. FUZZ-IEEE*, Reno, Nevada, May 2005, pp. 341–346.

[91] C. Lynch, H. Hagras, and V. Callaghan, "Embedded type-2 FLC for real-time speed control of marine & traction diesel engines," in *Proc. FUZZ-IEEE*, Reno, Nevada, May 2005, pp. 347–352.

[92] D. R. Wu and W. W. Tan, "Type-2 FLS modeling capability analysis," in *FUZZ-IEEE*, Reno, USA, May 2005, pp. 242–247.

[93] P. Persson, "Towards autonomous PID control," Ph.D. dissertation, Lund Institute of Technology, 1992.

Author's Publication List

1. D. R. Wu and W. W. Tan, "A type-2 fuzzy logic controller for the liquid-level process," in *Proc. FUZZ-IEEE*, vol. 2, Budapest, July 2004, pp. 953–958.

2. ——, "A simplified architecture for type-2 FLSs and its application to nonlinear control," in *Proc. IEEE Conf. Cybern. and Intell. Syst.*, Singapore, Dec. 2004, pp. 485–490.

3. ——, "Type-2 FLS modeling capability analysis," in *Proc. FUZZ-IEEE*, Reno, USA, May 2005, pp. 242–247.

This paper won the *Best Student Paper Award* in 2005 IEEE International Conference on Fuzzy Systems, May 22-25, Reno, Nevada.

4. ——, "Computationally efficient type-reduction strategies for a type-2 fuzzy logic controller," in *Proc. FUZZ-IEEE*, Reno, USA, May 2005, pp. 353–358.

5. ——, "Genetic learning and performance evaluation of type-2 fuzzy logic controllers," *Int. J. Eng. Applicat. of Artificial Intell.*, 2005, accepted for publication.

6. ——, "A simplified type-2 fuzzy controller for real-time control," *ISA Transactions*, 2005, accepted for publication.

7. ——, "Characteristics of type-2 fuzzy PI controllers," *IEEE Trans. Fuzzy Systems*, 2005, submitted.

8. ——, "A cellular neural network realization of Matsuoka's central pattern generator model," under preparation.